REGULATION OF ISOPRENE EMISSION FROM PLANTS

By

Ziru Li

A DISSERTATION

Submitted to
Michigan State University
in partial fulfillment of the requirements
for the degree of

DOCTOR OF PHILOSOPHY

Biochemistry and Molecular Biology

2012

ABSTRACT

REGULATION OF ISOPRENE EMISSION FROM PLANTS

By

Ziru Li

Isoprene emission from plants is the largest non-methane hydrocarbon flux into the atmosphere. This large hydrocarbon flux from the biosphere has a profound effect on ozone chemistry, aerosol formation and greenhouse gas lifetime in the atmosphere. Understanding the biochemical and molecular regulation of isoprene emission in response to environmental drivers will allow us to build models that better predict future atmospheric conditions. In addition, isoprene is produced through the plastidic methylerythritol phosphate (MEP) pathway, an essential pathway in plants, and accounts for over 90% of the MEP pathway flux. Studies of regulation of isoprene emission, therefore, also provide a unique opportunity for understanding regulation of the MEP pathway. My graduate work presented in this dissertation focused on two aspects of short-term control of isoprene emission: responses of isoprene emission to changes in 1) temperatures and 2) photon flux density. DMADP measurements using post-illumination isoprene emission suggest that the temperature dependence of isoprene emission reflects combined regulation from both isoprene synthase (IspS) and upstream MEP pathway enzymes. Analysis of transient response to elevated temperature shows that emission levels increase initially due to an increase in IspS activity, and then decrease over time as limited by substrate levels. An unexpected discovery from this work was the observation of a highly temperature-dependent “post-illumination isoprene burst”. It was hypothesized that this burst represents early metabolites in the MEP pathway that was trapped initially upon darkening, and then converted to isoprene in a later

phase. To understand the nature of this phenomenon I employed high pressure liquid chromatography-tandem mass spectrometry (HPLC-MS-MS) to measure metabolites in the MEP pathway under physiological conditions. Levels of intermediate metabolites, in particular methylerythritol cyclodiphosphate, were largely unaffected during phase I in darkness when isoprene emission declined exponentially. Quantitative comparison suggests this pool can account for the post-illumination isoprene burst. Steps in the MEP pathway that requires reducing power are likely the most susceptible steps in response to changes in light levels. This work represents one of the first studies that profiled MEP pathway metabolites in plants and it is suggested that the same technique can be used to understand short-term responses of isoprene emission to other environmental variables and to study metabolic control of the MEP pathway.

To my mom, dad and grandpa

謝謝你們這些年來的教誨。謹致此文, 以表寸心。

ACKNOWLEDGEMENTS

First and foremost I would like to thank my major advisor, Dr. Tom Sharkey, for his guidance throughout the past five years. I cannot overstate how I appreciate the many, many encouragements he gave when things are not working out the way they should, and I regret that oftentimes I was not trying hard enough. There were a lot of things that I learned from him, the most important ones not about isoprene but has to do with persistence, meticulousness and a deep sense of scholarship. I also thank him for the deep care he shows for his students, and for making my move from Madison to MSU as smooth as it can be. I was introduced to Tom in my junior year by Dr. Tammy Sage, a great professor herself whom I had the pleasure to work with for two years, and I wanted to thank Tammy once again for showing me the door to the wonderful world of plant biology.

I was fortunate to have another great mentor in the lab, Dr. Sean Weise who joined the lab at about the same time as we moved to MSU. Since then I have had the luxury of going up to him countless times with my questions and Sean always had the patience and often went out of his way to help me both in and out of the lab. So many of my experiments could not have been done without his help that he probably deserves to be on half of the publications I had (which he politely declined). As the lab manager he made the lab an organized and pleasant place to work in and he has certainly always kept us entertained (with his humorous manner). Thank you, Sean.

I wish to thank all my advisory committee members: Drs. Kevin Walker, Honggao Yan, Dan Jones and Kyung-Hwan Han. Thank you for your help/advices throughout the years. A special

thank you goes to Dan who not only bore with my many mass spec questions but also always made me feel better with a smile.

All the lab members that I have shared the bench with: Drs. Ru Zhang, Dennis Gray and Amy Wiberley; Aparajita Banerjee, Chris Harvey and the 20-plus undergraduate students that have rotated through the lab but especially Ellen Ratliff, Alex Corrion and Jennifer Yang, it was great to have you around and you have all made the lab a better place for me. I also gratefully acknowledge the stunning supporting staffs in the department and the facilities: Jessica Lawrence, Kaillathe Padmanabhan (Pappan), Teresa Vollmer, Alicia Pastor, Melinda Frame, Chao Li and Lijun Chen.

Last but certainly not the least, I thank the supports from my family and friends. There are so many of you (my buddies from the table tennis club, my international friends, my "science" friends …) that I simply cannot enumerate the names here. I also could not have pulled through this without the love and support from my girlfriend Danica. Thank you all for adding a colorful page in my graduate student life and I hope our friendship and love will last a lifetime.

TABLE OF CONTENTS

LIST OF TABLES

LIST OF FIGURES

KEY TO ABBREVIATIONS

A	assimilation/absorbance
ADP	adenosine diphosphate
ANOVA	analysis of variance
ATP	adenosine triphosphate
ATPase	ATP synthase
AtpC	CF_1-γ subunit of ATP synthase
BPG	bisphosphoglycerate
BVOC	biogenic volatile organic carbon
C_a	apparent CO_2 concentration
C_c	CO_2 concentration at site of carboxylation
CDPME	4-(cytidine 5'-diphospho)-2-*C*-methyl-D-erythritol
CDPMEP	4-(cytidine 5'-diphospho)-2-*C*-methyl-D-erythritol 2-phosphate
Chl	chlorophyll
C_i	intercellular CO_2 concentration
CMK	4-(cytidine 5'-diphospho)-2-*C*-methyl-D-erythritol kinase
CMP	cytidine monophosphate
CTP	cytidine triphosphate
Cyt b_6/f	cytochrome b_6/f complex
DGDG	digalactosyldiacylglycerol
dH_2O	distilled water
DIRK	dark-interval relaxation kinetics
DMADP	dimethylallyl diphosphate

DXP	1-deoxy-D-xylulose 5-phosphate
DXR	1-deoxy-D-xylulose 5-phosphate reductoisomerase
DXS	1-deoxy-D-xylulose 5-phosphate synthase
E	transpiration
E_a	Arrhenius activation energy
EC	enzyme commission
ECS	electrochromic shift
ER	endoplasmic reticulum
ESI	electrospray ionization
ETC	electron transport chain
FIS	fast isoprene sensor
F_v'/F_m'	photosystem II maximum efficiency
g	gravity
GAP	D-glyceraldehyde 3-phosphate
GGGT	galactolipid:galactolipid galactosyltransferase
g_{H}^{+}	proton conductance
g_{H2O}	stomatal conductance to water
GLV	green leaf volatiles
H_2O_2	hydrogen peroxide
HDR	4-hydroxy-3-methylbut-2-enyl diphosphate reductase
HDS	4-hydroxy-3-methylbut-2-enyl diphosphate synthase
HILIC	hydrophilic interaction chromatography
HMBDP	4-hydroxy-3-methylbut-2-enyl diphosphate
HPLC	high pressure liquid chromatography

IDI	isopentenyl diphosphate isomerase
IDP	isopentenyl diphosphate
IPCC	Intergovernmental Panel on Climate Change
IspS	isoprene synthase
J	linear electron transport rate
k_{cat}	turnover number
K_m	Michaelis-Menten constant
Lhcb1	light harvesting complex II type I chlorophyll *a*/*b* binding protein
LOD	limit of detection
m/z	mass-to-charge ratio
MBO	methylbutenol
MCT	2-*C*-methyl-D-erythritol 4-phosphate cytidylyltransferase
MDS	2-*C*-methyl-D-erythritol 2,4-cyclodiphosphate synthase
ME	methacrolein
MEcDP	2-*C*-methyl-D-erythritol 2,4-cyclodiphosphate
MEP	2-*C*-methyl-D-erythritol 4-phosphate
MGDG	monogalactosyldiacylglycerol
MS	mass spectrometry
MS-MS	tandem mass spectrometry
MVA	mevalonic acid
MVK	methyl vinyl ketone
NADH	nicotinamide adenine dinucleotide
NADPH	nicotinamide adenine dinucleotide phosphate
NMR	nuclear magnetic resonance
NoFOSpec	non-focusing optics flash spectrophotometer/fluorometer

P700	photosystem I primary donor
PA	phosphotidic acid
PC	phosphotidylcholine
PE	phosphotidylethanolamine
PEP	phosphoenolpyruvate
PG	phosphotidylglycerol
PGA	phosphoglycerate
P_i	inorganic phosphate
PI	phosphatidylinositol
PM	particulate matter
pmf	proton motive force
PPFD	photosynthetic photon flux density
PP_i	inorganic diphosphate
ppm	parts per million
PSI	photosystem I
PSII	photosystem II
PTR-TOF-MS	proton transfer reaction-time of flight-mass spectrometry
Q_E	energy-dependent non-photochemical quenching
RbcL	ribulose 1,5-bisphosphate carboxylase/oxygenase large subunit
RNAi	RNA interference
ROS	reactive oxygen species
Rubisco	ribulose 1,5-bisphosphate carboxylase/oxygenase
RuBP	ribulose 1,5-bisphosphate
SE	standard error
SQDG	sulfoquinovosyldiacylglycerol

TAG	triacylglycerol
TGDG	trigalactosyldiacylglycerol
TPS	terpene synthase
V_{cmax}	maximum carboxylation rate of ribulose 1,5-bisphosphate carboxylase/oxygenase
V_{max}	maximum rate of reaction
VOC	volatile organic carbon
WT	wild type
Δ_{ECS} /ΔA_{517}	total amplitude of electrochromic shift (change of absorbance at 517nm)
ΔG	Gibbs free energy
v_H^+	proton flux
τ_{ECS}	exponential time constant of the rapid phase (within 100ms) of electrochromic shift decay
τ_{ion}	exponential time constant of the slow and inverse phase (0.2 – 30s) of electrochromic shift decay
ΦPSII	photosystem II operating efficiency

CHAPTER 1

Function and Regulation of Isoprene Emission from Plants

Part of this chapter was adapted from the following submitted manuscript.
Li Z, Sharkey TD (2012) Biochemical and molecular controls of volatile organic carbon emissions. *In* Biology, controls and models of tree volatile organic compound emissions. Springer, Berlin. http://www.springer.com/series/6644

Introduction

Plant cells are amazing chemical factories that produce tens of thousands of compounds over their lifespan. These compounds fall into two general categories: primary metabolites such as proteins, sugars and nucleic acids which are required for "housekeeping" of the plant; and secondary (specialized) metabolites including the alkaloids, isoprenoids and phenolics, which are involved in many diverse but crucial functions such as defense, pollination, communication and stress responses. The isoprenoids, also called terpenoids, includes more than 22,000 members (Connolly and Hill, 1991) and is by far the largest family of the secondary metabolites.

The most basic member of the isoprenoid family is isoprene (C_5H_8, Fig. 1.1), which is also a common structural motif for higher-order isoprenoids. The terms terpene, terpenes, terpenoids, isoprenes and isoprenoids are often used interchangeably; while in other cases isoprenoids and terpenoids have been used to exclusively describe terpenes that are chemically modified (e.g. by oxidation). For the sake of simplicity, the general term "isoprenoids" will be used in this dissertation to comprise any compounds that include a C_5H_8 motif.

Biogenic production of isoprene

At room temperature, isoprene exists as a colorless liquid and is also a proven carcinogen (Melnick et al., 1994). In natural environments however, isoprene is usually a gas because of its

high volatility. Isoprene is produced from biogenic sources in tremendous quantities. Isoprene production from plants is estimated at ~ 600 Tg (6×10^{14}) per year, approximately equivalent to the methane flux and accounting for ~ 1/3 of the hydrocarbon input into the atmosphere (Guenther et al., 2006). This large hydrocarbon flux has a profound effect on atmospheric chemistry. Isoprene reacts with hydroxyl radicals in the atmosphere and contributes to the formation of tropospheric ozone, one of the two most significant air pollutants in the US (Trainer et al., 1987; Chameides et al., 1988). Tropospheric ozone contributes to asthma, and is estimated to account for ~ 20% in crop loss due to air pollution (Heck et al., 1982; Lippmann, 1989; Coleman et al., 1995; McConnell et al., 2002). Volatile organic carbons like isoprene has also been show to affect the formation of aerosols, a nucleating agent for cloud formation and the source of particulate matter (including both PM10 and PM2.5), the other significant air pollutant in this country (Went, 1960; Fehsenfeld et al., 1992; Kiendler-Scharr et al., 2009). In addition, reactions between isoprene and hydroxyl radicals could lengthen the lifetime of other greenhouse gases such as methane and thereby affect global climate change (Poisson et al., 2000).

Isoprene is produced from dimethylallyl diphosphate (DMADP) in plants. DMADP with its isomer isopentenyl diphosphate (IDP) are also the functional isoprene units in plants and animals and the building blocks of higher-order isoprenoids (Fig 1.1). Isoprene synthesis from DMADP is catalyzed by isoprene synthase (IspS), a close relative to other monoterpene and diterpene synthases and a member of the TPS-b family (Bohlmann et al., 1998). DMADP and IDP in plants can be synthesized through two pathways – the mevalonic acid (MVA) pathway, which resides exclusively in the cytosol, and the methylerythritol phosphate pathway (MEP pathway,

also called the non-mevalonate pathway) in the plastids. Isoprene is exclusively produced from the plastid DMADP pool synthesized by the MEP pathway.

The MEP pathway

The existence of a mevalonic acid-independent pathway for isoprenoid synthesis was not recognized until the early 1990s, where two separate groups found the observed labeling patterns in certain isoprenoids did not match predictions of a mevalonic acid pathway origin in ^{13}C-glucose and ^{13}C-acetate feeding experiments. An important step in understanding the new isoprenoid synthesis pathway was the discovery that labeled 1-deoxy-D-xylulose was incorporated into the side chains of ubiquinone (Broers 1994). The first metabolite in the MEP pathway was later shown to be the 1-deoxy-D-xylulose 5-phosphate (DXP).

Since then tremendous strides have been made towards elucidating the steps and enzymes in this pathway, using a combination of both traditional genetic methods and comparative genomic approaches. The entire MEP pathway was elucidated by 2003 (Fig. 1.2; Table 1.1, 1.2). The first enzyme in the pathway, DXP synthase (DXS), forms DXP from D-glyceraldehyde 3-phosphate and pyruvate. One CO_2 molecule is lost in this process. DXP produced by DXS is also a substrate in thiamine and pyridoxal synthesis. DXP reductoisomerase (DXR) then catalyzes the formation of 2-*C*-methyl-D-erythritol 4-phosphate (MEP), the first committed metabolite in this pathway that gives the pathway its name. The next enzyme, MEP cytidylyltransferase (MCT) transfers a cytidyl moiety to form 4-(cytidine 5'-diphospho)-2-*C*-methyl-D-erythritol (CDPME). This compound is phosphorylated by CDPME kinase (CMK) to produce CDPME 2-phosphate

(CDPMEP), which is then cyclized to 2-*C*-methyl-D-erythritol 2,4-cyclodiphosphate (MEcDP) by MEcDP synthase (MDS) with the loss of a cytidyl group. Finally, 4-hydroxy-3-methylbut-2-enyl diphosphate (HMBDP) is produced by HMBDP synthase (HDS) in the penultimate step in the pathway, and is then converted to DMADP and IDP by HMBDP reductase (HDR) in an approximately 1:5 ratio (Rohdich et al., 2002). Under steady state conditions the equilibrium ratio between DMADP and IDP is just the reverse at approximately 5:1, and the isomerization is accelerated *in vivo* by a plastidic IDP isomerase (IDI).

Isoprene synthase

DMADP produced from the MEP pathway is then acted upon by isoprene synthase (IspS) to produce isoprene in the chloroplasts. Due to its high volatility isoprene does not build to a substantial amount in plants, but instead passes through two membrane systems (the chloroplast membranes and plasma membrane) and is released into the atmosphere. Surprisingly high K_m values have been reported for isoprene synthase (0.5 – 8 mM) suggesting substrate concentration plays an important role in regulation of isoprene emission (Silver and Fall, 1995; Wildermuth and Fall, 1998; Wiberley et al., 2008). k_{cat} for isoprene synthase is approximately 1.8 s^{-1} (Silver and Fall, 1995; Wiberley et al., 2008). IspS evolved ca. 100 million years ago in multiple lineages and is a trait that has been gained and lost multiple times, perhaps similar to the evolution history of C_4 photosynthesis.

Why do plants make isoprene?

The "why" questions in biology are usually among the most difficult ones to answer, as the evolutionary advantages a certain trait can offer are often difficult to empirically quantify. This was particularly the case in the field of isoprene research. Isoprene emission represents a significant carbon loss from the plant – approximately 2% of recently assimilated carbons, and as high as 25% in certain circumstances – and thus should offer an evolutionary advantage that is at least commensurate to the carbon cost of isoprene. Intriguingly, this advantage was not obvious from the geographic or phylogenetic distribution of isoprene-emitting species. A number of hypotheses have been put forward to explain the function of isoprene.

Defense against heat stress

Eric Singsaas from this lab first proposed (1995) that isoprene may protect plants against heat stress, shown by a reduction in heat-induced increase in photosystem II chlorophyll fluorescence when isoprene is added into the air stream. Later, this hypothesis has been refined to suggest that isoprene specifically protects against moderate heat stress (the definition moderate heat stress varies between species, but in general, 40 – 44°C), and in particular rapid fluctuations in temperature that leaves experience in natural conditions. The large fluctuations in temperature may damage the integrity and structure of the thylakoid membranes, and isoprene may protect the intricate photosynthetic membranes from heat damage by intercalating into the lipid bilayers and stabilizing the membranes (Fig. 1.3). A number of observations support the thermotolerance hypothesis. First, photosynthesis is protected against heat stress when non-emitting species were

fumigated with isoprene (Sharkey et al., 2001). Second, thermotolerance from endogenous isoprene emission was shown when plants of an emitting species were compared with plants where isoprene emission was blocked by fosmidomycin (Sharkey et al., 2001; Velikova and Loreto, 2005). Third, *Arabidopsis* plants transformed with poplar and kudzu IspS and thus able to produce isoprene show enhanced tolerance to heat spikes (Sasaki et al., 2007; Sharkey et al., 2008). Fourth, poplar plants with IspS reduced using RNA interference are more susceptible to heat shocks (Behnke et al., 2007). Finally, there is biophysical evidence that isoprene can protect against damages to membrane integrity (Velikova et al., 2011).

Defense against oxidative stress

In addition to protection against heat spikes, it was also observed that isoprene quenches H_2O_2 and protects against lipid peroxidation in membranes exposed to ozone (Loreto et al., 2001; Loreto and Velikova, 2001; Velikova et al., 2008). It was suggested that isoprene is a potent antioxidant and a primary function of isoprene is to protect against reactive oxygen species (ROS, Vickers et al., 2009). More recently, methyl vinyl ketone and methacrolein was observed within leaves as breakdown products of isoprene (Jardine et al., 2012). However, the ratio of methyl vinyl ketone (MVK) and methacrolein (ME) production is different from what would be predicted from isoprene oxidation in air; and this may indicate MVK and ME observed in leaves come from a different source, for example, MVK may be produced as a breakdown product of fatty acids (Kai et al., 2012). From an evolutionary standpoint, it did not appear that ozone levels in the past would have provided significant selection pressure that would favor isoprene emission (Jacob, 1999), so the selection pressure likely comes from a different type of stress.

Defense against herbivores (plant-insect and/or plant-plant interactions)

Many plant volatiles include monoterpenes and sesquiterpenes are involved in plant defense against insects by either repelling the herbivores or attracting predatory arthropods (Turlings et al., 1990; De Moraes et al., 2001; Kessler and Baldwin, 2001; Kappers et al., 2005; Rasmann et al., 2005). The idea that isoprene may play a role in insect defense through tri-trophic interactions is alluring, although the effects of isoprene on plant-herbivore interactions have not been examined until very lately. Laothawornkitkul (2008) observed that tobacco plants that have been transformed with an IspS gene and emitting isoprene deterred caterpillar from feeding, and concluded that isoprene plays a role in herbivore defense. Another paper published at nearly the same time, however, used isoprene-emitting *Arabidopsis* plants to show that isoprene interferes with attracting natural enemies of herbivores (Loivamäki et al., 2008). It was argued in this case that since *Arabidopsis* plants do not naturally emit isoprene, isoprene may act as a "non-host-related volatile" for carnivorous insects that help determining host locations. However, the first study used tobacco plants, which is also a natural non-emitter. While it remains possible in theory that isoprene emission is beneficial to the plant in one case but detrimental in another (if co-evolution of the particular species of insects in question is faster), such circumstances are unlikely.

Aside from these two studies, there have been few reports that directly examined the effects of isoprene on plant-insect interactions. It appears that the effects of isoprene on herbivore decisions are, if anything, quite small. A major weakness in this hypothesis is that it does not explain why isoprene emitters produce a very large amount of isoprene constantly throughout the

day, when monoterpenes appear to be a much more targeted and therefore cheaper weapon against herbivores since they can be stored in discrete pockets and only released upon wounding (McKay et al, 2003).

The "safety valve"

Another hypothesis suggested isoprene emission may be involved in the regulation of MEP pathway metabolites (Logan et al., 2000; Rosenstiel et al., 2002). More specifically, it was suggested isoprene may be released to recoup the phosphate that was "inadvertently" added onto DMADP. On the other hand, results from this lab and others show that the MEP pathway is under tight feedback regulation (Wolfertz et al., 2003; Wolfertz et al., 2004; Banerjee A. and Sharkey T.D., unpublished data). The significant cost of isoprene (2% of fixed carbons) suggests isoprene emission is an adaptive trait, and releasing it as a waste product is unlikely. In addition, this hypothesis does not explain the temperature dependence of isoprene emission.

Mechanism of action

The majority in this field would probably agree that a primary function of isoprene is to protect against abiotic stresses (though it is in no way a consensus). A major debate still exists, however, over its mechanism of action. To understand how isoprene protects photosynthesis from heat stress one needs to understand how heat damages photosynthesis. The damage of heat stress to photosynthetic apparati is exhibited in three major aspects: 1) damage to photosynthetic membranes; 2) ROS production; and 3) induction of programmed cell death. In the short term,

membranes are likely the site of heat damage and isoprene protection (Sharkey and Schrader, 2006). Molecular modeling shows partition of isoprene into the hydrophobic phase of the membrane could effectively enhance membrane order that is equivalent to ~ 10°C decrease in temperature (Siwko et al., 2007). Circular dichroism, thermoluminescence, and electrochromic shift measurements show membrane stability is enhanced in poplars and transformed isoprene-emitting *Arabidopsis* but not their non-emitting counterparts (Velikova et al., 2011). However, membrane damage is usually tightly coupled to ROS production under stressed conditions, and more biophysical studies are needed to tell which is the cause and which is an effect. In the long term, both programmed cell death and necrosis occur in leaves. Once again, more studies are needed to unveil the underlying molecular mechanisms of these processes.

Biochemical and molecular regulation of isoprene emission

While monoterpenes and sesquiterpenes are often stored in storage bodies (e.g. resin ducts) and can accumulate to significant levels within plant tissues, volatile hemiterpenes such as isoprene are not retained in the leaf and are emitted immediately into the air (Loreto and Sharkey, 1990). The rates of emission of hemiterpenes are therefore much more dependent on the regulation of enzymes involved and more responsive to rapid changes in environmental variables. In particular, isoprene emission levels are characterized by rapid fluctuations in natural environments, presumably driven by changes in leaf temperatures due to rapid conductive heat exchange from the surrounding air currents. Isoprene emissions from plants are strongly light and temperature

dependent (Monson and Fall, 1989; Harley et al., 1998). Isoprene emission scales positively with light, and increases with increasing temperature until ~ 40 – 45°C where emission levels then falls sharply. Isoprene emission in many species decreases with increasing CO_2 concentrations, and the cause of this high-CO_2 suppression effect is unclear. The following sections will discuss and summarize present knowledge regarding regulation of isoprene emission in response to short-term environmental drivers, from a biochemical and molecular biology perspective.

Temperature

Unlike photosynthesis which peaks in activity at 25 – 30°C (Monson et al., 1992), isoprene emission exhibits strong temperature dependence up to 40 – 45°C, a temperature at which it is often considered as a significant heat stress (Fig. 1.4). The temperature response curves reported in the literature differ by as much as 8°C, and this is to a large extent due to differences in the methodologies. Isoprene emission at temperatures above 40°C is unstable (Singsaas and Sharkey, 2000). Therefore, depending on how fast leaf temperature is elevated, and whether the same leaf or different leaves were used for different temperature points, the temperature responses of isoprene emission rates may be expected to vary.

It was known for a long time that IspS activity increases strongly with temperature, and the link between emission levels and isoprene synthase has been postulated from very early on (Monson et al., 1992). It was also noticed that the temperature optimum for IspS is higher than that of isoprene emission, and the possibility of a substrate-side limitation was raised (Lehning et al., 1999). Rasoluv et al. (2009a) developed a method for measuring DMADP levels using integrated

post-illumination isoprene emission during the initial decline phase. Using this method, plastidic DMADP can be measured under physiological conditions. A major focus of my Ph.D. work was to understand how isoprene emission is regulated in response to changes in temperature, and this project will be discussed in detail in Chapter 2.

CO_2 and O_2

Isoprene emission often increases with increasing CO_2 concentrations between 0 and ~ 50 ppm CO_2, or approximately the CO_2 compensation point, where emission levels then start to decrease with increasing CO_2 concentrations (Fig. 1.5). The CO_2 response is temperature-dependent, and the high CO_2 suppression effect goes away at higher temperatures (Rasulov et al., 2010). The suppression of isoprene at high CO_2 concentrations is perplexing, as judging from the CO_2 response of photosynthesis we would predict just the contrary. Glyceraldehyde 3-phosphate (an end product of photosynthesis) is one of the two substrates for the MEP pathway, and $^{13}CO_2$ labeling studies have shown that under standard conditions a large proportion of isoprene emission comes from recent photosynthates (Delwiche and Sharkey, 1993; Karl et al., 2002; Loreto et al., 2004). Interestingly, at 0 ppm CO_2 a substantial amount of isoprene is emitted, at a rate that is comparable to emission at ambient CO_2 levels. Isoprene emission from leaves in CO_2-free air decreases slowly over time, but still does not reach zero after > 10 hours (Li Z. and Sharkey T.D., unpublished data). Carbon required for isoprene synthesis could obviously come from an alternative source (e.g. transitory starch).

Measurements of DMADP levels by non-aqueous fractionation showed CO_2 response of isoprene emission is regulated by substrate levels. Based on this experiment, Rosenstiel et al. (2003) proposed that CO_2 response of isoprene emission reflects an altered partition of phosphoenolpyruvate (PEP) between the cytosolic and plastidic compartments. PEP is required to produce pyruvate, one of the starting substrates of the MEP pathway. Specifically, it was suggested that PEP carboxylase activity increases with CO_2 concentration and this process could effectively compete with the MEP pathway for cytosolic PEP, which is presumably in equilibrium with plastidic PEP through the P_i/PEP transporter. An alternative hypothesis is that energetic cofactors required for the MEP pathway, such as ATP and NADPH, are affected at high CO_2 conditions (Rasulov et al., 2009b). As CO_2 concentrations increase, photosynthesis switches from being limited by Rubisco to being limited by linear electron transport that generates ATP and NADPH (Farquhar et al., 1980). At higher CO_2 concentrations, photosynthesis can be also feedback limited by inorganic phosphate levels which are determined by the speed of triose phosphate utilization (Sharkey, 1985). This decrease in phosphate levels reduces ATP synthesis (Kiirats et al., 2009). However, it is important to note that cellular phosphate levels could have multiple regulatory roles. Yet another explanation is that reduced plastidic phosphate levels at high CO_2 concentrations slow down the P_i/PEP antiporters on the chloroplast membranes, and reduce PEP transport into the chloroplast. In this case, we would expect to observe little decline in total cellular PEP levels at high CO_2, but simply an altered partition of PEP.

Under low O_2 conditions isoprene emission typically increases. Lower levels of photorespiration could lead to an increased availability of energetic cofactors, increasing the capacity for isoprene

synthesis. In the absence of both CO_2 and O_2 ("pure N_2" conditions), isoprene emission is quickly abolished; when CO_2 and O_2 are resupplied, a transient overshoot in isoprene emission is often seen.

Light

Isoprene emission increases with light level, in a similar way to the light responses of photosynthesis (Fig. 1.6). Despite the close relationship between photosynthetic end products and the MEP pathway, the responses of photosynthesis and isoprene emission to environmental variables such as temperature and CO_2/O_2 are, as discussed above, distinct from each other. This decoupling of emission levels from photosynthesis is also seen for methylbutenol emissions from pine needles (Gray et al., 2005). An interesting question to ponder then is, why do the light responses of isoprene emission and photosynthesis appear so similar? I will revisit this question in Chapter 4.

Two hypotheses had been put forward to explain the light response of isoprene emission in the past: 1) changes in DMADP levels (Loreto and Sharkey, 1993; Rosenstiel et al., 2002; Rasulov et al., 2009b) and 2) changes in IspS activation state (Wildermuth and Fall, 1996; Fall and Wildermuth, 1998; Sasaki et al., 2005). While light-dependent mRNA accumulation was shown for IspS (Sasaki et al., 2005) and IspS transcript levels also appears to be under circadian regulation (Loivamäki et al., 2007; Wiberley et al., 2009), these are processes that typically take place on a longer time scale and cannot explain the instantaneous responses to light levels. Measurement of DMADP by non-aqueous fractionation (Rosenstiel et al., 2002) and post-

illumination isoprene emission (Rasulov et al., 2009b) both showed DMADP varies while calculated isoprene synthase stays roughly constant with varying light intensities. These suggest substrate-level control of isoprene emission.

The question then becomes: which are the upstream steps that control light-dependent changes in DMADP? More generally, are the energetic cofactors (ATP and NADPH equivalents) or the carbon supply (GAP and pyruvate) the limiting factors in light response? An important clue can be gained from studies of isoprene emission during light-dark transients. When light is turned off on an emitting leaf, isoprene emission rapidly decreases to almost zero within 8-10 minutes (phase I). Emission level usually then starts to increase again in the dark, peaks at 20-25 minutes before dropping off again to zero in approximately 45 minutes (phase II) (Monson et al., 1991). I hypothesized that this "post-illumination isoprene burst" represent a pool of MEP pathway intermediate metabolites that were trapped upon darkening. To test this hypothesis as well as to understand regulation in the MEP pathway, I measured levels of intermediate metabolites in the MEP pathway, and this project is detailed in Chapter 3.

Modeling of global isoprene emission in a changing environment

Global greenhouse gas levels and temperature are both predicted to rise over the next century (IPCC, 2007), and future emission levels of isoprene are likely to change in response to changes in these environmental variables. A large effort therefore has been put into constructing future

models of biogenic volatile organic carbon emissions, of which isoprene was a major constituent (Guenther et al., 1995; Guenther et al., 2006; Heald et al., 2009; Hewitt et al., 2011). Modeling of isoprene emissions in the early years often took a top-down approach, using mathematical formulas that produce the best fit to empirical measurements. While this approach is pragmatic and has a certain degree of prediction power, it clearly neglected the underlying mechanisms by which isoprene emission is driven by environmental variables. Understanding the biochemical and molecular basis of isoprene emissions is therefore important, as this allows us to build bottom-up models that better reflect the genuine responses of biochemical regulations of isoprene in plants to different environments. A better understanding of the regulation of isoprene emissions also opens up the possibility for engineering low-emitting species (Behnke et al., 2011), which in the long run may alleviate the impact of global climate change on BVOC emissions.

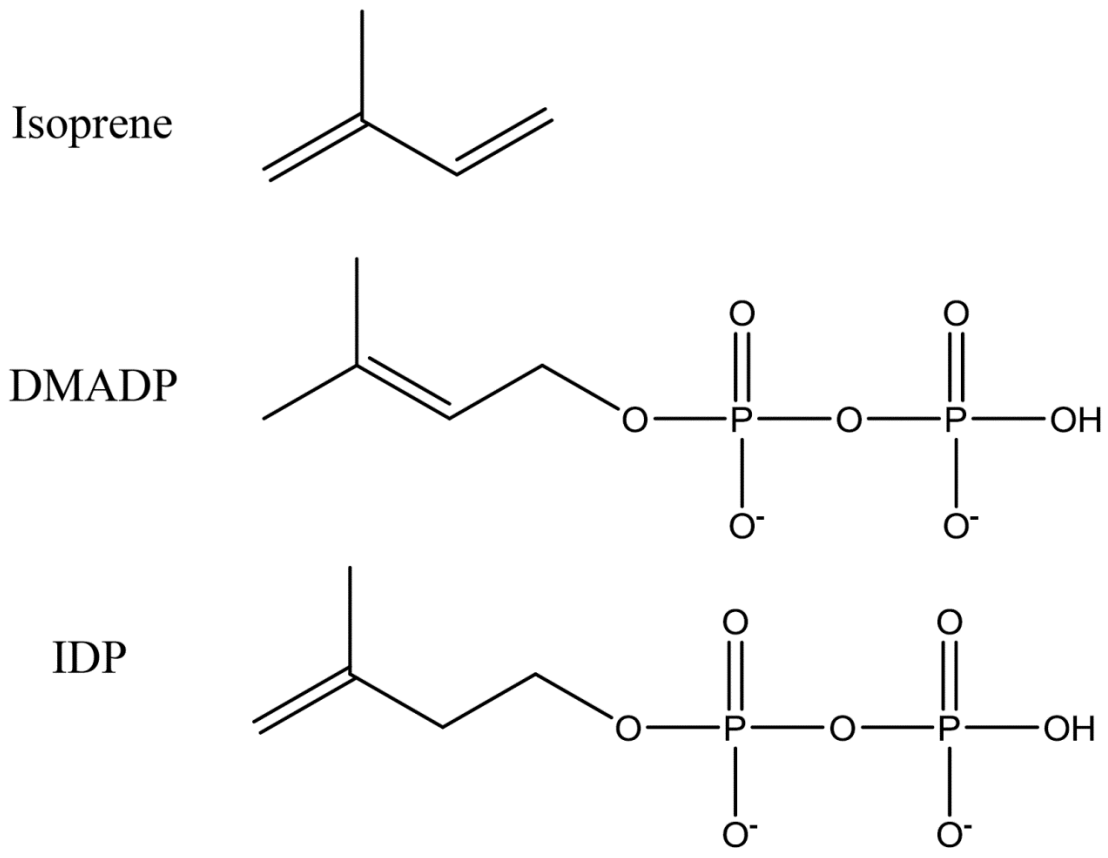

Figure 1.1 Isoprene and its activated forms in vivo (dimethylallyl diphosphate, DMADP and isopentenyl diphosphate, IDP).

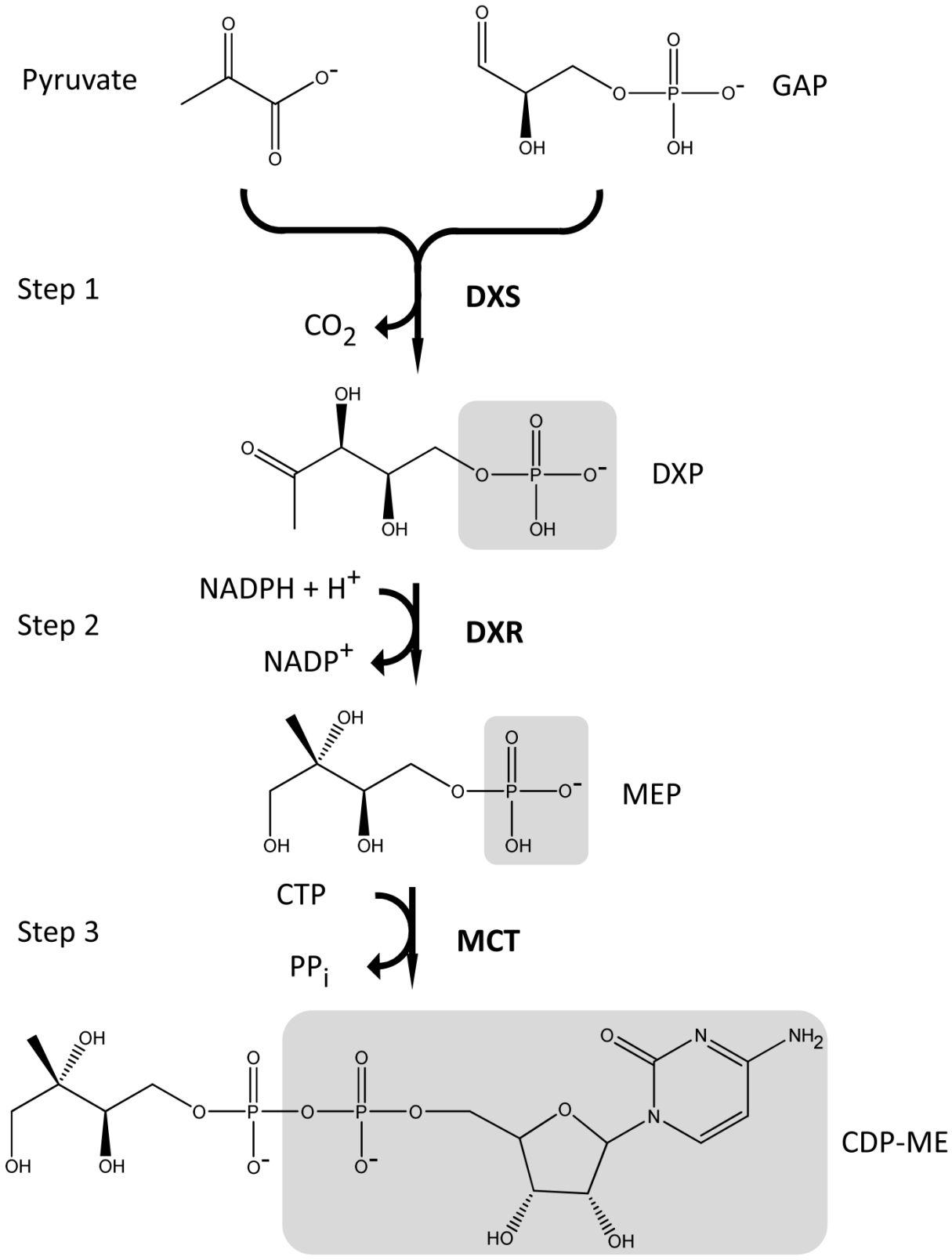

Figure 1.2 The MEP pathway in plants. Modified from Figure 1 of Li and Sharkey (2012 in press).

(Figure 1.2 continued)

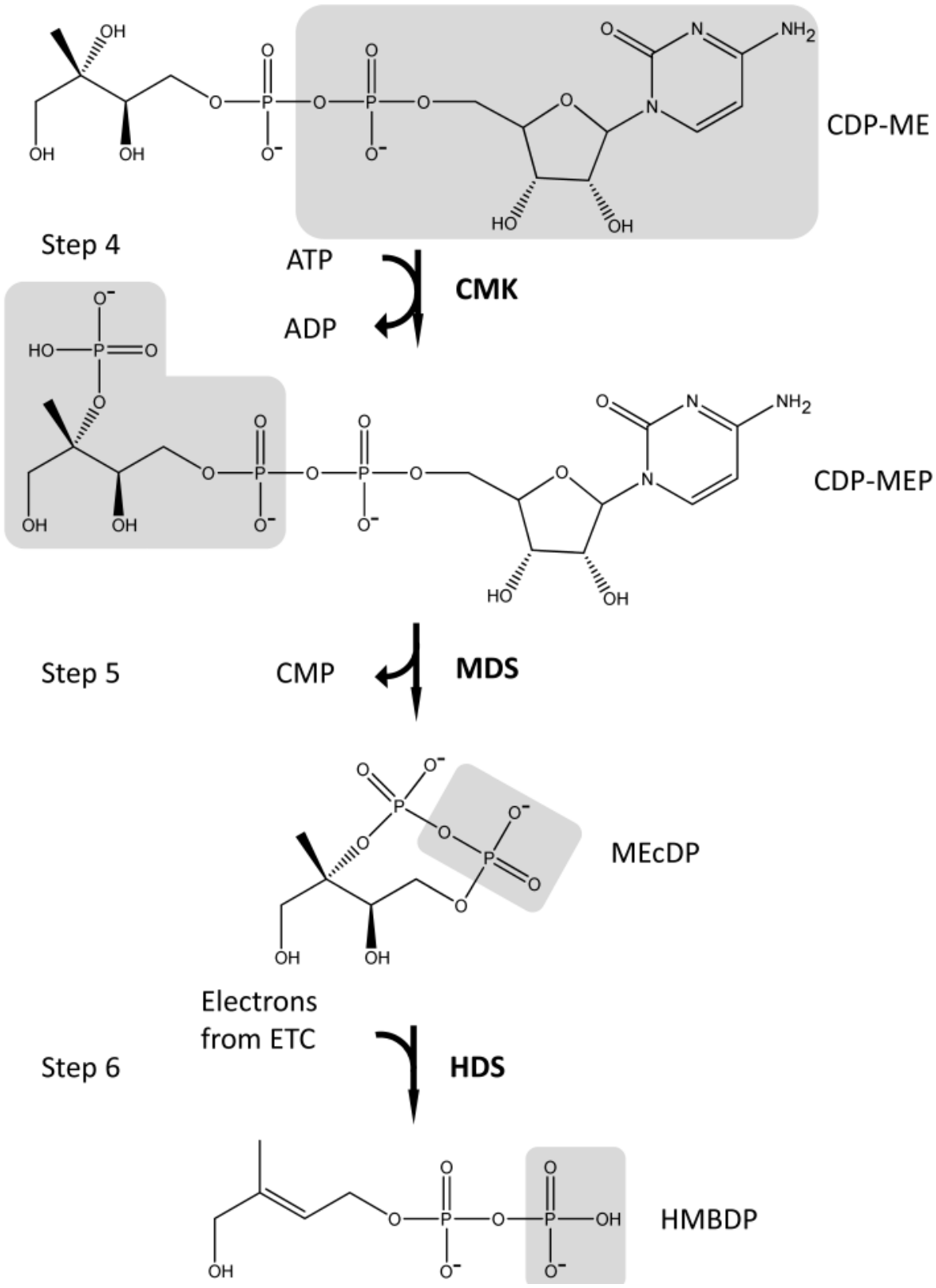

(Figure 1.2 continued)

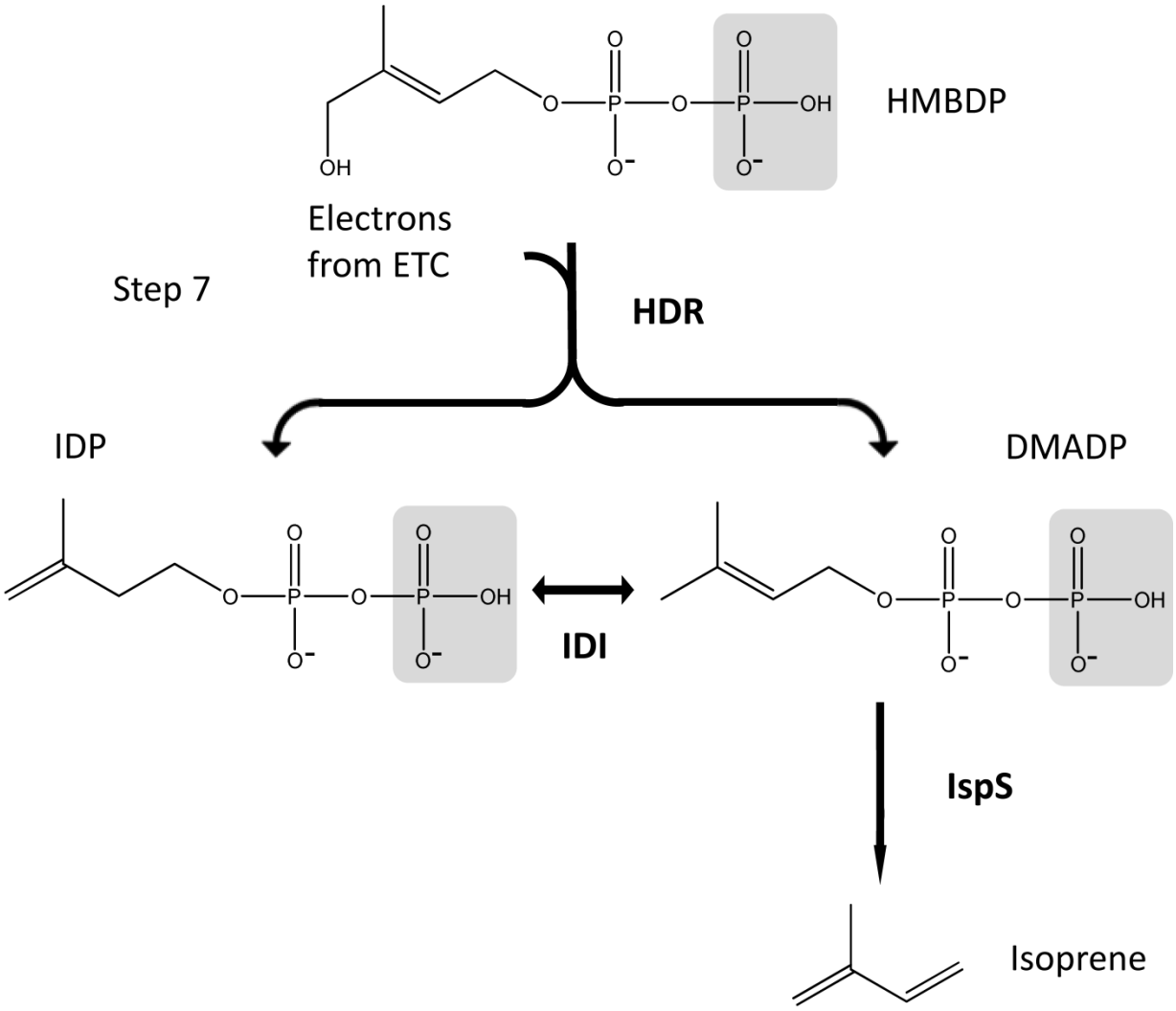

Table 1.1 Nomenclature of enzymes in the MEP pathway. Adapted from Table 1 in Phillips et al. (2008).

Step	Enzyme name	EC number	Abbreviation	Other abbreviations	*E. coli* gene	*A. thaliana* gene
1	1-deoxy-D-xylulose 5-phosphate synthase	2.2.1.7	DXS		*dxs*	*DXS* (At4g15560)
2	1-deoxy-D-xylulose 5-phosphate reductoisomerase	1.1.1.267	DXR		*ispC* (*yaeM , dxr*)	*DXR* (At5g62790)
3	2-*C*-methyl-D-erythritol 4-phosphate cytidylyltransferase	2.7.7.60	MCT	MECT, CMS	*ispD* (*ygbP*)	*MCT* (At2g02500)
4	4-(cytidine 5'-diphospho)-2-*C*-methyl-D-erythritol kinase	2.7.1.148	CMK	CMEK	*ispE* (*ychB*)	*CMK* (At2g26930)
5	2-*C*-methyl-D-erythritol 2,4-cyclodiphosphate synthase	4.6.1.12	MDS	MECPS, MECS, MCS	*ispF* (*ygbB*)	*MDS* (At1g63970
6	4-hydroxy-3-methylbut-2-enyl diphosphate synthase	1.17.7.1	HDS		*ispG* (*gcpE*)	*HDS* (At5g60600)
7	4-hydroxy-3-methylbut-2-enyl diphosphate reductase	1.17.1.2	HDR	IDS	*ispH* (*lytB*)	*HDR* (At4g34350)

Table 1.2 Kinetic parameters of MEP pathway enzymes reported in the literature up to date. If kinetic data from a plant enzyme are available then only data from the plant enzymes are used, otherwise values are derived from bacterial enzymes and are denoted by an asterisk. The median values of reported numbers for each enzyme are listed here. k_{cat}/K_m values are not calculated from K_m and k_{cat} in this table but were instead empirically determined as reported in the literature (if available). All numbers were rounded to two significant digits.

Enzymes	Substrate	K_m (mM)	k_{cat} (s^{-1})	k_{cat}/K_m ($mM^{-1}s^{-1}$)	References
DXS	GAP	0.12*	14*	14*	Kuzuyama et al., 2000; Hahn et al., 2001; Bailey et al., 2002; Eubanks and Poulter, 2003; Lee et al., 2007; Brammer and Meyers, 2009
	pyruvate	0.096*		-	
DXR	DXP	0.14	4.4	20*	Engprasert et al., 2005; Rohdich et al., 2006; Jawaid et al., 2009; Takenoya et al., 2010
	NADPH	0.056		-	
MCT	MEP	0.50	26	-	Rohdich et al., 2000
	CTP	0.11		-	
CMK	CDPME	0.14*	-	-	Bernal et al., 2005; Sgraja et al., 2008
	ATP	0.32*		-	
MDS	CDPMEP	0.48	2.5	-	Geist et al., 2010
HDS[1]	MEcDP	0.56	0.4*	-	Kollas et al., 2002; Seemann et al., 2005; Zepeck et al., 2005; Seemann et al., 2006
HDR[1]	HMBDP	0.31*	3.7	-	Altincicek et al., 2002; Gräwert et al., 2004
IDI	IDP	0.0057	0.69*	-	Spurgeon et al., 1984; Jones et al., 1985; Dogbo and Camara, 1987; Lützow and Beyer, 1988
IspS	DMADP	2.5	1.8	-	Silver and Fall, 1995; Wildermuth and Fall, 1996; Schnitzler et al., 2005; Wiberley et al., 2008; Rasulov et al., 2009a

[1]The HDS enzyme in *Arabidopsis* can obtain electrons directly from photosynthesis, possibly via ferredoxin (Seemann et al., 2006). HDR displays activity in presence of ferredoxin/ferredoxin-$NADP^+$/NADPH system but its electron source in planta is less clear (Rohdich et al., 2002). No kinetic data has been reported yet for the second substrate (the electron donor) for either of the two enzymes.

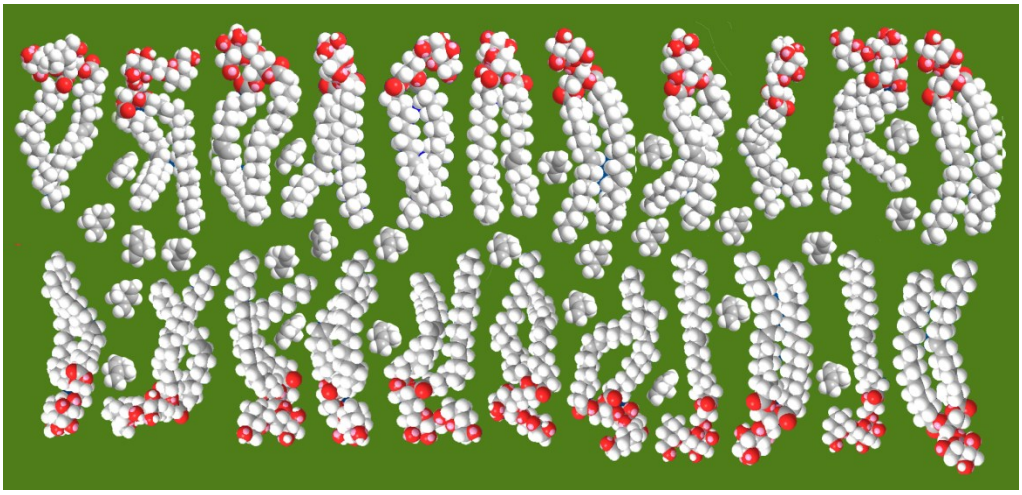

Figure 1.3 The thermotolerance model. A hypothetical biomembrane consisting entirely of digalactosyldiacylglycerol is depicted here. When isoprene passes through membranes, it could partition into the hydrophobic phase and stabilize membrane structures. For interpretation of the references to color in this and all other figures, the reader is referred to the electronic version of this dissertation.

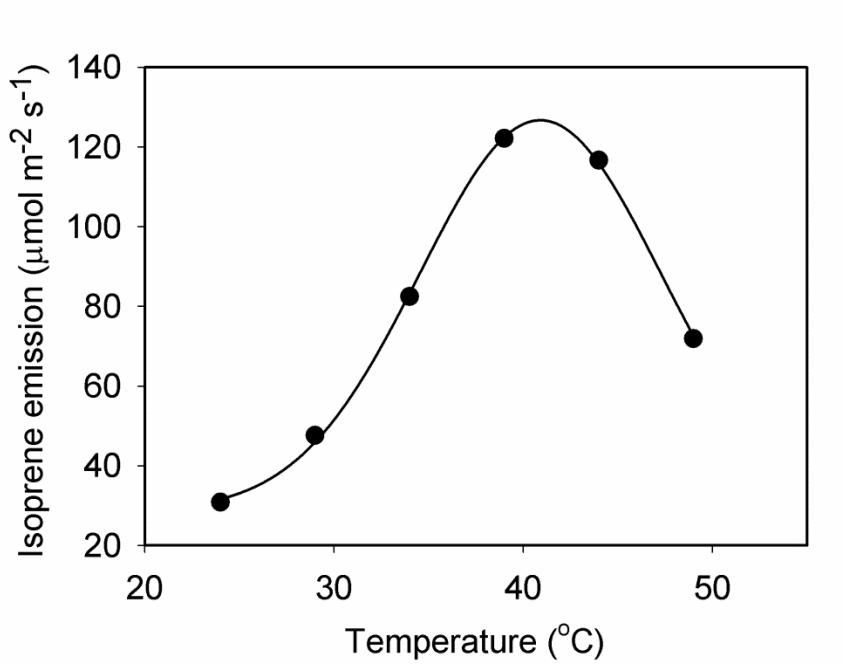

Figure 1.4 Temperature response of isoprene emission from a poplar leaf (Li Z. and Sharkey T.D., unpublished data). Photosynthetic photon flux density = 1000 μmol m^{-2} s^{-1}.

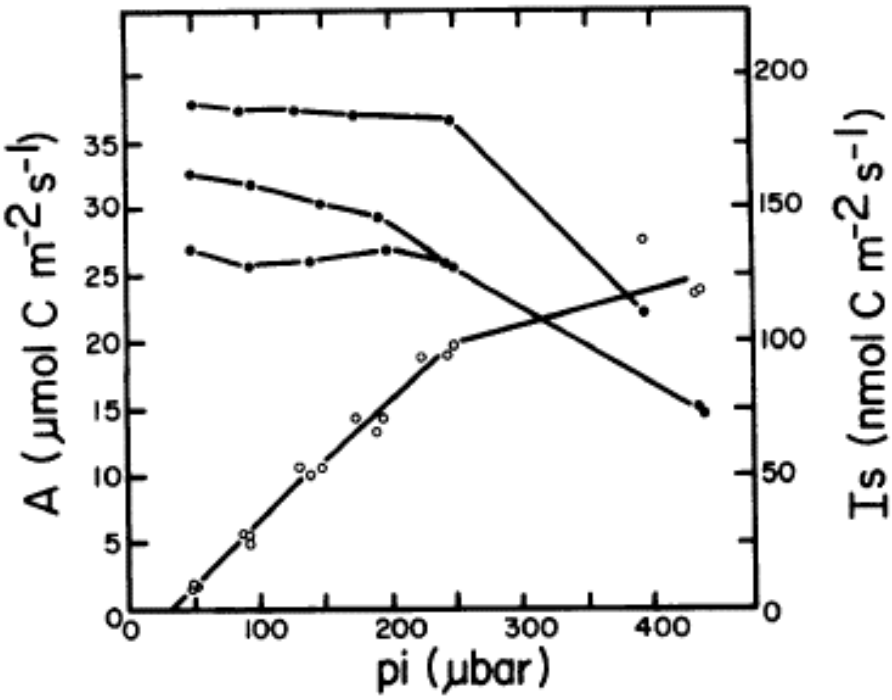

Figure 1.5 Response of isoprene emission and carbon assimilation to changes in CO_2. Open circles, assimilation; solid circles, isoprene emission. Figure is taken from Monson and Fall (1989).

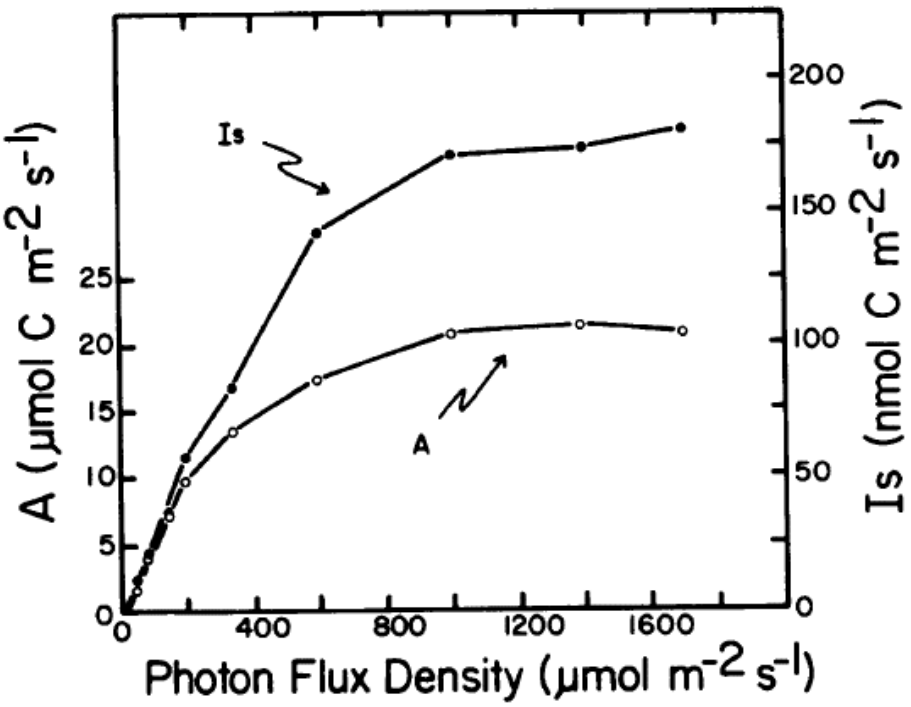

Figure 1.6 Response of isoprene emission and carbon assimilation to changes in light levels. Open circles, assimilation; solid circles, isoprene emission. Figure is taken from Monson and Fall (1989).

LITERATURE CITED

LITERATURE CITED

Altincicek B, Duin EC, Reichenberg A, Hedderich R, Kollas A-K, Hintz M, Wagner S, Wiesner J, Beck E, Jomaa H (2002) LytB protein catalyzes the terminal step of the 2-C-methyl-D-erythritol-4-phosphate pathway of isoprenoid biosynthesis. FEBS Letters **532:** 437-440

Bailey AM, Mahapatra S, Brennan PJ, Crick DC (2002) Identification, cloning, purification, and enzymatic characterization of *Mycobacterium tuberculosis* 1-deoxy-d-xylulose 5-phosphate synthase. Glycobiology **12:** 813-820

Behnke K, Ehlting B, Teuber M, Bauerfeind M, Louis S, Hansch R, Polle A, Bohlmann J, Schnitzler JP (2007) Transgenic, non-isoprene emitting poplars don't like it hot. Plant Journal **51:** 485-499

Behnke K, Grote R, Brüggemann N, Zimmer I, Zhou G, Elobeid M, Janz D, Polle A, Schnitzler J-P (2011) Isoprene emission-free poplars – a chance to reduce the impact from poplar plantations on the atmosphere. New Phytologist **194:** 70-82

Bernal C, Mendez E, Terencio J, Boronat A, Imperial S (2005) A spectrophotometric assay for the determination of 4-diphosphocytidyl-2-C-methyl-d-erythritol kinase activity. Analytical Biochemistry **340:** 245-251

Bohlmann J, Meyer-Gauen G, Croteau R (1998) Plant terpenoid synthases: Molecular biology and phylogenetic analysis. Proceedings of the National Academy of Sciences of the United States of America **95:** 4126-4133

Brammer LA, Meyers CF (2009) Revealing substrate promiscuity of 1-deoxy-d-xylulose 5-phosphate synthase. Organic Letters **11:** 4748-4751

Broers STJ (1994) Über die frühen stufen der biosynthese von isoprenoiden in *Escherichia coli*. PhD Thesis, ETH Zürich, Switzerland

Chameides WL, Lindsay RW, Richardson J, Kiang CS (1988) The role of biogenic hydrocarbons in urban photochemical smog: Atlanta as a case study. Science **241:** 1473-1475

Coleman MD, Isebrands JG, Dickson RE, Karnosky DF (1995) Photosynthetic productivity of aspen clones varying in sensitivity to tropospheric ozone. Tree Physiology **15:** 585

Connolly JD, Hill RA (1991) Dictionary of terpenoids, Vol 1. Chapman & Hall/CRC

De Moraes CM, Mescher MC, Tumlinson JH (2001) Caterpillar-induced nocturnal plant volatiles repel conspecific females. Nature **410:** 577-580

Delwiche CF, Sharkey TD (1993) Rapid appearance of ^{13}C in biogenic isoprene when $^{13}CO_2$ is fed to intact leaves. Plant, Cell and Environment **16:** 587-591

Dogbo O, Camara B (1987) Purification of isopentenyl pyrophosphate isomerase and geranylgeranyl pyrophosphate synthase from *Capsicum* chromoplasts by affinity chromatography. Biochimica et Biophysica Acta (BBA) - Lipids and Lipid Metabolism **920:** 140-148

Engprasert S, Taura F, Shoyama Y (2005) Molecular cloning, expression and characterization of recombinant 1-deoxy-d-xylulose-5-phosphate reductoisomerase from *Coleus forskohlii* Briq. Plant Science **169:** 287-294

Eubanks LM, Poulter CD (2003) *Rhodobacter capsulatus* 1-deoxy-d-xylulose 5-phosphate synthase: steady-state kinetics and substrate binding. Biochemistry **42:** 1140-1149

Fall R, Wildermuth MC (1998) Isoprene synthase: From biochemical mechanism to emission algorithm. Journal of Geophysical Research [Atmospheres] **103:** 25599-25609

Farquhar GD, Caemmerer S, Berry JA (1980) A biochemical model of photosynthetic CO_2 assimilation in leaves of C_3 species. Planta **149:** 78-90

Fehsenfeld F, Calvert J, Fall R, Goldan P, Guenther AB, Hewitt CN, Lamb B, Liu S, Trainer M, Westberg H (1992) Emissions of volatile organic compounds from vegetation and the implications for atmospheric chemistry: Natural sources of acid precursors, neutralizing compounds, and oxidants. Global Biogeochemical Cycles **6:** 389-430

Geist JG, Lauw S, Illarionova V, Illarionov B, Fischer M, Gräwert T, Rohdich F, Eisenreich W, Kaiser J, Groll M, Scheurer C, Wittlin S, Alonso-Gómez JL, Schweizer WB, Bacher A, Diederich F (2010) Thiazolopyrimidine inhibitors of 2-methylerythritol 2,4-cyclodiphosphate synthase (IspF) from *Mycobacterium tuberculosis* and *Plasmodium falciparum*. ChemMedChem **5:** 1092-1101

Gräwert T, Kaiser J, Zepeck F, Laupitz R, Hecht S, Amslinger S, Schramek N, Schleicher E, Weber S, Haslbeck M, Buchner J, Rieder C, Arigoni D, Bacher A, Eisenreich W, Rohdich F (2004) IspH protein of *Escherichia coli*: Studies on iron-sulfur cluster implementation and catalysis. Journal of the American Chemical Society **126:** 12847-12855

Gray DW, Goldstein AH, Lerdau MT (2005) The influence of light environment on photosynthesis and basal methylbutenol emission from *Pinus ponderosa*. Plant, Cell & Environment **28:** 1463-1474

Guenther A, Hewitt CN, Erickson D, Fall R, Geron C, Graedel T, Harley P, Klinger L, Lerdau M, McKay WA, Pierce T, Scholes B, Steinbrecher R, Tallamraju R, Taylor J, Zimmerman P (1995) A global model of natural volatile organic compound emissions. Journal of Geophysical Research **100:** 8873-8892

Guenther A, Karl T, Harley P, Wiedinmyer C, Palmer PI, Geron C (2006) Estimates of global terrestrial isoprene emissions using MEGAN (Model of Emissions of Gases and Aerosols from Nature). Atmospheric Chemistry and Physics Discussions **6:** 107–173

Hahn FM, Eubanks LM, Testa CA, Blagg BSJ, Baker JA, Poulter CD (2001) 1-deoxy-d-xylulose 5-phosphate synthase, the gene product of open reading frame (ORF) 2816 and ORF 2895 in *Rhodobacter capsulatus*. Journal of Bacteriology **183:** 1-11

Harley P, Fridd-stroud V, Greenberg J, Guenther A, Vasconcellos P (1998) Emission of 2-methyl-3-buten-2-ol by pines: a potentially large natural source of reactive carbon to the atmosphere. Journal of Geophysical Research **103:** 25479-25486

Heald CL, Wilkinson MJ, Monson RK, Alo CA, Wang G, Guenther A (2009) Response of isoprene emission to ambient CO_2 changes and implications for global budgets. Global Change Biology **15:** 1127-1140

Heck WW, Taylor OC, Adams R, Bingham G, Miller J, Preston E, Weinstein L (1982) Assessment of crop loss from ozone. Journal of the Air Pollution Control Association **32:** 353-361

Hewitt CN, Ashworth K, Boynard A, Guenther A, Langford B, MacKenzie AR, Misztal PK, Nemitz E, Owen SM, Possell M, Pugh TAM, Ryan AC, Wild O (2011) Ground-level ozone influenced by circadian control of isoprene emissions. Nature Geoscience **4:** 671-674

IPCC (2007) Climate Change 2007: Synthesis Report, Summary for policy makers. *In* IPCC, ed, pp 1-22

Jacob DJ (1999) Introduction to Atmospheric Chemistry. *In*. Princeton University Press, Princeton, pp 1-267

Jardine KJ, Monson RK, Abrell L, Saleska SR, Arneth A, Jardine A, Ishida FY, Serrano AMY, Artaxo P, Karl T, Fares S, Goldstein A, Loreto F, Huxman T (2012) Within-plant isoprene oxidation confirmed by direct emissions of oxidation products methyl vinyl ketone and methacrolein. Global Change Biology **18:** 973-984

Jawaid S, Seidle H, Zhou W, Abdirahman H, Abadeer M, Hix JH, van Hoek ML, Couch RD (2009) Kinetic characterization and phosphoregulation of the *Francisella tularensis* 1-deoxy-D-xylulose 5-phosphate reductoisomerase (MEP synthase). PLoS ONE **4:** e8288

Jones BL, Porter JW, John H. Law HCR (1985) [26] Enzymatic synthesis of phytoene. *In* Methods in Enzymology, Vol 110. Academic Press, pp 209-220

Kai H, Hirashima K, Matsuda O, Ikegami H, Winkelmann T, Nakahara T, Iba K (2012) Thermotolerant cyclamen with reduced acrolein and methyl vinyl ketone. Journal of Experimental Botany**:** DOI: 10.1093/jxb/ers1110

Kappers IF, Aharoni A, van Herpen TWJM, Luckerhoff LLP, Dicke M, Bouwmeester HJ (2005) Genetic engineering of terpenoid metabolism attracts bodyguards to arabidopsis. Science **309:** 2070-2072

Karl TK, Fall RF, Rosenstiel TR, Prazeller PP, Larsen BL, Seufert GS, Lindinger WL (2002) On-line analysis of the $^{13}CO_2$ labeling of leaf isoprene suggests multiple subcellular origins of isoprene precursors. Planta **215:** 894-905

Kessler A, Baldwin IT (2001) Defensive function of herbivore-induced plant volatile emissions in nature. Science **291:** 2141-2144

Kiendler-Scharr A, Wildt J, Dal Maso M, Hohaus T, Kleist E, Mentel TF, Tillmann R, Uerlings R, Schurr U, Wahner A (2009) New particle formation in forests inhibited by isoprene emissions. Nature **461:** 381-384

Kiirats O, Cruz JA, Edwards GE, Kramer DM (2009) Feedback limitation of photosynthesis at high CO_2 acts by modulating the activity of the chloroplast ATP synthase. Functional Plant Biology **36:** 893-901

Kollas A-K, Duin EC, Eberl M, Altincicek B, Hintz M, Reichenberg A, Henschker D, Henne A, Steinbrecher I, Ostrovsky DN, Hedderich R, Beck E, Jomaa H, Wiesner J (2002) Functional characterization of GcpE, an essential enzyme of the non-mevalonate pathway of isoprenoid biosynthesis. FEBS Letters **532:** 432-436

Kuzuyama T, Takagi M, Takahashi S, Seto H (2000) Cloning and characterization of 1-deoxy-d-xylulose 5-phosphate synthase from *Streptomyces sp.* strain CL190, which uses both the mevalonate and nonmevalonate pathways for isopentenyl diphosphate biosynthesis. Journal of Bacteriology **182:** 891-897

Laothawornkitkul J, Paul ND, Vickers CE, Possell M, Taylor JE, Mullineaux PM, Hewitt CN (2008) Isoprene emissions influence herbivore feeding decisions. Plant, Cell and Environment **31:** 1410-1415

Lee J-K, Oh D-K, Kim S-Y (2007) Cloning and characterization of the *dxs* gene, encoding 1-deoxy-d-xylulose 5-phosphate synthase from *Agrobacterium tumefaciens*, and its overexpression in *Agrobacterium tumefaciens*. Journal of Biotechnology **128:** 555-566

Lehning A, Zimmer I, Steinbrecher R, Bruggemann N, Schnitzler JP (1999) Isoprene synthase activity and its relation to isoprene emission in *Quercus robur* L. leaves. Plant, Cell and Environment **22:** 495-504

Lippmann M (1989) Health effects of ozone: a critical review. Journal of the Air Pollution Control Association **39:** 672

Logan BA, Monson RK, Potosnak MJ (2000) Biochemistry and physiology of foliar isoprene production. Trends in Plant Science **5:** 477-481

Loivamäki M, Louis S, Cinege G, Zimmer I, Fischbach RJ, Schnitzler J-P (2007) Circadian rhythms of isoprene biosynthesis in grey poplar leaves. Plant Physiology **143:** 540-551

Loivamäki M, Mumm R, Dicke M, Schnitzler JP (2008) Isoprene interferes with the attraction of bodyguards by herbaceous plants. Proceedings of the National Academy of Sciences of the United States of America **105:** 17430-17435

Loreto F, Mannozzi M, Maris C, Nascetti P, Ferranti F, Pasqualini S (2001) Ozone quenching properties of isoprene and its antioxidant role in leaves. Plant Physiology **126:** 993-1000

Loreto F, Pinelli P, Brancaleoni E, Ciccioli P (2004) ^{13}C labelling reveals chloroplastic and extra-chloroplastic pools of dimethylallyl piroposphate and their contribution to isoprene formation. Plant Physiology **135:** 1903-1907

Loreto F, Sharkey TD (1990) A gas-exchange study of photosynthesis and isoprene emission in *Quercus rubra* L. Planta 182: 523-531

Loreto F, Sharkey TD (1993) On the relationship between isoprene emission and photosynthetic metabolites under different environmental conditions. Planta **189:** 420-424

Loreto F, Velikova V (2001) Isoprene produced by leaves protects the photosynthetic apparatus against ozone damage, quenches ozone products, and reduces lipid peroxidation of cellular membranes. Plant Physiology **127:** 1781-1787

Lützow M, Beyer P (1988) The isopentenyl-diphosphate Delta-isomerase and its relation to the phytoene synthase complex in daffodil chromoplasts. Biochimica et Biophysica Acta (BBA) - Lipids and Lipid Metabolism **959:** 118-126

McKay SAB, Hunter WL, Godard K-A, Wang SX, Martin DM, Bohlmann Jr, Plant AL (2003) Insect attack and wounding induce traumatic resin duct development and gene expression of (-)-pinene synthase in Sitka spruce. Plant Physiology 133: 368-378

McConnell R, Berhane K, Gilliland F, London SJ, Islam T, Gauderman WJ, Avol E, Margolis HG, Peters JM (2002) Asthma in exercising children exposed to ozone: a cohort study. The Lancet **359:** 386-391

Melnick RL, Sills RC, Roycroft JH, Chou BJ, Ragan HA, Miller RA (1994) Isoprene, an endogenous hydrocarbon and industrial chemical, induces multiple organ neoplasia in rodents after 26 weeks of inhalation exposure. Cancer Research **54:** 5333-5339

Monson RK, Fall R (1989) Isoprene emission from aspen leaves: influence of environment and relation to photosynthesis and photorespiration. Plant Physiology **90:** 267-274

Monson RK, Hills AJ, Zimmerman PR, Fall RR (1991) Studies of the relationship between isoprene emission rate and CO_2 or photon-flux density using a real-time isoprene analyser. Plant, Cell and Environment **14:** 517-523

Monson RK, Jaeger CH, Adams WW, Driggers EM, Silver GM, Fall R (1992) Relationships among isoprene emission rate, photosynthesis, and isoprene synthase activity as influenced by temperature. Plant Physiology **98:** 1175-1180

Phillips MA, León P, Boronat A, Rodríguez-Concepción M (2008) The plastidial MEP pathway: unified nomenclature and resources. Trends in Plant Science **13:** 619-623

Poisson N, Kanakidou M, Crutzen PJ (2000) Impact of non-methane hydrocarbons on tropospheric chemistry and the oxidizing power of the global troposphere: 3-dimensional modelling results. Journal of Atmospheric Chemistry **36:** 157-230

Rasmann S, Kollner TG, Degenhardt J, Hiltpold I, Toepfer S, Kuhlmann U, Gershenzon J, Turlings TCJ (2005) Recruitment of entomopathogenic nematodes by insect-damaged maize roots. Nature **434:** 732-737

Rasulov B, Copolovici L, Laisk A, Niinemets Ü (2009a) Postillumination isoprene emission: in vivo measurements of dimethylallyldiphosphate pool size and isoprene synthase kinetics in aspen leaves. Plant Physiology **149:** 1609-1618

Rasulov B, Hüve K, Bichele I, Laisk A, Niinemets Ü (2010) Temperature response of isoprene emission in vivo reflects a combined effect of substrate limitations and isoprene synthase activity: a kinetic analysis. Plant Physiology **154:** 1558-1570

Rasulov B, Hüve K, Valbe M, Laisk A, Niinemets Ü (2009b) Evidence that light, carbon dioxide, and oxygen dependencies of leaf isoprene emission are driven by energy status in hybrid aspen. Plant Physiology **151:** 448-460

Rohdich F, Hecht S, Gärtner K, Adam P, Krieger C, Amslinger S, Arigoni D, Bacher A, Eisenreich W (2002) Studies on the nonmevalonate terpene biosynthetic pathway: metabolic role of IspH (LytB) protein. Proceedings of the National Academy of Sciences of the United States of America **99:** 1158-1163

Rohdich F, Lauw S, Kaiser J, Feicht R, Köhler P, Bacher A, Eisenreich W (2006) Isoprenoid biosynthesis in plants – 2C-methyl-d-erythritol-4-phosphate synthase (IspC protein) of *Arabidopsis thaliana*. FEBS Journal **273:** 4446-4458

Rohdich F, Wungsintaweekul J, Eisenreich W, Richter G, Schuhr CA, Hecht S, Zenk MH, Bacher A (2000) Biosynthesis of terpenoids: 4-diphosphocytidyl-2C-methyl-d-erythritol synthase of *Arabidopsis thaliana*. Proceedings of the National Academy of Sciences of the United States of America **97:** 6451-6456

Rosenstiel TN, Fisher AJ, Fall R, Monson RK (2002) Differential accumulation of dimethylallyl diphosphate in leaves and needles of isoprene- and methylbutenol-emitting and nonemitting species. Plant Physiology **129:** 1276-1284

Rosenstiel TN, Potosnak MJ, Griffin KL, Fall R, Monson RK (2003) Increased CO_2 uncouples growth from isoprene emission in an agriforest ecosystem. Nature **421:** 256-259

Sasaki K, Ohara K, Yazaki K (2005) Gene expression and characterization of isoprene synthase from *Populus alba*. FEBS Letters **579:** 2514-2518

Sasaki K, Saito T, Lamsa M, Oksman-Caldentey KM, Suzuki M, Ohyama K, Muranaka T, Ohara K, Yazaki K (2007) Plants utilize isoprene emission as a thermotolerance mechanism. Plant and Cell Physiology **48:** 1254

Schnitzler JP, Zimmer I, Bachl A, Arend M, Fromm J, Fischbach RJ (2005) Biochemical properties of isoprene synthase in poplar (*Populus* × *canescens*). Planta **222:** 777-786

Seemann M, Tse Sum Bui B, Wolff M, Miginiac-Maslow M, Rohmer M (2006) Isoprenoid biosynthesis in plant chloroplasts via the MEP pathway: direct thylakoid/ferredoxin-dependent photoreduction of GcpE/IspG. FEBS Letters **580:** 1547-1552

Seemann M, Wegner P, Schünemann V, Bui BTS, Wolff M, Marquet A, Trautwein AX, Rohmer M (2005) Isoprenoid biosynthesis in chloroplasts via the methylerythritol phosphate pathway: the (E)-4-hydroxy-3-methylbut-2-enyl diphosphate synthase (GcpE) from *Arabidopsis thaliana* is a [4Fe-4S] protein. Journal of Biological Inorganic Chemistry **10:** 131-137

Sgraja T, Alphey MS, Ghilagaber S, Marquez R, Robertson MN, Hemmings JL, Lauw S, Rohdich F, Bacher A, Eisenreich W, Illarionova V, Hunter WN (2008) Characterization of Aquifex aeolicus 4-diphosphocytidyl-2C-methyl-d-erythritol kinase – ligand recognition in a template for antimicrobial drug discovery. FEBS Journal **275:** 2779-2794

Sharkey TD (1985) Photosynthesis in intact leaves of C_3 plants: Physics, physiology and rate limitations. The Botanical Review **51:** 53-105

Sharkey TD, Chen X, Yeh S (2001) Isoprene increases thermotolerance of fosmidomycin-fed leaves. Plant Physiology **125:** 2001-2006

Sharkey TD, Schrader SM (2006) High temperature stress. In KVM Rao, AS Raghavendra, K Reddy, eds, Phyiology and Molecular Biology of Stress Tolerance in Plants. Springer, The Netherlands, pp 101-129

Sharkey TD, Wiberley AE, Donohue AR (2008) Isoprene emission from plants: why and how. Annals of Botany **101:** 5-18

Silver GM, Fall R (1995) Characterization of aspen isoprene synthase, an enzyme responsible for leaf isoprene emission to the atmosphere. Journal of Biological Chemistry **270:** 13010

Singsaas EL, Sharkey TD (2000) The effects of high temperature on isoprene synthesis in oak leaves. Plant, Cell and Environment **23:** 751-757

Siwko ME, Marrink SJ, de Vries AH, Kozubek A, Schoot Uiterkamp AJM, Mark AE (2007) Does isoprene protect plant membranes from thermal shock? A molecular dynamics study. BBA-Biomembranes **1768:** 198-206

Spurgeon SL, Sathyamoorthy N, Porter JW (1984) Isopentenyl pyrophosphate isomerase and prenyltransferase from tomato fruit plastids. Archives of Biochemistry and Biophysics **230:** 446-454

Takenoya M, Ohtaki A, Noguchi K, Endo K, Sasaki Y, Ohsawa K, Yajima S, Yohda M (2010) Crystal structure of 1-deoxy-d-xylulose 5-phosphate reductoisomerase from the hyperthermophile *Thermotoga maritima* for insights into the coordination of conformational changes and an inhibitor binding. Journal of Structural Biology **170:** 532-539

Trainer M, Williams EJ, Parrish DD, Buhr MP, Allwine EJ, Westberg HH, Fehsenfeld FC, Liu SC (1987) Models and observations of the impact of natural hydrocarbons on rural ozone. Nature **329:** 705-707

Turlings TCJ, Tumlinson JH, Lewis WJ (1990) Exploitation of herbivore-induced plant odors by host-seeking parasitic wasps. Science **250:** 1251-1253

Velikova V, Fares S, Loreto F (2008) Isoprene and nitric oxide reduce damages in leaves exposed to oxidative stress. Plant, Cell and Environment **31:** 1882 - 1894

Velikova V, Loreto F (2005) On the relationship between isoprene emission and thermotolerance in *Phragmites australis* leaves exposed to high temperatures and during the recovery from a heat stress. Plant Cell and Environment **28:** 318

Velikova V, Várkonyi Z, Szabó M, Maslenkova L, Nogues I, Kovács L, Peeva V, Busheva M, Garab G, Sharkey TD, Loreto F (2011) Increased thermostability of thylakoid membranes in isoprene-emitting leaves probed with three biophysical techniques. Plant Physiology **157:** 905-916

Vickers CE, Possell M, Cojocariu CI, Velikova VB, Laothawornkitkul J, Ryan A, Mullineaux PM, Nicholas Hewitt C (2009) Isoprene synthesis protects transgenic tobacco plants from oxidative stress. Plant, Cell and Environment **32:** 520-531

Went FW (1960) Blue hazes in the atmosphere. Nature **187:** 641-643

Wiberley AE, Donohue AR, Meier ME, Westphal MM, Sharkey TD (2008) Regulation of isoprene emission in *Populus trichocarpa* leaves subjected to changing growth temperature. Plant Cell and Environment **31:** 258-267

Wiberley AE, Donohue AR, Westphal MM, Sharkey TD (2009) Regulation of isoprene emission from poplar leaves throughout a day. Plant Cell and Environment **32:** 939-947

Wildermuth MC, Fall R (1996) Light-dependent isoprene emission - characterization of a thylakoid-bound isoprene synthase in *Salix discolor* chloroplasts. Plant Physiology **112:** 171-182

Wildermuth MC, Fall R (1998) Biochemical characterization of stromal and thylakoid-bound isoforms of isoprene synthase in willow leaves. Plant Physiology **116:** 1111-1123

Wolfertz M, Sharkey TD, Boland W, Kuhnemann F (2004) Rapid regulation of the methylerythritol 4-phosphate pathway during isoprene synthesis. Plant Physiology **135:** 1939-1945

Wolfertz M, Sharkey TD, Boland W, Kuhnemann F, Yeh S, Weise SE (2003) Biochemical regulation of isoprene emission. Plant, Cell and Environment **26:** 1357-1364

Zepeck F, Gräwert T, Kaiser J, Schramek N, Eisenreich W, Bacher A, Rohdich F (2005) Biosynthesis of isoprenoids. Purification and properties of IspG protein from *Escherichia coli*. Journal of Organic Chemistry **70:** 9168-9174

CHAPTER 2

Effects of Temperature on Post-illumination Isoprene Emission

Research work described in this chapter was originally published in Plant Physiology.
Li Z, Ratliff EA, Sharkey TD (2011) Effect of temperature on post-illumination isoprene emission in oak and poplar. Plant Physiology **155**: 1037-1046 © 2011 American Society of Plant Biologists http://www.plantphysiol.org/

Abstract

Isoprene emission from broadleaf trees is highly temperature dependent, accounts for much of the hydrocarbon emission from plants, and has a profound effect on atmospheric chemistry. Here I studied temperature response of post-illumination isoprene emission in oak (*Quercus robur*) and poplar (*Populus deltoides*) leaves in order to understand the regulation of isoprene emission as affected by temperature. Upon darkening a leaf, isoprene emission fell nearly to zero but then increased for several minutes before falling back to nearly zero (a "burst" of isoprene). Time of appearance of this burst was highly temperature dependent, occurring sooner at higher temperatures. I hypothesize that this burst represents an intermediate pool of metabolites, probably early metabolites in the methylerythritol 4-phosphate pathway, accumulated upstream of dimethylallyl diphosphate (DMADP). The amount of this early metabolite(s) was on average 2.9 times the amount of plastidic DMADP. DMADP increased with temperature up until 35°C before starting to decrease; in contrast, the isoprene synthase rate constant increased up to 40°C, the highest temperature it could be assessed. Temperature responses of early metabolites were similar with those of DMADP. During a rapid temperature switch from 30°C to 40°C, isoprene emission increased transiently. It was found that an increase in isoprene synthase activity is primarily responsible for this transient increase in emission levels, while DMADP level stayed constant during the switch. One hour after switching to 40°C the amount of DMADP fell but the rate constant for isoprene synthase remained constant indicating that the high temperature fall off in isoprene emission results from a reduction in the supply of DMADP rather than changes in isoprene synthase activity.

Introduction

It has long been known that isoprene emission from plants is highly temperature dependent (Sanadze and Kalandaze, 1966; Tingey et al., 1979; 1987; Monson et al., 1992). Isoprene emission increases up to 35 to 40°C even when carbon assimilation is declining. This uncoupling of emission from photosynthesis contributed to the hypothesis that isoprene may protect plants against heat stress (Sharkey and Singsaas, 1995; Singsaas et al., 1997). The rate of isoprene emission declines above its optimum but the optimum temperature is significantly affected by the protocol of isoprene emission measurement (Singsaas et al., 1999; Singsaas, 2000). If measurements are made quickly the optimum is much higher than if the measurements are made slowly. This occurs because isoprene emission above 35°C is unstable, increasing when the temperature is first raised but then falling back after 10 to 20 min at the higher temperature. A mechanistic understanding of the regulation of isoprene emission with changes in temperature is important to accurately model isoprene output in future environments where global mean temperature is predicted to rise.

Whether isoprene emission is primarily controlled by enzyme activity or substrate (dimethylallyl diphosphate, DMADP) availability has been under debate. While it was originally proposed that changes in isoprene synthase (IspS) activity accounts for changes in emission levels (Fall and Wildermuth, 1998; Lehning et al., 1999), recent evidence suggests that instead, variations in substrate levels may be responsible (Schnitzler et al., 2005; Rasulov et al., 2009b). In vitro K_m values determined for IspS are in the mM range; these unusually high values indicate changes in substrate levels could affect the reaction rate (Wildermuth and Fall, 1996; Schnitzler et al., 2005).

A recently developed method using post-illumination isoprene emission to measure DMADP levels, in particular, contributed to the understanding of regulation of isoprene emission (Rasulov et al., 2009). The principle of this method is similar to in vivo measurement of ribulose 1,5-bisphosphate (RuBP) by post-illumination CO_2 assimilation (Laisk et al., 1984; Ruuska et al., 1998). Assuming the MEP pathway is rapidly shut off by darkness while isoprene synthase remains active, total isoprene released during darkness stoichiometrically approximates plastidic DMADP levels. Using this non-intrusive method it has been reported that in poplar (*Populus* spp.) trees, dependence of isoprene emission on light, carbon dioxide, and oxygen is regulated by changes in substrate levels, and temperature response reflects mixed regulations on both enzyme activities and substrate levels (Rasulov et al., 2009b; 2010).

In this study the effects of temperature on post-illumination isoprene emission in oak (*Quercus robur*) and poplar (*Populus deltoides*) leaves were investigated. Following the initial decline in isoprene emission rate upon darkening of the leaf a burst of isoprene emission was observed. The time of appearance of this burst is highly temperature-dependent, and its size was markedly larger than the DMADP peak. Assuming this post-illumination burst represents a separate pool of MEP pathway metabolites, I measured isoprene emission and substrate levels under different temperatures in an effort to understand temperature regulation of MEP pathway metabolites and gain insight into the nature of the post-illumination burst. Isoprene emission and metabolite levels as determined by post-illumination isoprene emission during a rapid temperature switch from 30°C to 40°C were also measured and the findings discussed.

Results

Characteristics of post-illumination isoprene emission

Post-illumination isoprene emissions in oak leaves at different temperatures were measured following procedures of Rasulov et al. (2009). At a leaf temperature of 30°C, isoprene emission initially dropped to nearly zero after light was turned off (Fig. 2.1a). This initial decline was exponential, consistent with one homogenous pool being converted to isoprene (Fig. 2.1a, inset). The rate of isoprene emission rose again in darkness and then slowly dropped and leveled off in 30 min. When integrated and corrected for system clearing, this showed up as a second peak apart from the classic DMADP peak on the post-illumination emission trace (Fig. 2.1b). It was hypothesized that this peak represents an intermediate pool of metabolites that accumulated upstream of DMADP, possibly in the methylerythritol 4-phosphate (MEP) pathway. This pool is hereafter referred to as the "early metabolites". This phenomenon was also observed in poplar.

Time of appearance of this burst was highly temperature dependent in both oak and poplar (Fig. 2.2). The peak appeared sooner at higher temperatures, and at temperatures >40°C it appeared to merge with the initial decline in isoprene emission. This peak was observed even at the lowest temperature used, 25°C. At this temperature, the peak took >15 min before appearing and occurred over a much longer time (>30 min) than at higher temperatures.

Temperature response of isoprene emission, DMADP and early metabolites

Isoprene emission in oak leaves increased with temperature until 35°C – 40°C, at which point it started to decrease (Fig. 2.3a). Carbon assimilation decreased with temperature at temperatures above 30°C, and became negative at 50°C. The carbon cost of isoprene emission as a percentage of net assimilation increased exponentially with temperature, up to 20% at 45°C (Fig. 2.3b, inset). This percentage rose to more than 100% at 50°C as net assimilation had become negative at this temperature.

Plastidic DMADP levels increased with temperature between 25°C and 35°C before decreasing at 40°C (Fig. 2.3c). DMADP and early metabolite levels at temperatures >40°C could not be obtained since I could not separate the two peaks at higher temperatures (Fig. 2.2a). DMADP levels at 35°C were approximately 30% more than at 25°C. The variations, however, were not significant due to large standard errors ($P = 0.137$, one-way repeated measures ANOVA). The calculated rate constant for isoprene synthase (isoprene emission rate divided by amount of DMADP) increased steadily during 25°C - 40°C with an Arrhenius activation energy (E_a) of 50.4 kJ mol^{-1} (Fig. 2.3d). The early metabolites showed a similar temperature response curve as DMADP, increasing with temperature between 25 and 35°C and decreasing at 40°C (Fig. 2.3e). Pools of early metabolites were 1.7 – 3.6 times the size of DMADP pools, and this ratio increased with temperature (Fig. 2.3e, inset). The early metabolites pool is on average 2.9 times the size of the DMADP pool. Variations in early metabolites were statistically significant ($P = 0.007$). The "rate constant" for the process of early metabolites depletion did not increase between 25°C and 35°C, but increased when temperature was raised to 40°C (Fig. 2.3f).

Total MEP pathway metabolites were calculated by integrating the total area below the post-illumination emission curve. The size of this pool increased with temperature up to 35°C before decreasing to very low levels at 45°C and 50°C (Fig. 2.3g). The "rate constant" for the process of total MEP pathway metabolite depletion increased up to 45°C with an E_a of 33.6 kJ mol^{-1}, and decreased only slightly at 50°C (Fig. 2.3h).

CO_2 response of isoprene emission, DMADP and early metabolites

To determine if the early metabolite pool was related to Calvin-Benson cycle intermediates, isoprene emission was measured over a range of CO_2 concentrations in oak leaves. Metabolite levels at 200, 400, 800 and 1200 ppm CO_2 were then determined with post-illumination isoprene emission. Isoprene emission stayed steady with increasing CO_2 concentrations in this range and carbon assimilation increased with CO_2 concentrations (Fig. 2.4a, b). DMADP levels decreased slightly at high CO_2 concentrations ($P = 0.157$, Fig. 2.4c). Both early metabolites and total MEP pathway metabolites stayed constant with increasing CO_2 concentrations (Fig. 2.4d, e). The time at which the early metabolites peak appeared was not affected by CO_2 concentration (data not shown).

Changes in isoprene emission and metabolites during a rapid temperature switch from 30°C to 40°C

When temperature of an oak leaf was rapidly raised from 30°C to 40°C, isoprene emission initially increased but then fell 20 min after the switch, and eventually leveled off, often to pre-switch levels (Fig. 2.5). Fig. 2.6a shows emission levels before the temperature switch, 20 min after switch (when emission was at a maximum), and 1 hr after the switch (when emission level had dropped and leveled off). Total MEP pathway metabolites as measured by post-illumination isoprene emission followed the same trend as emission rates, and were highest at 20 min after switch (Fig. 2.6b). However, contributions from DMADP and early metabolites to the total pool were disparate (Fig. 2.6c). DMADP levels did not increase upon the temperature increase. Early metabolites, being a bigger pool by itself, increased significantly and was primarily responsible for the increase in total MEP pathway metabolites. Both DMADP and the early metabolite pool decreased when the high temperature was maintained. Calculated rate constants for isoprene synthase more than doubled during the temperature switch, and remained constant when high temperature was maintained (Fig. 2.6d).

Discussion

Characteristics and source of post-illumination isoprene emission

In addition to the post-illumination isoprene emission that declined exponentially, I observed a later burst of isoprene emission in darkness (Fig. 2.1a). This peak could be measured at 25°C but became more prominent as temperature increased (Fig. 2.2). It also occurred earlier at higher temperature and at 45°C it fused with the initial post-illumination isoprene emission that is believed to come from DMADP present when the light is turned off.

The use of post-illumination isoprene emission as a measure of DMADP was first suggested by Rasulov et al. (2009). This method depends on darkness stopping DMADP production at a point in metabolism where DMADP is the only significant metabolite pool between the block caused by darkness and isoprene. Potential points at which DMADP production could be stopped by imposing darkness are shown in Fig. 2.7. These steps are most susceptible because energetic cofactors produced from electron transport chain are quickly depleted in darkness (Sharkey et al., 1986; Rasulov et al., 2009). In this view, the observation of a post-illumination isoprene burst is interesting. This phenomenon was first documented by Monson et al. (1991) where it was suggested isoprene emission may be controlled by ATP levels. A "light-independent isoprene emission process" was also observed at higher temperatures by Rasulov et al. (2010). Assuming there is only one homogeneous DMADP pool in the chloroplasts, this burst of isoprene in darkness has to represent DMADP that is either transported into chloroplasts, or synthesized *de*

novo from some unknown metabolite, "metabolite X". The following possible sources are explored and discussed below.

a) *Cytosolic DMADP.* DMADP can also be produced by the mevalonic acid (MVA) pathway in the cytosol and this pool can be large. However, reports that examined DMADP transport into chloroplasts showed this activity is very low (Bick and Lange, 2003). Crosstalk between the MEP pathway and MVA pathway is limited and unidirectional out of chloroplasts (Bick and Lange, 2003; Laule et al., 2003; Dudareva et al., 2005; Hampel et al., 2005). Rasulov et al. (2009) measured total leaf DMADP and found a significant pool of DMADP in darkened leaves which they hypothesized to be cytosolic DMADP and that cytosolic DMADP cannot be used for isoprene production. I agree.

b) *Plastidic IDP*. This is unlikely since the plastidic DMADP pool is considerably larger than the IDP pool in the presence of IDP isomerase (IDI). IDI is needed in isoprene-emitting plants to increase the DMADP pool for isoprene production since 5 times more IDP than DMADP is produced in the last step of the MEP pathway (Adam et al., 2002; Rohdich et al., 2002; 2003; Tritsch et al., 2010). Different groups have reported equilibrium DMADP:IDP ratios ranging from 3:1 to 13:1 in the presence of IDI (Agranoff et al., 1960; Koyama et al., 1983; Lützow and Beyer, 1988; Ramos-Valdivia et al., 1997). The "metabolite X" in this study is much larger than the pool size of DMADP, so it is unlikely to be IDP (Fig. 2.3e, inset). Besides, assuming IDI is active in darkness, IDP should isomerize to DMADP and convert to isoprene during the first phase of post-illumination isoprene emission (1^{st} peak in Fig. 2.1b). It is likely that the first phase of post-illumination isoprene emission represents both DMADP and IDP (DMADP being

the majority) and that "metabolite X" is further upstream in the metabolic pathway leading to isoprene.

c) *Metabolites upstream of the MEP pathway, for example, sugar phosphates in Calvin-Benson cycle.* Sugars and sugar phosphates, e.g. ribulose bisphosphate (RuBP), 3-phosphoglycerate (3-PGA) and triose phosphates are large pools and ultimately the source of plastidic DMADP. Nonetheless, the amount of "metabolite X" was unchanged over a large range of CO_2 concentrations (Fig. 2.4d). Changes in CO_2 would affect the amount of PGA and RuBP present in leaves when the light is turned off, though the effect is less on the amount of glyceraldehyde 3-phosphate (GAP) (Badger et al., 1984; Loreto and Sharkey, 1993). However, GAP levels fall to very low levels within 5 min of darkness (Sharkey et al., 1986; Loreto and Sharkey, 1993). In addition, a previous study showed carbon isotope labeling is unchanged during the post-illumination period (Kreuzwieser et al., 2002), supporting the view that "metabolite X" and DMADP are located in the same pathway. It thus appears unlikely that this post-illumination burst represents a metabolite in the Calvin-Benson cycle upstream of MEP pathway.

d) *MEP pathway metabolites (upstream of DMADP).* Metabolites in the MEP pathway upstream of IDP and DMADP seem to be the most likely source. While the regulation of the MEP pathway is still not well understood, several enzymes such as deoxyxylulose phosphate (DXP) synthase (DXS), DXP reductoisomerase (DXR), hydroxymethylbutenyl diphosphate (HMBDP) synthase (HDS) and HMBDP reductase (HDR) have all been proposed as highly regulated steps which could potentially let intermediate metabolites build up to significant levels (Sharkey et al., 2008; Rivasseau et al., 2009). For instance, a recent report suggested that a cyclic intermediate in

the MEP pathway, methylerythritol cyclodiphosphate (MEcDP), accumulates to measurable levels in spinach leaves (Rivasseau et al., 2009). Maybe early metabolites upstream of DMADP, such as MEcDP, are converted to DMADP in darkness. But some tricky questions remain to be answered: Why should these early metabolites convert to DMADP, if reducing power is depleted in darkness? Why is the conversion of early metabolites to DMADP delayed in darkness?

This phenomenon can be explained if the MEP pathway is limited by energetic cofactors in the short term and by carbon supply in the long term. When light is turned off, electron transport stops essentially immediately. This effectively shuts off the MEP pathway as the second and the last two steps of the MEP pathway all require reducing power (Fig. 2.7). In addition, steps requiring ATP are also turned off within a few seconds. HDR may be the most susceptible enzyme as it accepts electrons directly from ferredoxin in light (Seemann et al., 2005; 2006; Seemann and Rohmer, 2007). If the ATP supply limits more than reducing power during the first few seconds then post-illumination isoprene emission will measure several metabolites in addition to DMADP. Given that ATP can be made from a stored proton motive force across the thylakoid membranes after the light is turned off it seems much less likely that ATP supply is more limiting than the reduced ferredoxin supply in the first moments of darkness.

The subsequent increase in isoprene emission could occur when HDR switches to NADPH as a source of reducing power during darkness (Zepeck et al., 2005; Seemann et al., 2006). NADPH (or NADH) (Adam et al., 2002) produced elsewhere in chloroplast could supply the MEP pathway leading to a rise in isoprene emission, but this would take time. There is likely also to be NADH in the plastid though generally NADH:NAD ratios are lower than NADPH:NADP ratios.

Because plastidic GAP dehydrogenase can use either NADH or NADPH (McGowan and Gibbs, 1974) it is not clear whether these redox pairs would be in different ratios. Thus I cannot speculate on how NADH may affect the observed results. Another way that a delay could be introduced comes from the redox regulation of the reductive phase of the pentose phosphate pathway. The first two steps of this pathway produce NADPH but are inhibited in the light by regulatory dithiols. These enzymes could become activated over a period of minutes after darkening the leaf.

In the long term, carbon supply to the MEP pathway may become the limiting factor causing emission to fall eventually. The amount of GAP is rapidly reduced in darkness (Sharkey et al., 1986; Loreto and Sharkey, 1993). When light is turned off, 3-PGA levels increase initially, which could lead to an excess of pyruvate (Fig. 2.7), but then falls quickly to low levels at 10 min into darkness (Loreto and Sharkey, 1993). I suspect this is because low levels of NADPH and ATP during the first few minutes of darkness drives the reactions between 3-PGA and GAP in the reverse direction, depleting GAP and pushing up 3-PGA levels. On a longer time frame, redox-sensitive enzymes in the Calvin-Benson cycle such as phosphoribulokinase and GAP dehydrogenase are turned off causing a drop in PGA levels (Wara-Aswapati et al., 1980; Wedel and Soll, 1998; Scheibe et al., 2002). Thus, the first decline in isoprene emission following darkness may result from a lack of reduced ferredoxin while the second decline may result from a lack of carbon intermediates.

The amount of plastidic DMADP found in our study (approx. 1 μmol m^{-2} under standard conditions) is in good agreement with previous reports (Rasulov et al., 2009; 2009b; 2010). The

rate constant of isoprene synthase derived from this number predicts that the entire DMADP pool turns over in 39 seconds under standard conditions. On the other hand, the early metabolites comprise a much larger pool and turns over in 146 seconds, or approx. $2^1/_2$ min, under the same conditions.

Temperature and CO_2 response of DMADP and early metabolites in oak

Our results support the view that isoprene emission under different temperature regimes is regulated both by enzyme activity and substrate levels. DMADP levels increase with temperature until 35°C where it starts to drop (Fig. 2.3c). This trend was also observed in aspen (Rasulov et al., 2010). The rate constant of isoprene synthase increased with temperature at 25°C – 40°C, and the rate constant for depletion of total MEP pathway metabolites increased up to 45°C (Fig. 2.3d, 2.3h). Again this is in agreement with IspS activity measured in vitro and in vivo (Monson et al., 1992; Lehning et al., 1999; Rasulov et al., 2009b). The early metabolites showed a similar temperature response to DMADP, increasing up to 35°C before it dropped at 40°C. The changes in early metabolites were, however, much sharper: early metabolites at 35°C more than doubled the amount at 25°C, whereas DMADP increased by just 30% (Fig. 2.3c, 2.3e). This is reflected in the "rate constant" calculated for each of these two metabolites: while IspS activity rose sharply with temperature, the activities that converted early metabolites to isoprene (via DMADP) remained relatively unchanged from 25°C to 35°C before increasing at higher temperatures (Fig. 2.3d, 2.3f). This shows variation of early metabolites with temperature is non-enzymatic but instead regulatory, implying a complex regulatory role that early metabolites play in temperature response of isoprene emission.

Isoprene emission and substrate levels did not respond to increased CO_2 concentrations in this study (Fig. 2.4). Reduced isoprene emissions at elevated CO_2 concentrations are often reported in CO_2 response studies (Jones and Rasmussen, 1975; Monson and Fall, 1989; Loreto and Sharkey, 1990; Rosenstiel et al., 2003; Scholefield et al., 2004; Possell et al., 2005; Calfapietra et al., 2008; Wilkinson et al., 2009; Rasulov et al., 2009b among others). However, in one study, CO_2 response of isoprene emission in red oak (*Quercus rubra*) was variable (Loreto and Sharkey, 1990). In another, isoprene emission from leaves of red oak was significantly higher under high CO_2 growth conditions, and did not change with increasing experimental CO_2 concentrations (Sharkey et al., 1991). Under field conditions, an increase (in oak) or no change (in poplar) in isoprene emission in trees grown under elevated CO_2 conditions have been reported (Calfapietra et al., 2007; Loreto et al., 2007). It was also reported by some that the reduction in emission at high CO_2 concentrations, when observed, is temperature sensitive (Loreto and Sharkey, 1990; Rasulov et al., 2010). Our results here further demonstrate that CO_2 response of isoprene emission between experiments can be different.

Metabolite levels during a rapid switch from 30°C to 40°C

It was observed in this lab some years ago that upon a rapid increase in temperature, isoprene emission in oak increases, but only transiently when the high temperature was maintained (Singsaas et al., 1999; Singsaas and Sharkey, 2000). I was able to repeat this result (Fig. 2.5) and used post-illumination isoprene emission to measure changes in metabolite levels in this experiment.

Our results show that a change in emission levels during the fast temperature switch is attributable to an increase in IspS activity rather than substrate level (Fig. 2.6c, d). DMADP levels at 30°C and 40°C were similar. This is consistent with the temperature response curve of DMADP (Fig. 2.3). Early metabolites were high just after the temperature switch (Fig. 2.6b, c) but declined after 1 hr. The early metabolites may serve as a buffer allowing for short-term high rates of isoprene emission. However, IspS appears to be able to drain the early metabolite pool faster than it can be refilled at 40°C causing the control of the rate of isoprene emission to shift from DMADP concentration plus IspS kinetics to upstream reactions needed to make the early metabolites. In the field, temperatures of red oak leaves could rise up to 39°C and vary by >10°C on a sunny day (Singsaas et al., 1999). The rapid temperature shift used in this experiment in a sense mimics a real-world scenario where leaf temperature rises rapidly in a sun fleck. It appears that metabolic control can shift at these physiologically relevant temperatures.

When high temperature is maintained for a period of time, metabolite levels drop and enzyme activity is maintained (Fig. 2.6b, c, d). This could be explained by a limitation on energetic cofactors. Rates of photosynthetic electron transport decrease (Niinemets et al., 1999) and thylakoid membrane conductance increases at higher temperatures (Zhang et al., 2009; Zhang and Sharkey, 2009), causing a drop in proton motive force. This leads to a decrease in ATP synthesis. On the other hand, ATP and NADPH usage increases as photorespiration increases. This drawdown of energetic cofactors could affect the MEP pathway, where 3 NADPH and 3 ATP equivalents are needed for synthesis of one isoprene molecule.

Conclusions

In this study I examined the effect of temperature on the post-illumination isoprene burst and discussed possible sources of this phenomenon. Timing of this burst is highly temperature dependent. This burst likely represents a pool of metabolite(s) that has accumulated in the MEP pathway, but identity of this metabolite and the mechanism by which it is converted to DMADP remains unclear. It will be useful to perform more studies to extend our understanding of chloroplast energetic status during the post-illumination period.

Our results also confirm previous finding that response of isoprene emission to temperature is regulated both by enzyme activity and substrate availability. Isoprene emission and metabolite levels did not respond to high CO_2 concentrations in this study. During a rapid temperature switch from 30°C to 40°C, isoprene emission increased initially due to an increase in enzyme activity and then decreased over time as substrate became limiting.

Materials and methods

Plant material

Leaves were harvested from oak (*Quercus robur*) trees on Michigan State University campus (42°43'N, 84°28'W) between April and September 2010. Whenever possible, leaves from the

periphery (sun exposed) of the canopy were harvested. Small twigs with desired leaves were cut from the trees with razor blades or a pole pruner and immediately re-cut underwater with a sharp razor blade. Leaves with a small portion of branch were then transferred underwater to a floral tube and carried back to the lab to be analyzed. I have found in the past that leaves harvested this way were physiologically active for at least 6 hours. To maintain consistency, leaves used in the same experiment were harvested from the same tree.

Poplar trees (*Populus deltoides*) were propagated by stem cuttings in soil (Baccto planting mix, Michigan Peat Co., Houston, Texas) and grown in a 25/23°C 14 hr photoperiod growth chamber. Photosynthetic photon flux density (PPFD) at leaf level was set at 500 μmol m^{-2} s^{-1}. Mature leaves from 2-month old plants were used in this study. Poplar leaves remained attached during the experiment.

Gas exchange

During an experiment leaves were enclosed in a custom-built aluminum cuvette with a glass window. Air in cuvette was mixed with three small Micronel D241L fans (Micronel US, Carlsbad, California). Synthetic air used for gas exchange was mixed from cylinders of N_2, O_2 and 5% CO_2 in air and humidified as described in Tennessen et al. (1994). CO_2 concentration was controlled to 400 ppm unless otherwise noted. Total flow rate through chamber was measured with a flow meter before the air entered the leaf chamber. CO_2 levels in reference and sample air were measured with a LI-6262 CO_2/H_2O analyzer (LI-COR Biosciences, Lincoln, Nebraska). Air coming out of analyzer was then connected to a fast isoprene sensor (FIS, Hills

Scientific, Boulder, Colorado), and isoprene was measured at 5-second intervals. Temperature of the leaf chamber was controlled by two water baths linked to a six-way valve that allowed ultra-fast switching between different temperatures. Both leaf and air temperatures were monitored with thermocouples; only leaf temperatures were used and reported.

Experiments were carried out under standard conditions (30°C, 1000 μmol m^{-2} s^{-1} PPFD at leaf level) unless otherwise noted. Light was provided with an SL3500 white light-emitting diode array (Photon Systems Instruments, Drasov, Czech). Each leaf was acclimatized for at least 45 min before starting the experiment. Assimilation rate was calculated according to methods used by von Caemmerer and Farquhar (1981).

Measurement of post-illumination isoprene emission

Post-illumination isoprene emission and chamber clearing was measured according to procedures described by Rasulov et al. (2009). Light in the chamber was turned off by quickly switching off the LED light and at the same time covering the chamber window with a thick stack of paper. This procedure drops light level in the chamber to essentially zero (0.00 μmol m^{-2} s^{-1} as measured by a quantum sensor in the same condition). In practice, it was found that a first dark period in the experiment caused the post-illumination burst to appear earlier than succeeding dark periods, while subsequent darkenings caused consistent responses in following dark periods. This problem was overcome by giving the leaf one dark period for which the data was not used before the actual experiment began.

To generate the chamber clearing trace, a small flow of external isoprene source (Airgas Great Lakes, Independence, Ohio) was first fed into the chamber until isoprene levels in the chamber were steady. The isoprene source was then cut off at the chamber while isoprene level was monitored at the FIS (Fig. 2.1a).

The true post-illumination isoprene emission was obtained by subtracting chamber clearing from the observed emission. This usually generated two distinct peaks: the 1st assumed to be DMADP and the 2nd referred to as early metabolites (Fig. 2.1b). Since the kinetics of reactions that convert the early metabolites to isoprene is currently not known, the two-peaked post-illumination trace cannot be precisely deconvoluted. A realistic estimate is obtained by simply drawing a vertical line at the minimum between the two peaks and separating the two peaks by this line (Fig. 2.1b, inset). This data analysis process is automated using the Peak Analyzer module in Origin® (Originlab, Northampton, Massachusetts).

Data analysis

One-way ANOVA and t-tests ($p < 0.05$) were used to detect significant differences between groups. Mann-Whitney and Kruskal-Wallis tests were used in cases where normality test failed. Statistical tests were carried out in SigmaPlot® (Systat Software Inc., Chicago, Illinois).

Acknowledgement

Assistance from Ellen Ratliff, who was also a co-author on the publication resulting from this project, is gratefully acknowledged. This work was supported by the National Science Foundation (grant no. IOS-0950574 to T.D.S.).

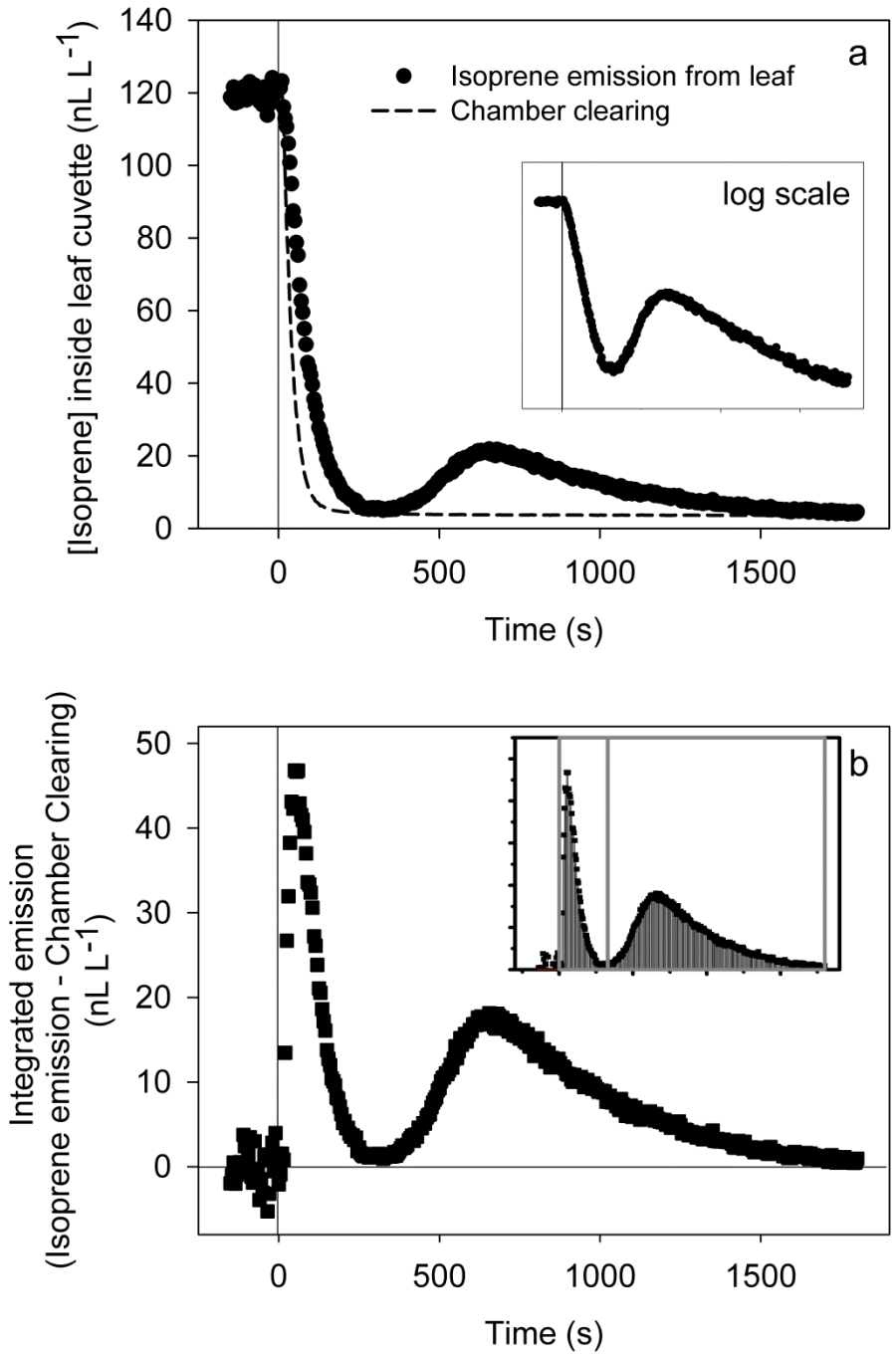

Figure 2.1 A typical post-illumination isoprene emission trace in oak leaf under standard conditions. Light was turned off at time 0. After emission dropped to almost zero in ~ 5 min, isoprene emission increased again and then fell slowly in 20 - 30 min (a). The decline in the first part of the trace was exponential (a, inset). In the chamber clearing trace, pre-clearing isoprene levels were normalized to pre-darkness emission levels in the emission trace. Subtracting clearing trace from emission trace yielded the true post-illumination isoprene emission (b). This difference showed up as two distinct peaks at temperatures < 45°C. DMADP (1st peak) and early metabolites (2nd peak) were then separated and integrated in Origin® (b, inset).

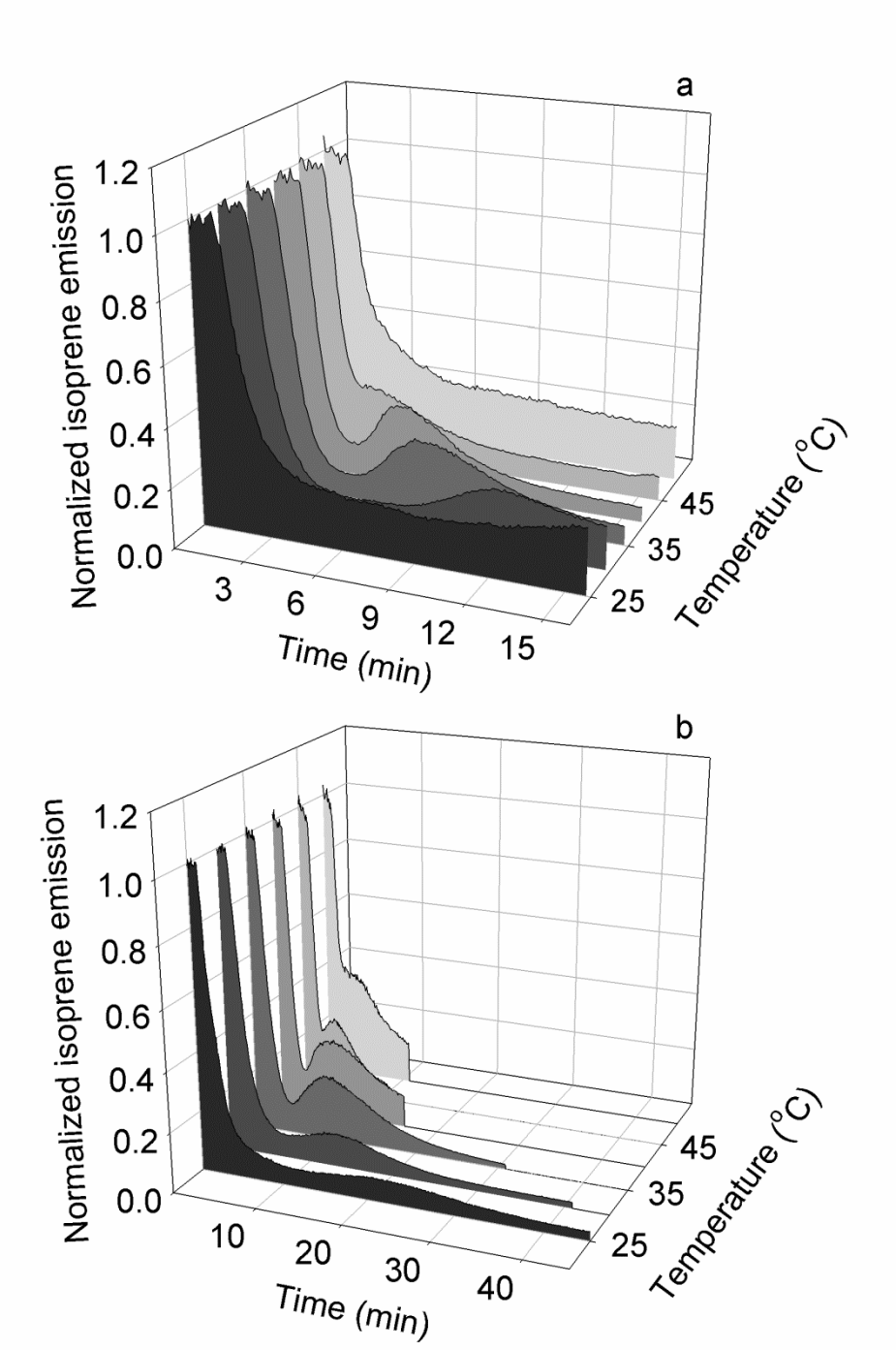

Figure 2.2 Time of appearance of the post-illumination burst is temperature dependent in both oak (a) and poplar (b). In both cases, the peak in the post-illumination isoprene emission trace appeared progressively sooner at higher temperatures, and merged with the initial decline in isoprene emission at temperatures > 40°C. Light is turned off at t = 50 s. Isoprene emissions at different temperatures were normalized to pre-darkness levels. Post-illumination period (darkness) in (b) was intentionally shortened at higher temperatures. This was intended to minimize thermodamage since heat damage is exacerbated in darkness.

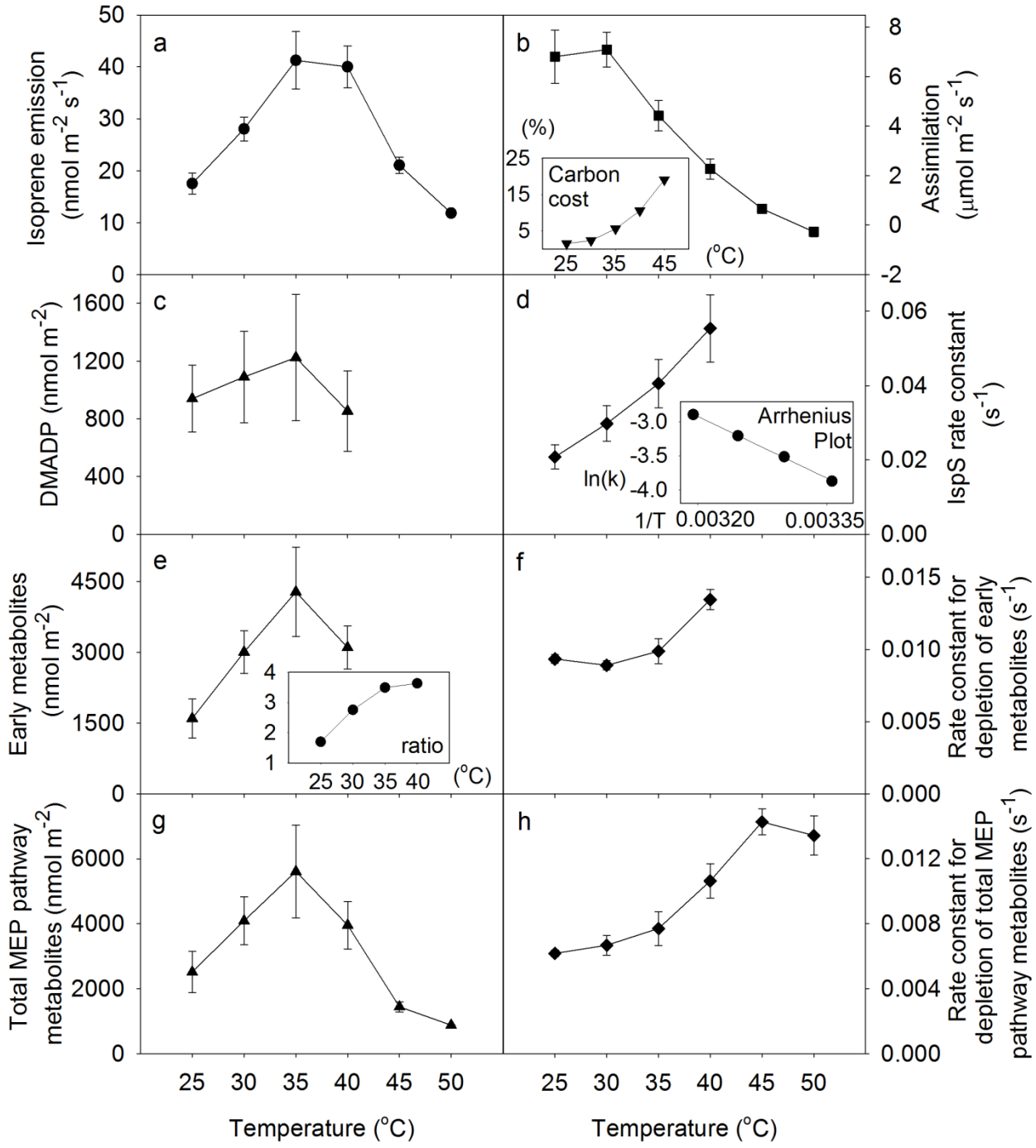

Figure 2.3 Temperature dependence of isoprene emission rate (a), assimilation rate (b), DMADP (c), IspS rate constant (d), early metabolites (e), "rate constant" for depletion of early metabolites (f), total MEP pathway metabolites (g) and "rate constant" for depletion of total MEP pathway metabolites (h) in oak leaf. Amount of early metabolites and total MEP pathway metabolites are in isoprene units. Carbon cost of isoprene as a percentage of assimilation at a given temperature was calculated assuming synthesis of each isoprene requires

(Figure 2.3 continued)

six fixed carbons (b, inset). The "rate constant" for depletion of a certain metabolite was calculated by dividing isoprene emission rate by the amount of the metabolite. Arrhenius plot of ln(k) vs. 1/T (in Kelvin) for isoprene synthase is shown in (d) inset. Early metabolites to DAMDP ratio is shown in (e) inset. DMADP and early metabolites data for temperatures over 40°C could not be obtained since it was impossible to separate the two peaks at higher temperatures. Each point denotes mean ± standard error (n = 4).

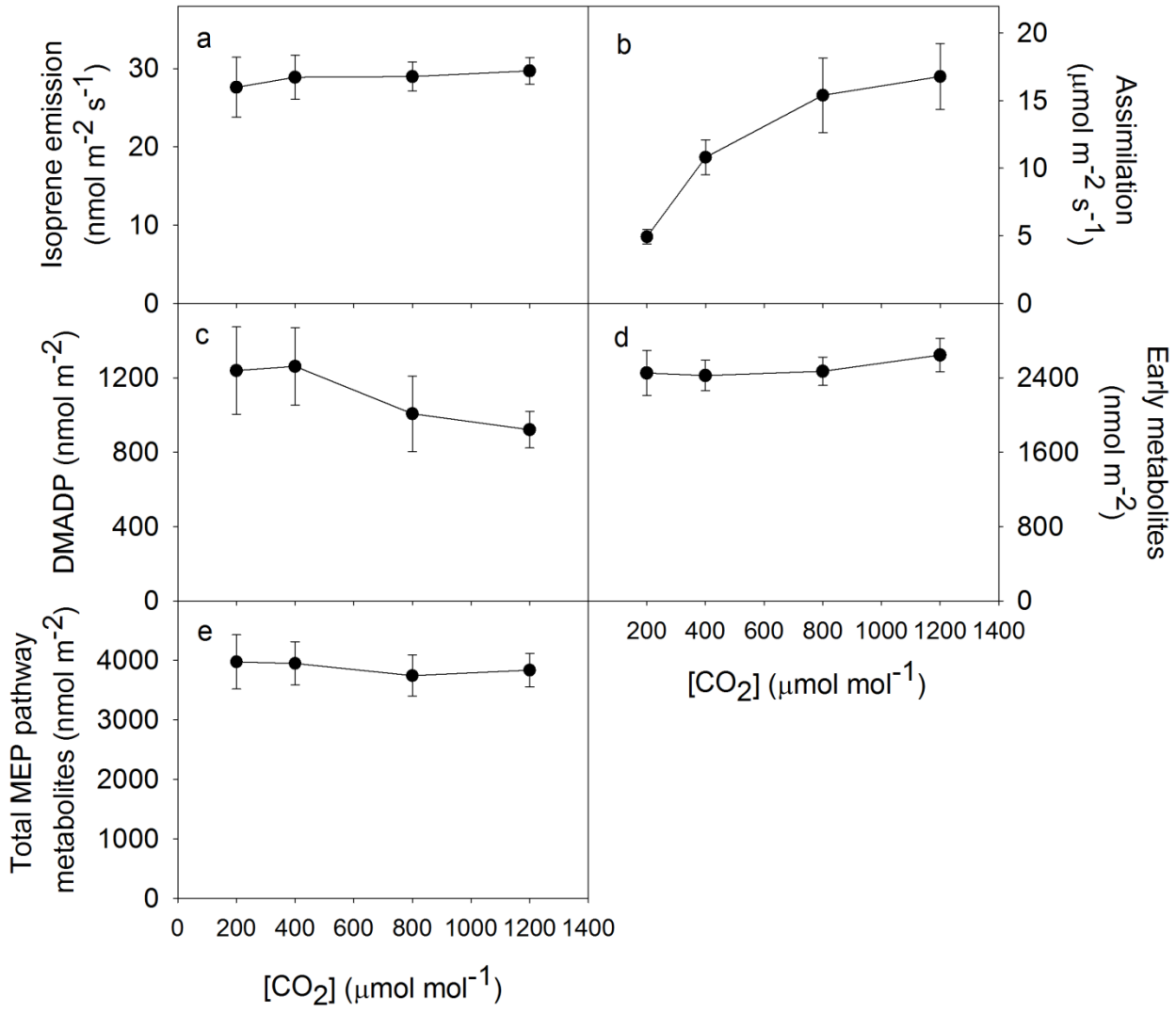

Figure 2.4 CO_2 response of isoprene emission (a), assimilation rate (b), DMADP (c), early metabolites (d) and total MEP pathway metabolites (e) in oak leaf. Amount of early metabolites and total MEP pathway metabolites are in isoprene units. Each point denotes mean ± standard error (n = 3).

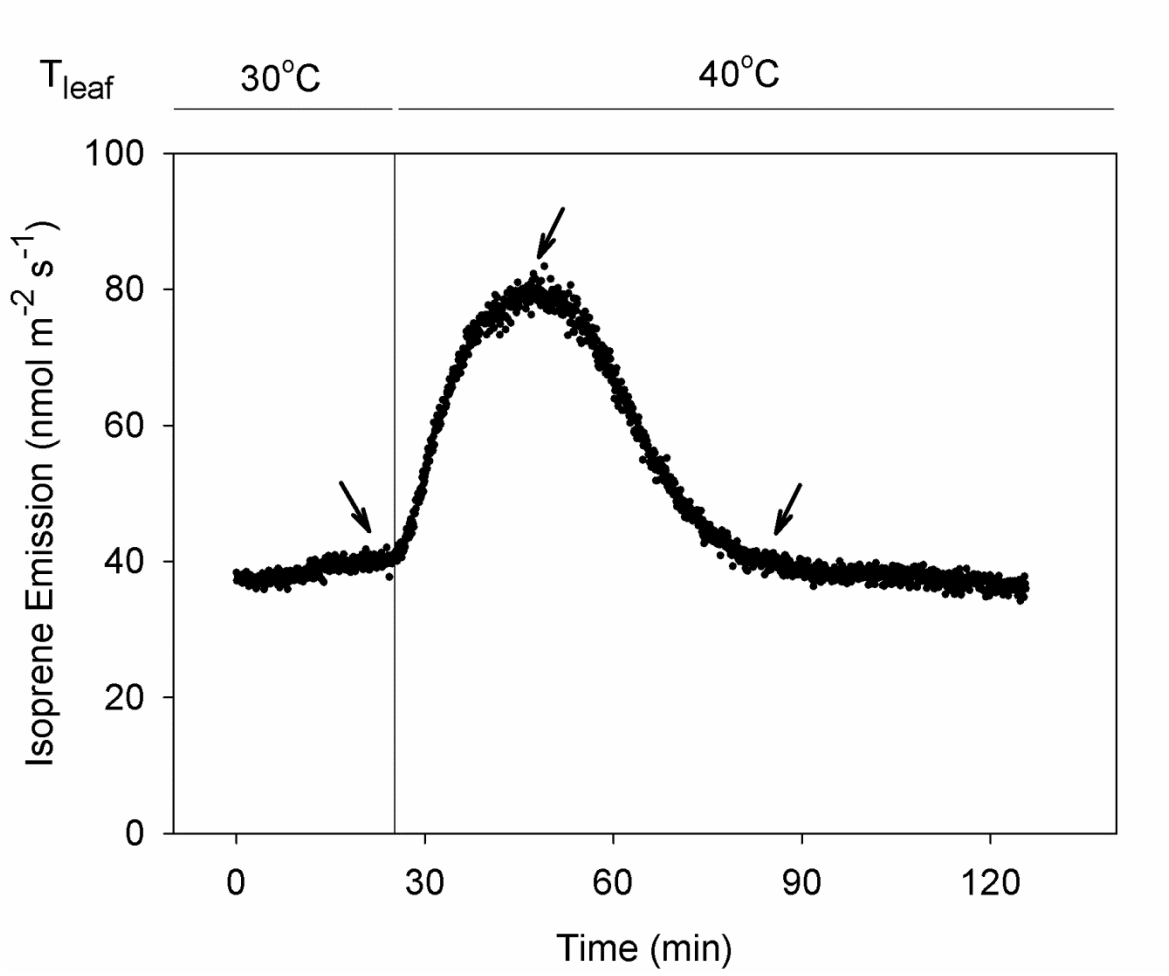

Figure 2.5 Isoprene emission of an oak leaf during a rapid switch from 30°C to 40°C. Isoprene emission increased initially upon the switch but then fell at approximately 20 min after the switch. Isoprene emission then leveled off, often to pre-switch levels, within one hour after switch. Measurements in Fig. 2.6 were made at time points shown by the arrows.

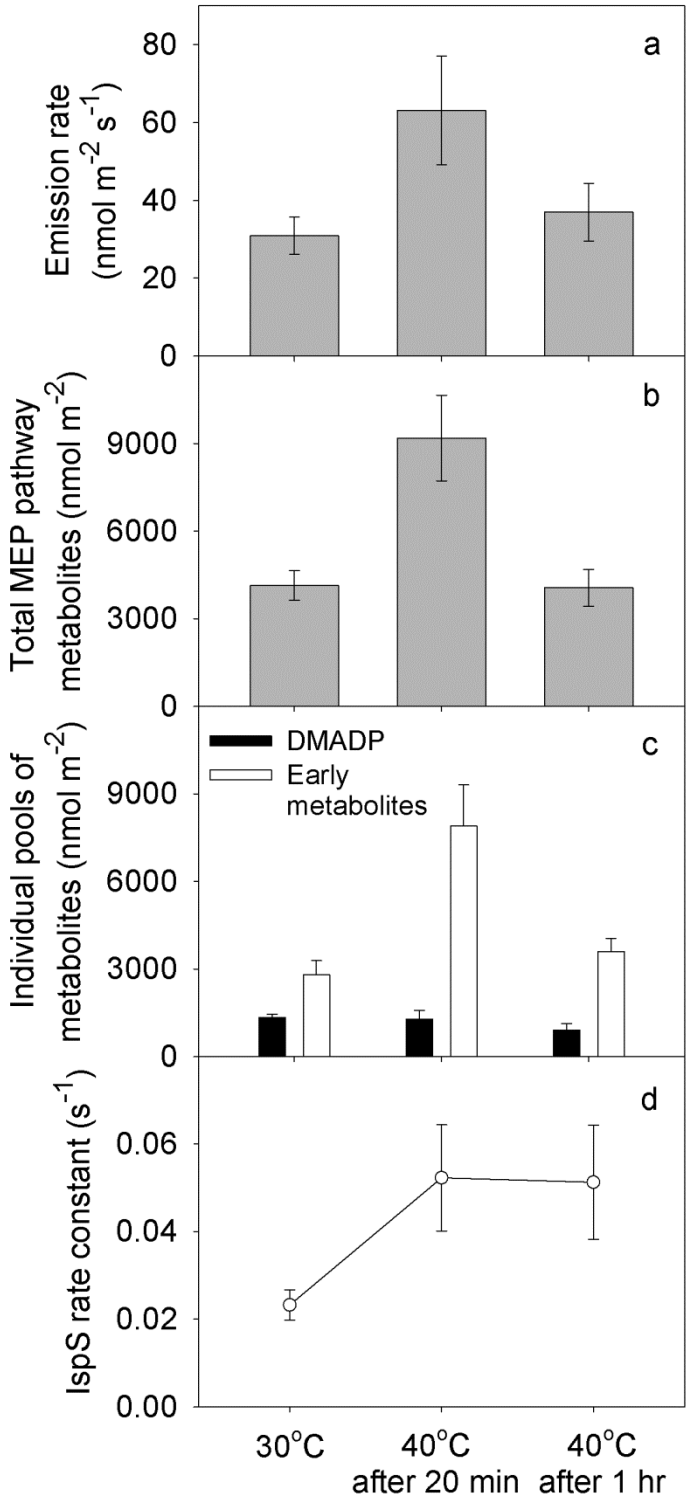

Figure 2.6 Isoprene emission rates (a), total MEP pathway metabolites (b), DMADP and early metabolites (c), and IspS rate constant (d) during a rapid switch from 30°C to 40°C in oak leaf. Amount of total MEP pathway metabolites and early metabolites are in isoprene units. Rate constant for isoprene synthase was calculated by dividing emission rate by DMADP level. Each point denotes mean ± standard error (n = 3).

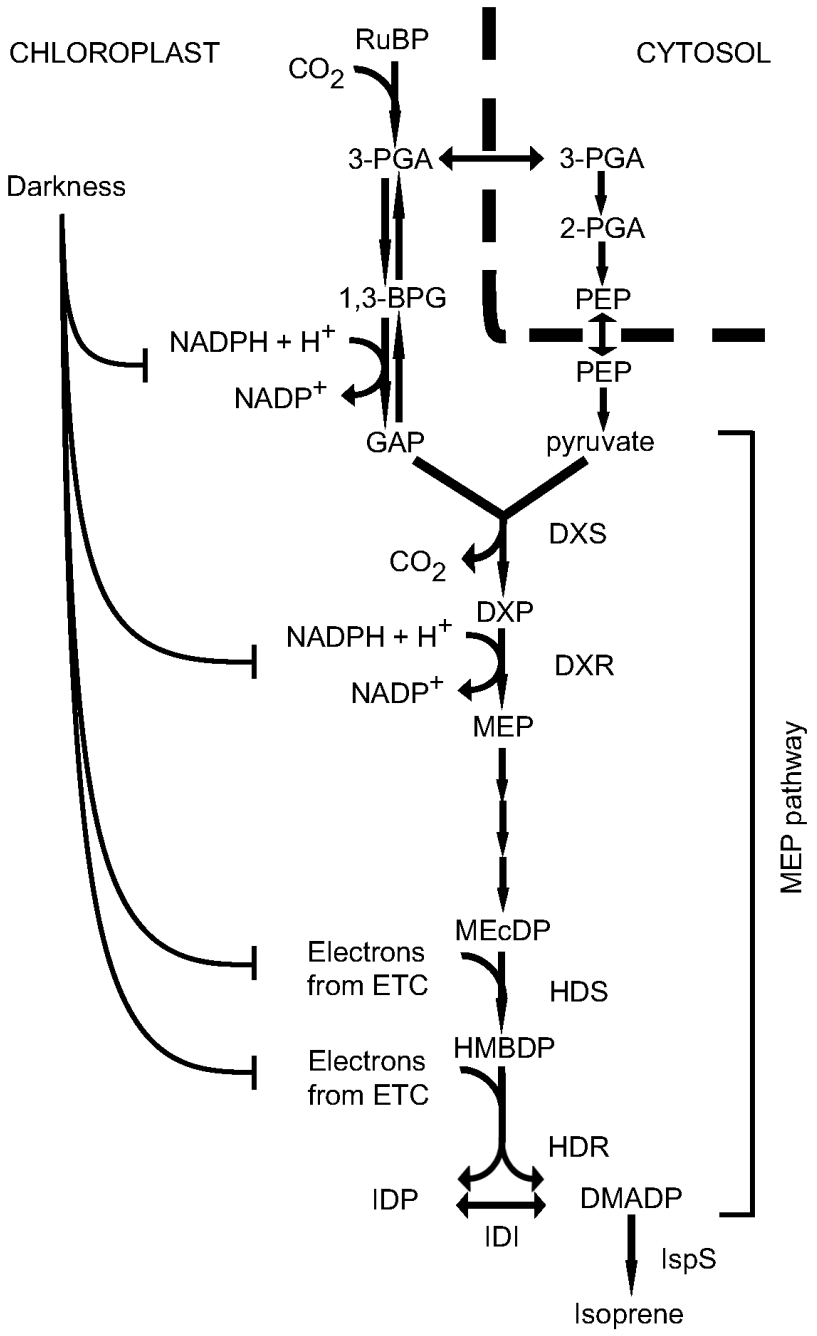

Figure 2.7 Proposed inhibition by darkness of steps leading to isoprene production in the short term. Steps in the MEP pathway expected to be most susceptible to depletion of reducing power upon darkening are indicated here. ETC = electron transport chain. PGA = phosphoglycerate; PEP = phosphoenolpyruvate; 1,3-BPG = 1,3-bisphosphoglycerate; GAP = glyceraldehyde 3-phosphate; DXS = deoxyxylulose 5-phosphate (DXP) synthase; DXR = DXP reductoisomerase; MEcDP = methylerythritol 2,4-cyclodiphosphate; HDS = hydroxymethylbutenyl diphosphate (HMBDP) synthase; HDR = HMBDP reductase; IDP = isopentenyl diphosphate; IDI = IDP isomerase. ATPs are omitted here for simplicity. Steps between 3-PGA and GAP are reversible. Coupling of NADPH is only shown in the forward reaction for simplicity.

LITERATURE CITED

LITERATURE CITED

Adam P, Hecht S, Eisenreich WG, Kaiser J, Grawert T, Arigoni D, Bacher A, Rohdich F (2002) Biosynthesis of terpenes: Studies on 1-hydroxy-2-methyl-2-(E)-butenyl 4-diphosphate reductase. Proceedings of the National Academy of Sciences of the United States of America **99:** 12108-12113

Agranoff BW, Eggerer H, Henning U, Lynen F (1960) Biosynthesis of terpenes 7. Isopentenyl pyrophosphate isomerase. Journal of Biological Chemistry **235:** 326-332

Badger MR, Sharkey TD, Von Caemmerer S (1984) The relationship between steady-state gas exchange of bean leaves and the levels of carbon-reduction-cycle intermediates. Planta **160:** 305-313

Bick JA, Lange BM (2003) Metabolic cross talk between cytosolic and plastidial pathways of isoprenoid biosynthesis: unidirectional transport of intermediates across the chloroplast envelope membrane. Archives of Biochemistry and Biophysics **415:** 146-154

Calfapietra C, Mugnozza GS, Karnosky DF, Loreto F, Sharkey TD (2008) Isoprene emission rates under elevated CO_2 and O_2 in two field-grown aspen clones differing in their sensitivity to O_3. New Phytologist **179:** 55-61

Calfapietra C, Wiberley AE, Falbel TG, Linskey AR, Mugnozza GS, Karnosky DF, Loreto F, Sharkey TD (2007) Isoprene synthase expression and protein levels are reduced under elevated O_3 but not under elevated CO_2 (FACE) in field-grown aspen trees. Plant, Cell and Environment **30:** 654-661

Dudareva N, Andersson S, Orlova I, Gatto N, Reichelt M, Rhodes D, Boland W, Gershenzon J (2005) The nonmevalonate pathway supports both monoterpene and sesquiterpene formation in snapdragon flowers. Proceedings of the National Academy of Sciences of the United States of America **102:** 933

Fall R, Wildermuth MC (1998) Isoprene synthase: From biochemical mechanism to emission algorithm. Journal of Geophysical Research [Atmospheres] **103:** 25599-25609

Hampel D, Mosandl A, Wüst M (2005) Biosynthesis of mono-and sesquiterpenes in carrot roots and leaves (*Daucus carota* L.): metabolic cross talk of cytosolic mevalonate and plastidial methylerythritol phosphate pathways. Phytochemistry **66:** 305-311

Jones CA, Rasmussen RA (1975) Production of isoprene by leaf tissue. Plant Physiology **55:** 982-987

Koyama T, Katsuki Y, Ogura K (1983) Studies on isopentenyl pyrophosphate isomerase with artificial substrates: Z-E isomerization of Z-3-methyl-3-pentenyl pyrophosphate. Bioorganic Chemistry **12:** 58-70

Kreuzwieser J, Graus M, Wisthaler A, Hanse A, Rennenberg H, Schnitzler JP (2002) Xylem-transported glucose as an additional carbon source for leaf isoprene formation in *Quercus robur*. New Phytologist **156:** 171-178

Laisk A, Kiirats O, Oja V (1984) Assimilatory power (postillumination CO_2 uptake) in leaves: measurement, environmental dependencies, and kinetic properties. Plant Physiology **76:** 723

Laule O, Fürholz A, Chang HS, Zhu T, Wang X, Heifetz PB, Gruissem W, Lange M (2003) Crosstalk between cytosolic and plastidial pathways of isoprenoid biosynthesis in *Arabidopsis thaliana*. Proceedings of the National Academy of Sciences of the United States of America **100:** 6866

Lehning A, Zimmer I, Steinbrecher R, Bruggemann N, Schnitzler JP (1999) Isoprene synthase activity and its relation to isoprene emission in *Quercus robur* L. leaves. Plant, Cell and Environment **22:** 495-504

Loreto F, Centritto M, Barta C, Calfapietra C, Fares S, Monson RK (2007) The relationship between isoprene emission rate and dark respiration rate in white poplar (*Populus alba* L.) leaves. Plant, Cell and Environment **30:** 662-669

Loreto F, Sharkey TD (1990) A gas-exchange study of photosynthesis and isoprene emission in *Quercus rubra* L. Planta **182:** 523-531

Loreto F, Sharkey TD (1993) On the relationship between isoprene emission and photosynthetic metabolites under different environmental conditions. Planta **189:** 420-424

Lützow M, Beyer P (1988) The isopentenyl-diphosphate Δ-isomerase and its relation to the phytoene synthase complex in daffodil chromoplasts. Biochimica et Biophysica Acta, Lipids and Lipid Metabolism **959:** 118-126

McGowan RE, Gibbs M (1974) Comparative enzymology of the glyceraldehyde 3-phosphate dehydrogenases from *Pisum sativum*. Plant Physiology **54:** 312-319

Monson RK, Fall R (1989) Isoprene emission from aspen leaves: influence of environment and relation to photosynthesis and photorespiration. Plant Physiology **90:** 267-274

Monson RK, Hills AJ, Zimmerman PR, Fall RR (1991) Studies of the relationship between isoprene emission rate and CO_2 or photon-flux density using a real-time isoprene analyser. Plant, Cell and Environment **14:** 517-523

Monson RK, Jaeger CH, Adams WW, Driggers EM, Silver GM, Fall R (1992) Relationships among isoprene emission rate, photosynthesis, and isoprene synthase activity as influenced by temperature. Plant Physiology **98:** 1175-1180

Niinemets Ü, Tenhunen JD, Harley PC, Steinbrecher R (1999) A model of isoprene emission based on energetic requirements for isoprene synthesis and leaf photosynthetic properties for *Liquidambar* and *Quercus*. Plant, Cell and Environment **22:** 1319-1335

Possell M, Hewitt CN, Beerling DJ (2005) The effects of glacial atmospheric CO_2 concentrations and climate on isoprene emissions by vascular plants. Global Change Biology **11:** 60-69

Ramos-Valdivia AC, Heijden R, Verpoorte R (1997) Isopentenyl diphosphate isomerase: a core enzyme in isoprenoid biosynthesis. A review of its biochemistry and function. Natural product reports **14:** 591-603

Rasulov B, Copolovici L, Laisk A, Niinemets Ü (2009) Postillumination isoprene emission: in vivo measurements of dimethylallyldiphosphate pool size and isoprene synthase kinetics in aspen leaves. Plant Physiology **149:** 1609-1618

Rasulov B, Hüve K, Bichele I, Laisk A, Niinemets Ü (2010) Temperature response of isoprene emission in vivo reflects a combined effect of substrate limitations and isoprene synthase activity: a kinetic analysis. Plant Physiology **154:** 1558-1570

Rasulov B, Hüve K, Valbe M, Laisk A, Niinemets Ü (2009b) Evidence that light, carbon dioxide, and oxygen dependencies of leaf isoprene emission are driven by energy status in hybrid aspen. Plant Physiology **151:** 448-460

Rivasseau C, Seemann M, Boisson A-M, Streb P, Gout E, Douce R, Rohmer M, Bligny R (2009) Accumulation of 2-C-methyl-D-erythritol 2,4-cyclodiphosphate in illuminated plant leaves at supraoptimal temperatures reveals a bottleneck of the prokaryotic methylerythritol 4-phosphate pathway of isoprenoid biosynthesis. Plant, Cell and Environment **32:** 82-92

Rohdich F, Hecht S, Gärtner K, Adam P, Krieger C, Amslinger S, Arigoni D, Bacher A, Eisenreich W (2002) Studies on the nonmevalonate terpene biosynthetic pathway: metabolic role of IspH (LytB) protein. Proceedings of the National Academy of Sciences of the United States of America **99:** 1158-1163

Rohdich F, Zepeck F, Adam P, Hecht S, Kaiser J, Laupitz R, Grawert T, Amslinger S, Eisenreich W, Bacher A, Arigoni D (2003) The deoxyxylulose phosphate pathway of isoprenoid biosynthesis: Studies on the mechanisms of the reactions catalyzed by IspG and IspH protein. Proceedings of the National Academy of Sciences of the United States of America **100:** 1586-1591

Rosenstiel TN, Potosnak MJ, Griffin KL, Fall R, Monson RK (2003) Increased CO_2 uncouples growth from isoprene emission in an agriforest ecosystem. Nature **421:** 256-259

Ruuska S, Andrews TJ, Badger MR, Hudson GS, Laisk A, Price GD, von Caemmerer S (1998) The interplay between limiting processes in C_3 photosynthesis studied by rapid-

response gas exchange using transgenic tobacco impaired in photosynthesis. Australian Journal of Plant Physiology **25:** 859-870

Sanadze GA, Kalandaze AN (1966) Light and temperature curves of the evolution of C_5H_8. Soviet Plant Physiology **13:** 458-461

Scheibe R, Wedel N, Vetter S, Emmerlich V, Sauermann SM (2002) Co-existence of two regulatory NADP-glyceraldehyde 3-P dehydrogenase complexes in higher plant chloroplasts. European Journal of Biochemistry **269:** 5617-5624

Schnitzler JP, Zimmer I, Bachl A, Arend M, Fromm J, Fischbach RJ (2005) Biochemical properties of isoprene synthase in poplar (*Populus* × *canescens*). Planta **222:** 777-786

Scholefield PA, Doick KJ, Herbert BMJ, Hewitt CNS, Schnitzler JP, Pinelli P, Loreto F (2004) Impact of rising CO_2 on emissions of volatile organic compounds: isoprene emission from *Phragmites australis* growing at elevated CO_2 in a natural carbon dioxide spring. Plant Cell and Environment **27:** 393-401

Seemann M, Rohmer M (2007) Isoprenoid biosynthesis via the methylerythritol phosphate pathway: GcpE and LytB, two novel iron-sulphur proteins. Comptes Rendus Chimie **10:** 748-755

Seemann M, Tse Sum Bui B, Wolff M, Miginiac-Maslow M, Rohmer M (2006) Isoprenoid biosynthesis in plant chloroplasts via the MEP pathway: direct thylakoid/ferredoxin-dependent photoreduction of GcpE/IspG. FEBS Letters **580:** 1547-1552

Seemann M, Wegner P, Schünemann V, Bui BTS, Wolff M, Marquet A, Trautwein AX, Rohmer M (2005) Isoprenoid biosynthesis in chloroplasts via the methylerythritol phosphate pathway: the (E)-4-hydroxy-3-methylbut-2-enyl diphosphate synthase (GcpE) from *Arabidopsis thaliana* is a [4Fe-4S] protein. Journal of Biological Inorganic Chemistry **10:** 131-137

Sharkey TD, Loreto F, Delwiche CF (1991) High carbon dioxide and sun/shade effects on isoprene emission from oak and aspen tree leaves. Plant Cell and Environment **14:** 333-338

Sharkey TD, Seemann JR, Pearcy RW (1986) Contribution of metabolites of photosynthesis to postillumination CO_2 assimilation in response to lightflecks. Plant Physiology **82:** 1063-1068

Sharkey TD, Singsaas EL (1995) Why plants emit isoprene. Nature **374:** 769-769

Sharkey TD, Wiberley AE, Donohue AR (2008) Isoprene emission from plants: why and how. Annals of Botany **101:** 5-18

Singsaas EL (2000) Terpenes and the thermotolerance of photosynthesis. New Phytologist **146:** 1-2

Singsaas EL, Laporte MM, Shi JZ, Monson RK, Bowling DR, Johnson K, Lerdau M, Jasentuliytana A, Sharkey TD (1999) Kinetics of leaf temperature fluctuation affect isoprene emission from red oak (*Quercus rubra*) leaves. Tree Physiology **19:** 917-924

Singsaas EL, Lerdau M, Winter K, Sharkey TD (1997) Isoprene increases thermotolerance of isoprene-emitting species. Plant Physiology **115:** 1413-1420

Singsaas EL, Sharkey TD (2000) The effects of high temperature on isoprene synthesis in oak leaves. Plant, Cell and Environment **23:** 751-757

Tennessen DJ, Singsaas EL, Sharkey TD (1994) Light emitting diodes as a light source for photosynthesis research. Photosynthesis Research **39:** 85-92

Tingey DT, Evans RC, Bates EH, Gumpertz ML (1987) Isoprene emissions and photosynthesis in three ferns - the influence of light and temperature. Physiologia Plantarum **69:** 609-616

Tingey DT, Manning M, Grothaus LC, Burns WF (1979) The influence of light and temperature on isoprene emission rates from live oak. Physiologia Plantarum **47:** 112-118

Tritsch D, Hemmerlin A, Bach TJ, Rohmer M (2010) Plant isoprenoid biosynthesis via the MEP pathway: In vivo IPP/DMAPP ratio produced by (E)-4-hydroxy-3-methylbut-2-enyl diphosphate reductase in tobacco BY-2 cell cultures. FEBS Letters **584:** 129-134

Von Caemmerer S, Farquhar GD (1981) Some relationships between the biochemistry of photosynthesis and the gas exchange of leaves. Planta **153:** 376-387

Wara-Aswapati O, Kemble RJ, Bradbeer JW (1980) Activation of glyceraldehyde-phosphate dehydrogenase (NADP) and phosphoribulokinase in *Phaseolus vulgaris* leaf extracts involves the dissociation of oligomers. Plant Physiology **66:** 34

Wedel N, Soll J (1998) Evolutionary conserved light regulation of Calvin cycle activity by NADPH-mediated reversible phosphoribulokinase / CP12 / glyceraldehyde-3-phosphate dehydrogenase complex dissociation. Proceedings of the National Academy of Sciences of the United States of America **95:** 9699

Wildermuth MC, Fall R (1996) Light-dependent isoprene emission - characterization of a thylakoid-bound isoprene synthase in *Salix discolor* chloroplasts. Plant Physiology **112:** 171-182

Wilkinson MJ, Monson RK, Trahan N, Lee S, Brown E, Jackson RB, Polley HW, Fay PA, Fall R (2009) Leaf isoprene emission rate as a function of atmospheric CO_2 concentration. Global Change Biology **15:** 1189-1200

Zepeck F, Gräwert T, Kaiser J, Schramek N, Eisenreich W, Bacher A, Rohdich F (2005) Biosynthesis of isoprenoids. Purification and properties of IspG protein from *Escherichia coli*. Journal of Organic Chemistry **70:** 9168-9174

Zhang R, Cruz JA, Kramer DM, Magallanes-Lundback ME, Dellapenna D, Sharkey TD (2009) Moderate heat stress reduces the pH component of the transthylakoid proton motive force in light-adapted, intact tobacco leaves. Plant, Cell and Environment **32:** 1538-1547

Zhang R, Sharkey TD (2009) Photosynthetic electron transport and proton flux under moderate heat stress. Photosynthesis Research **100:** 29-43

CHAPTER 3

The Metabolic Source of Post-illumination Isoprene Burst

Research work described in this chapter was originally published in Plant, Cell and Environment. (In press) **Li Z, Sharkey TD** (2012) Metabolic profiling of the methylerythritol phosphate pathway reveals the source of post-illumination isoprene burst. Plant, Cell and Environment

Abstract

The response of isoprene emission to environmental conditions in the short term is to a large extent regulated by levels of DMADP, produced by the methylerythritol phosphate pathway. However, there have been few studies to date on regulation of the MEP pathway in plants under physiological conditions. In this study I combined gas exchange techniques and HPLC-MS-MS and measured the profile of MEP pathway metabolites in leaves under different conditions. I report that in the MEP pathway, metabolites immediately preceding steps requiring reducing power were in high concentrations. Inhibition of the MEP pathway by fosmidomycin caused deoxyxylulose phosphate accumulation in leaves as expected. Evidence is presented that accumulation of MEP pathway intermediates, primarily methylerythritol cyclodiphosphate, is responsible for the post-illumination isoprene burst phenomenon. Pools of intermediate metabolites stayed at approximately the same level ten minutes after light was turned off, but declined eventually under prolonged darkness. In contrast, a strong inhibition of the second-to-last step of the MEP pathway caused suppression of isoprene emission in pure N_2. The energetics and regulation of the MEP pathway under physiological conditions is discussed.

Introduction

The methylerythritol phosphate (MEP) pathway is one of two pathways in plants responsible for the biosynthesis of dimethylallyl diphosphate (DMADP) and isopentenyl diphosphate (IDP), the building blocks of all isoprenoids including carotenoids, monoterpenes, and prenyl chains of chlorophylls and quinones (Fig. 3.1). The MEP pathway in plants is essential as it has been shown that mutants lacking this pathway were unable to develop functional chloroplasts (Mandel et al., 1996; Lois et al., 1998). MEP-pathway-derived DMADP also leads to the production of approximately 600 Tg of isoprene (C_5H_8) per year, or about $^1/_3$ of global hydrocarbon emission from all sources (Guenther et al., 2006). This biogenic isoprene contributes to tropospheric ozone formation (Chameides et al., 1988). However, relatively little is known about the regulation of the MEP pathway in plants.

A useful probe of the MEP pathway flux in vivo is isoprene emission. In emitting plant species, isoprene emission accounts for well over 90% of the flux through the MEP pathway (Sharkey et al., 1991). When light is turned off, isoprene emission from a leaf quickly declines to almost zero within 10 min, presumably because the MEP pathway requires energetic cofactors from the light reactions of photosynthesis (three ATP- and three NADPH-equivalents per C_5 molecule) (Sharkey et al., 2008). The integral of post-illumination isoprene emission has been proposed to reflect the pool size of plastidic DMADP (Rasulov et al., 2009). Interestingly, it had been observed in poplars and oaks that isoprene emission rises again in darkness before eventually falling off to zero on a longer time scale ("post-illumination burst") (Monson et al., 1991; Rasulov et al., 2010; Li et al., 2011; Rasulov et al., 2011). In a revisit to this phenomenon, I

hypothesized that a pool of intermediate metabolites in the MEP pathway may be trapped upon an almost instantaneous depletion of reducing power during the first few moments of darkness, and that these metabolites were later converted to isoprene as reducing power becomes available (Li et al., 2011). The size of the pool of metabolites giving rise to the post-illumination burst is comparable to the size of the DMADP pool and these two pools responded similarly to environmental variables (Li et al., 2011; Rasulov et al., 2011).

To understand the nature of post-illumination isoprene burst and gain insights into regulation of the MEP pathway, it would be useful to measure levels of leaf MEP pathway metabolites under physiological conditions. Some of the best efforts to date include studies using radioisotopes and ^{31}P-NMR studies. Using ^{31}P-NMR, it has been shown that methylerythritol cyclodiphosphate (MEcDP), a cyclic compound produced by MEcDP synthase (MDS, step 5), accumulates in leaves (Rivasseau et al., 2009; Mongélard et al., 2011). MEcDP was the only MEP pathway metabolite detectable by ^{31}P-NMR (Rivasseau et al., 2009).

In this study I present a method for profiling of MEP pathway metabolites in leaves based on high performance liquid chromatography-tandem mass spectrometry (HPLC-MS-MS). With the exception of diphosphocytidylyl methylerythritol phosphate (CDP-MEP), an unstable intermediate, all MEP pathway metabolites were successfully measured. I show that metabolites immediately before steps in the MEP pathway that require reducing power are in high concentrations while other metabolites are present in very low concentrations. The MEP pathway intermediate metabolites (MEcDP in particular) were the sources of post-illumination isoprene

burst. Leaves exposed to pure N_2 accumulated very high levels of MEcDP, suggesting the second-to-last step of the pathway was inhibited in the absence of both CO_2 and O_2.

Results

Separation and quantitation of MEP pathway metabolites by HPLC-MS-MS

To separate MEP pathway metabolites that are highly polar, I employed hydrophilic interaction chromatography (HILIC) using a zwitterionic stationary phase attached to polymeric beads. A binary gradient was used for separation of the metabolites (Table 3.1). Standards of MEP pathway metabolites eluted between 4.4 and 9.1 min (Fig. 3.2). DMADP and IDP could not be differentiated based on fragmentation patterns or by chromatography in this study. MEP pathway metabolites in leaves were extracted in a 3:1:1 acetonitrile-isopropanol-water buffer. This extraction buffer was chosen as it approximated the initial mobile phase and ensured rapid arrest of cellular metabolism at the same time (Weise S.E., Sutter A.E.., Banerjee A., Li Z. and Sharkey T.D., unpublished data). Recovery ratios of standards added to leaf samples were determined for each metabolite (Table 3.2). With the exception of CDP-MEP, all metabolites were recovered in leaves with good consistency (within 15% of standard error). Low recovery of CDP-MEP is likely due to the innate instability of this compound possibly because of the three high-energy phosphodiester bonds it contains.

Levels of MEP pathway metabolites in leaves during a light-to-dark switch

When light was switched off, isoprene emission from an aspen leaf initially declined (phase I) and then rose in the dark before declining again to approximately zero (phase II, Fig. 3.3a). To determine the source of the post-illumination isoprene burst, MEP pathway metabolites were measured in leaf samples taken at three time points: in light, 10 min into darkness (before the burst), and 40 min into darkness (after the burst) (Fig. 3.3a). In the light, three intermediate metabolites – deoxyxylulose phosphate (DXP), methylerythritol cyclodiphosphate (MEcDP) and hydroxymethylbutenyl diphosphate (HMBDP) – accumulated to significant levels (> 100 nmol m^{-2}). In particular, MEcDP measured 0.92 μmol m^{-2}. Levels of MEP and CDP-MEP were below limits of detection (LOD). Whole-leaf DMADP and IDP measured 0.79 μmol m^{-2} in total. After light was switched off for 10 min and isoprene emission declined to its first minimum (Fig. 3.3a), DMADP/IDP levels were reduced to 13% of previous levels in light. In contrast, levels of MEcDP were unaffected and slightly increased to 0.96 μmol m^{-2}. Levels of other metabolites were reduced to between 18% (CDP-ME) and 64% (HMBDP) of their respective levels under light. At 40 min into darkness the amount of all metabolites decreased, to between 3.6% (CDP-ME) and 18% (DXP) of their levels in light. The amount of isoprene emitted during phase II is compared with the amount of decrease in metabolites in phase II, in Fig. 3.3b, second panel.

Levels of MEP pathway metabolites in fosmidomycin-fed leaves, and leaves acclimated in pure N_2

Isoprene emission levels and MEP pathway metabolites were measured in leaves fed with 20 μM fosmidomycin for over 80 min (Fig. 3.4a). Fosmidomycin inhibits DXR, the enzyme catalyzing step 2 of the MEP pathway (Fig. 3.1). Isoprene emission of fosmidomycin-fed leaves was reduced by 93% compared with the control emission levels. DXP levels increased 40-fold in fosmidomycin-fed leaves while other downstream metabolites were reduced to between 16% (CDP-ME) and 38% (HMBDP) of their control levels (Fig. 3.4b).

Acclimation of a leaf in N_2 quickly inhibited isoprene emission, in a similar fashion to the suppression of isoprene emission by darkness (Fig. 3.5a). However, no "burst" was observed in N_2. A large overshoot in isoprene emission was observed when O_2 and CO_2 were switched back on, and isoprene emission was reduced by ~ 20% after N_2 treatment. The reduction in emission capacity following the N_2 treatment did not recover in two hours. In leaves acclimated in N_2, MEcDP increased 32-fold while DMADP/IDP decreased to 6% of control levels (Fig. 3.5b). Levels of other metabolites decreased to between 26% (CDP-ME) and 85% (DXP) of their respective controls.

Discussion

MEP pathway metabolites accumulate before steps requiring reducing equivalents

In leaves under standard conditions, DXP, MEcDP and HMBDP accumulated to significant levels (Fig. 3.3b). In particular, MEcDP accumulated to 0.92 μmol m^{-2}, or approximately 39 μM inside the chloroplasts using chloroplast volume estimated from (Winter et al., 1994). The metabolites shown to be accumulating here are precursors in steps of the MEP pathway that require reducing power. DXP is reduced by DXP reductoisomerase (DXR, step 2) to form MEP, a reaction that requires NADPH as a cofactor (Kuzuyama et al., 1998; Takahashi et al., 1998). Inhibition of this step by fosmidomycin led to accumulation of DXP and depletion of downstream metabolites in leaves (Fig. 3.4). The last two enzymes of the pathway convert MEcDP to HMBDP and then to IDP and DMADP in a 5:1 ratio (step 6 and 7). Both steps require reducing equivalents either directly from ferredoxin or in the form of NADPH (Charon et al., 1999; Hecht et al., 2001; Rohdich et al., 2002; Seemann et al., 2006; Seemann and Rohmer, 2007). The energetic status of leaves has long been proposed to regulate MEP pathway and isoprene emission (Monson and Fall, 1989; Loreto and Sharkey, 1990; Niinemets et al., 1999; Martin et al., 2000; Zimmer et al., 2000). A significant role for ATP was suggested (Loreto and Sharkey, 1990) but data reported here indicates that reducing power may be a key regulator of isoprene emission rate in leaves.

Intermediate metabolites in the MEP pathway can account for post-illumination isoprene burst

Upon darkening of a leaf, isoprene emission dropped rapidly to almost zero within 10 min (phase I, Fig. 3.3a). This decline in isoprene emission could be, in theory, caused by a decrease in 1) carbon input into the MEP pathway; 2) ATP levels; 3) ferredoxin levels or 4) levels of NADPH. In this study, I show that in phase I DMADP/IDP levels were reduced by 87% while MEcDP levels slightly increased. Under prolonged darkness (phase II), MEcDP eventually decreased to 12% of the level found in illuminated leaves. This suggests steps between MEcDP and DMADP/IDP (step 6 and 7) were blocked in phase I. This blockage was reversed over time, and intermediate metabolites in the MEP pathway were metabolized to isoprene leading to the post-illumination isoprene burst in phase II.

Step 6 in the MEP pathway, catalyzed by the iron-sulfur protein HMBDP synthase (HDS), is tightly coupled to photosynthesis (Seemann et al., 2002; Seemann et al., 2006). In contrast to its homolog in *E. coli*, the plant HDS cannot use the NADPH/flavodoxin/flavodoxin reductase system, but instead could use isolated thylakoid preparations as the sole electron donor upon illumination (Seemann et al., 2005; Seemann et al., 2006). Reducing power required by HDS in light can be directly shuttled via ferredoxin from electron transport of the light reactions and in the absence of NADPH (Okada and Hase, 2005; Seemann and Rohmer, 2007). Therefore, it is likely that this step is rapidly slowed down (incompletely inhibited) upon darkness, trapping the MEcDP pool. Over time, this inhibition is relieved as HDS switches to NADPH as its electron source in dark (Seemann and Rohmer, 2007). NADPH could be low immediately after switching the light off and then be replenished through the pentose phosphate pathway. The first step in the

pentose phosphate pathway catalyzed by plastidic glucose-6-phosphate dehydrogenase is redox sensitive and is activated in darkness by oxidation (Lendzian and Ziegler, 1970; Wenderoth et al., 1997). The levels of DXP and HMBDP were decreased by less than 50% in phase I, while other metabolites (CDP-ME and DMADP/IDP) showed much larger reductions, suggesting step 2 and step 7 were also slowed down in phase I consistent with control by redox status. It is likely that no new carbon came into the MEP pathway in darkness, otherwise additional isoprene emission would have been observed.

The DMADP/IDP measured in this study includes both plastidic and cytosolic pools. It is generally accepted that the darkness-labile or fosmidomycin-labile part of DMADP/IDP pool is in the chloroplasts, while the remaining portion is of cytosolic origin (Rosenstiel et al., 2002). The integral of isoprene emission during phase I has also been hypothesized to be a measure of the plastidic DMADP pool in vivo (Rasulov et al., 2009). In this study, I show that the size of post-illumination burst (integrated emission in phase II) agrees well with the sum of the metabolic intermediates that are lost during the burst (Fig. 3.3b). The size of plastidic DMADP pool measured in the current study is in good agreement with previous reports (Behnke et al., 2007; Rasulov et al., 2009).

Acclimation in nitrogen turns off isoprene emission by inhibiting the second-to-last step of the MEP pathway

It has been reported long ago that isoprene emission is rapidly abolished in pure N_2 (Fig. 3.5a) (Loreto and Sharkey, 1993). The suppression of isoprene production in N_2 is not due to a

limitation on carbon supply as isoprene emission is much less affected in CO_2-free air in which photorespiration would cause a significantly more negative carbon balance (Loreto and Sharkey, 1990). In leaves acclimated in N_2, MEcDP accumulated to very high levels while DMADP decreased by over 90%. Leaves followed for 1 hour in N_2 did not show a second burst, indicating that inhibited flow through step 6 cannot be reestablished during sustained exposure to N_2 the way it can be in sustained darkness (Fig. 3.5b). The subsequent overshoot in isoprene emission when O_2 and CO_2 were restored to the air around the leaf presumably came from accumulated MEcDP. In the absence of O_2 and CO_2, Rubisco will be inactive resulting in very little sink for electrons from photosynthetic electron transport. The NADP-malate dehydrogenase activation state can be used as a proxy for plastidic redox status and it has been shown that NADP malate dehydrogenase in *Phaseolus vulgaris* leaves exposed to a nitrogen atmosphere becomes fully activated (Scheibe, 1987; Weise et al., 2006). I suggest that in N_2 the redox poise of the cell is disrupted causing a depletion of reducing equivalents required for step 6; alternatively, the [4Fe-4S] cluster of HDS is oxygen sensitive (Seemann et al., 2005; Rivasseau et al., 2009), and perhaps it suffered from increased turnover rate. This is supported by the observation that, following an initial burst of isoprene emission upon returning to air, emission capacity was irreversibly reduced (Fig. 3.5a).

In conclusion, I show that darkness and N_2 inhibit MEP pathway at the same step (step 6) in a different fashion. Profiling of the MEP pathway metabolites suggest this step and the two other steps requiring reducing power are likely the points of regulation of isoprene emission under different environment conditions. Indeed, flux through HDS measured by ^{31}P-NMR positively correlates with light intensity and temperature (Mongélard et al., 2011). Understanding the

regulation of MEP pathway has important practical implications, as the MEP pathway in bacteria and pathogens represent an ideal therapeutic target for development of new drugs. In addition, there is a growing interest in metabolic engineering of the MEP pathway to produce compounds of important medical and commercial values, such as taxol, vitamins and biofuels.

Materials and methods

Plant material

Hybrid aspen (*Populus tremula* × *alba*) grown in Michigan State University greenhouses were used for this study. Unless otherwise stated, whole plants were brought into the lab in insulated transporters and attached leaves were used for gas exchange experiments. In the fosmidomycin-feeding experiment where detached leaves were used, the leaf was swiftly cut at the base of the petiole with a fresh razor blade, and then immediately recut underwater and transported to a floral tube underwater.

Gas exchange experiments

The experimental setup for gas exchange were described by Li et al. (2011). Synthetic air of 80% N_2 and 20% O_2 was mixed using mass flow controllers and supplied to a LI-6400 Portable Photosynthesis System (LI-COR Biosciences, Lincoln, NE), where CO_2 was added to bring the

air to 400 ppm CO_2. A custom-built leaf cuvette was put in-line with the LI-6400 chamber to allow real-time monitoring and recording of gas exchange parameters (e.g. carbon assimilation, transpiration and C_i). The exhaust gas of LI-6400 was connected to a Fast Isoprene Sensor (FIS, Hills Scientific, Boulder, CO) where simultaneous isoprene measurements were made. Air was humidified by passing an adjustable portion of N_2 through a humidifier. Cuvette temperature was controlled by passing water from a water bath through the leaf chamber. Leaf temperature was monitored using a thermocouple wired from LI-6400 into the leaf cuvette. The light source was an SL3500 white light emitting diode array (Photon Systems Instruments, Drasov, Czech Republic). All leaves were acclimated at standard conditions (30°C leaf temperature, 1,000 μmol m^{-2} s^{-1} photosynthetic photon flux density at leaf level) for at least one hour before the start of an experiment.

Extraction of leaf metabolites

During a gas exchange experiment, the leaf was quickly taken out of the cuvette and immediately frozen in liquid N_2. The whole leaf was then ground up in liquid N_2 and extracted with 3:1:1 acetonitrile-isopropanol-50 mM ammonium acetate in dH_2O (adjusted to pH 10 with ammonium hydroxide). The leaf extract was centrifuged at 14,000 x *g* for 10 min and the supernatant was stored at -80°C for later analysis.

High performance liquid chromatography-tandem mass spectrometry (HPLC-MS-MS)

Metabolites of the MEP pathway were separated and quantified on a ZIC-*p*HILIC column (Merck SeQuant, Umeå, Sweden) fitted to a 3200 Q-TRAP mass spectrometer (Applied Biosystems, Carlsbad, CA) that was coupled with two LC-20AD HPLC pumps and a SIL-HTc autosampler (Shimadzu, Kyoto, Japan). Standards of MEP pathway metabolites were separated using a binary gradient consisting of 50 mM ammonium acetate adjusted to pH 10.0 with ammonium hydroxide (solvent A) and acetonitrile (solvent B) (Table 3.1). Electrospray ionization (ESI) in negative ion mode was used. Enhanced product ion scans were first run to assess fragmentation patterns and determine the optimal product ions for monitoring. Compound-dependent MS parameters were then optimized by repeated injection of standards with analysis using a range of instrument parameters including source temperatures, and transport and collision potentials (Table 3.3). Mass spectra were acquired in multiple reaction monitoring mode for the optimized precursor/product ion pairs (Fig. 3.1).

Since isotope-labeled standards were not commercially available, metabolite levels in leaf samples were quantified based on linearly fitted curves of unlabeled external standards. Standards of MEP pathway metabolites, including DXP, MEP, CDP-ME, MEcDP, HMBDP, DMADP and IDP were acquired from Echelon Biosciences. Due to their short shelf life under even deep freeze conditions, CDP-MEP standards were freshly prepared from CDP-ME, by the CMK-catalyzed reaction using a CDP-MEP Synthesis Kit (Echelon Biosciences, Logan, UT). Newly synthesized CDP-MEP was quantified in two ways, by measuring ATP consumption and

CDP-ME consumption in the reaction. All other reagents used were analytical or HPLC grade and used without further purification.

Quality control and data analysis

Recovery ratios were determined by spiking of leaf samples with authentic standards. For paired comparisons, leaves frozen in liquid N_2 were divided into two similar-sized fractions, one of which was spiked during the grinding step. The unspiked sample was then normalized to the pellet weight of the spiked sample for determination of endogenous metabolite levels. Recovery ratios have been taken into account in data presented in this paper. Limits of detection (LOD) were defined as the lowest concentrations that gave a signal-to-noise ratio of two. One-way analysis of variance and unpaired *t* tests ($P < 0.05$) were used to detect significant differences between groups. Statistical analyses were carried out in Origin (OriginLab, Northampton, MA).

Acknowledgements

I thank Dr. Frank Telewski for providing poplar trees; Drs. A. Daniel Jones, Chao Li and Lijun Chen for assistance with LC-MS-MS; Echelon Biosciences for the gift of CDP-MEP synthesis kit; and Alex Corrion and Dr. Sean E. Weise for assistance with gas exchange experiments. This work was supported by National Science Foundation Grant IOS-0950574 to T.D.S.

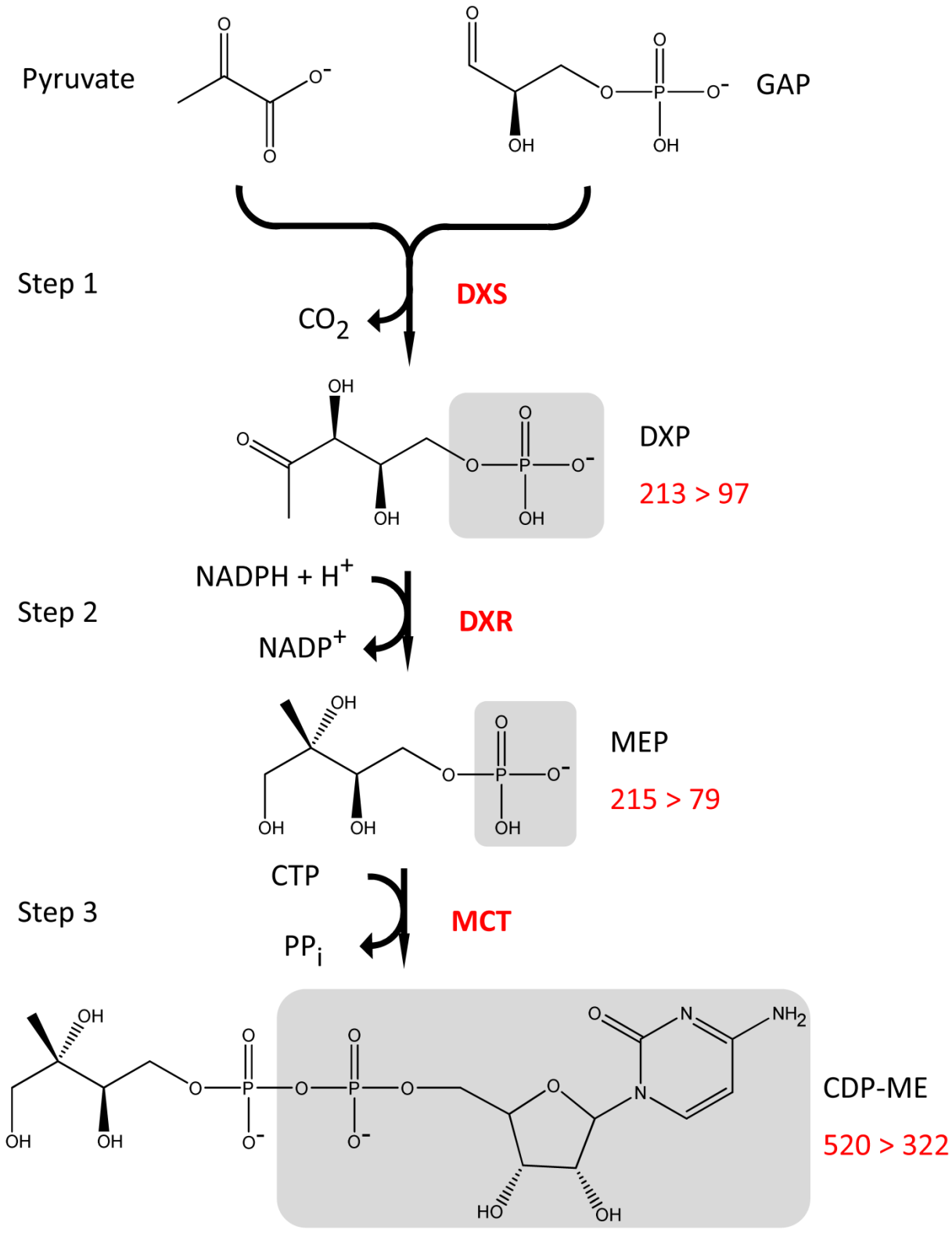

Figure 3.1 Metabolites in the MEP pathway. GAP, glyceraldehyde 3-phosphate; DXS, deoxyxylulose phosphate (DXP) synthase; DXR, DXP reductoisomerase; MEP, methylerythritol

(Figure 3.1 continued)

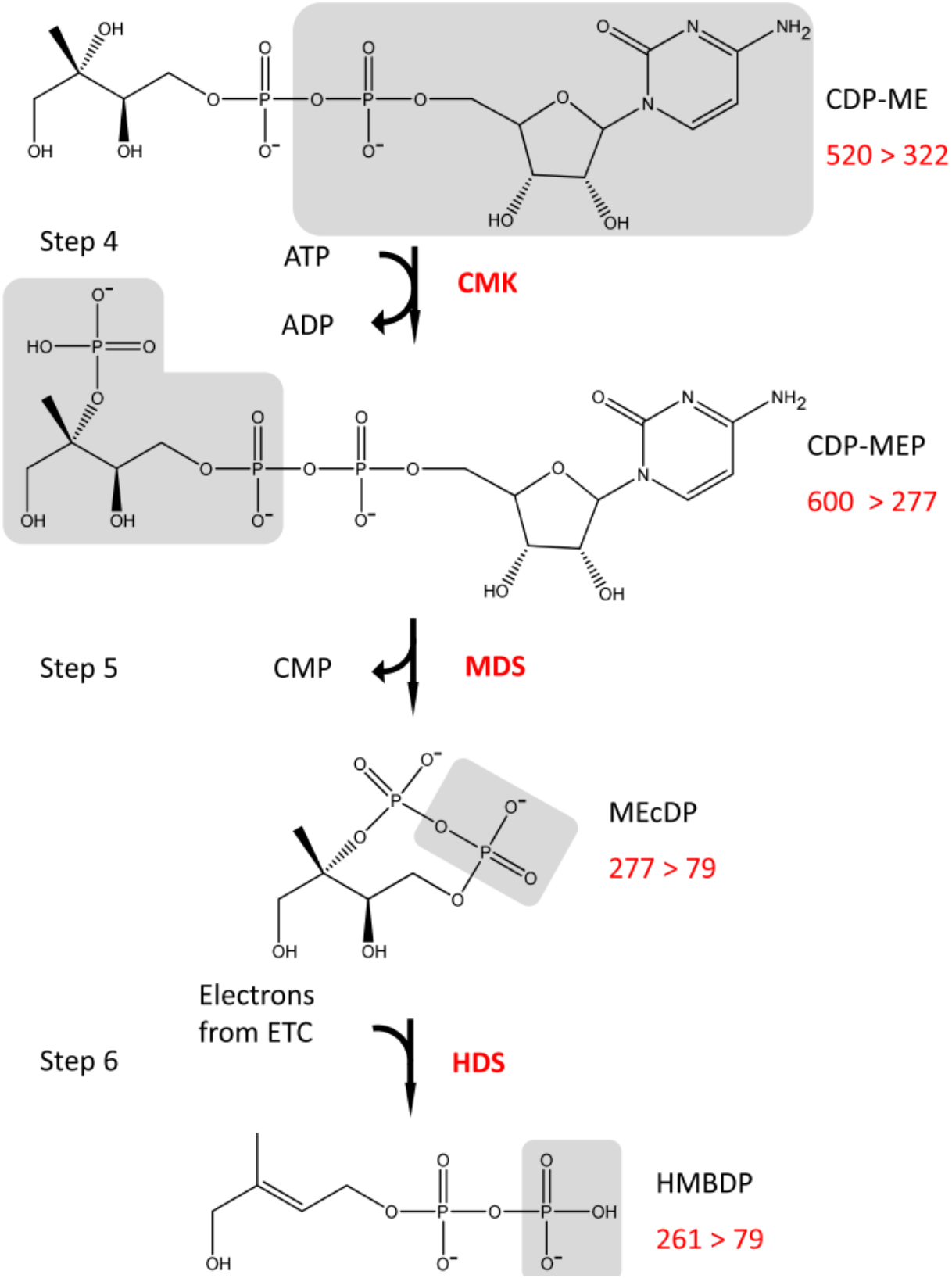

(Figure 3.1 continued)

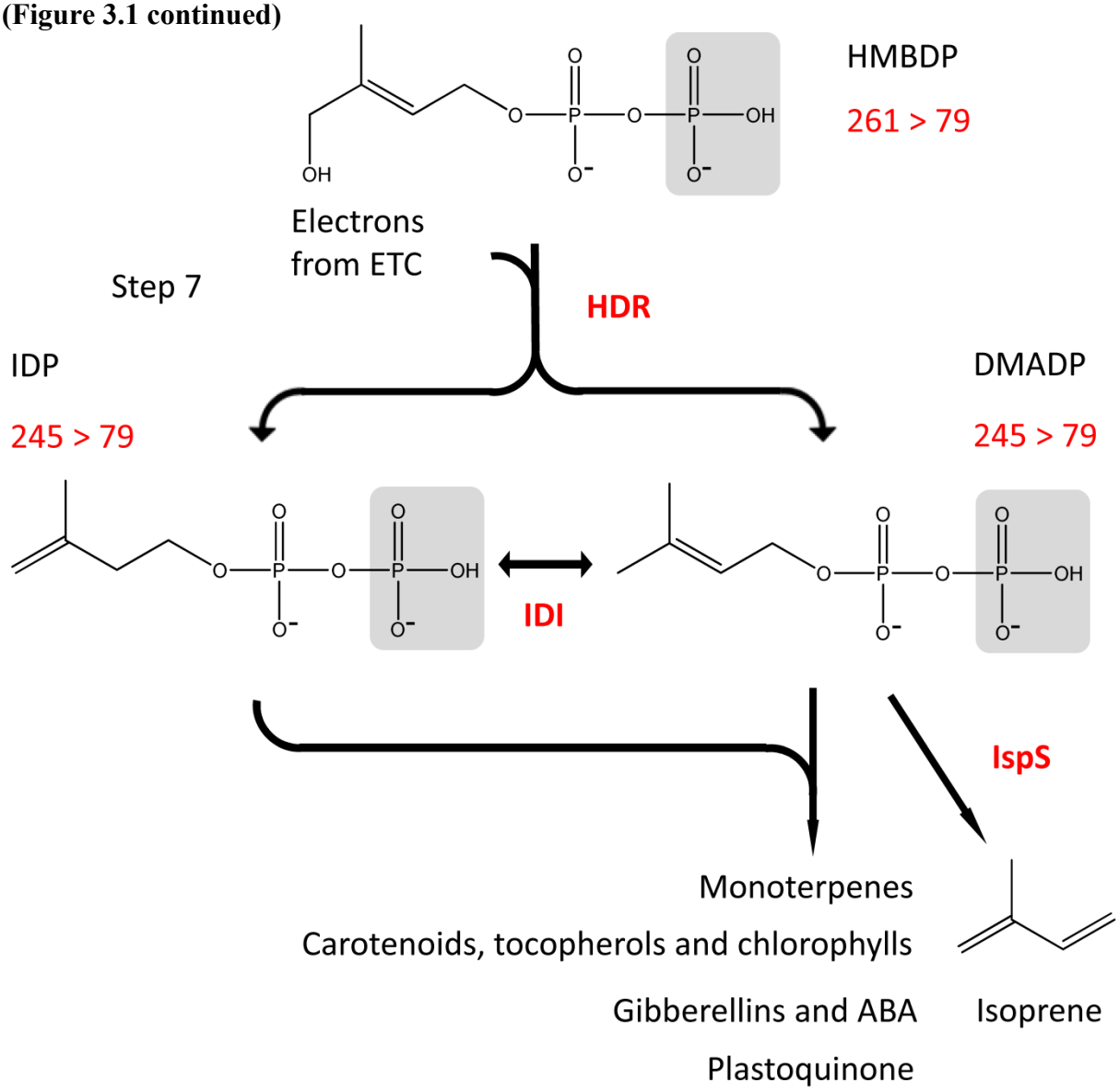

phosphate; CTP, cytidine triphosphate; PP_i, inorganic diphosphate; MCT, MEP cytidylyltransferase; CDP-ME, diphosphocytidylyl methylerythritol; CMK, CDP-ME kinase; CDP-MEP, CDP-ME phosphate; CMP, cytidine monophosphate; MDS, methylerythritol cyclodiphosphate (MEcDP) synthase; ETC, electron transport chain; HDS, hydroxymethylbutenyl diphosphate (HMBDP) synthase; HDR, HMBDP reductase; IDP, isopentenyl diphosphate; IDI, IDP isomerase; DMADP, dimethylallyl diphosphate; IspS, isoprene synthase. Names of the metabolites and enzymes follow suggested nomenclature in Phillips *et al.* (2008). The mass-to-charge ratios (m/z) of precursor and product ions used in this study are indicated beside the names of each metabolite. Product ions are shaded in grey background.

Table 3.1 Solvent composition used in the binary gradient for elution of MEP pathway metabolites. Solvent A, 50mM ammonium acetate adjusted to pH 10 with ammonium hydroxide; Solvent B, acetonitrile.

Time (min)	A (%)	B (%)
0.00	20	80
2.00	20	80
2.01	30	70
6.50	30	70
7.50	60	40
10.00	60	40
10.01	20	80
15.00	20	80

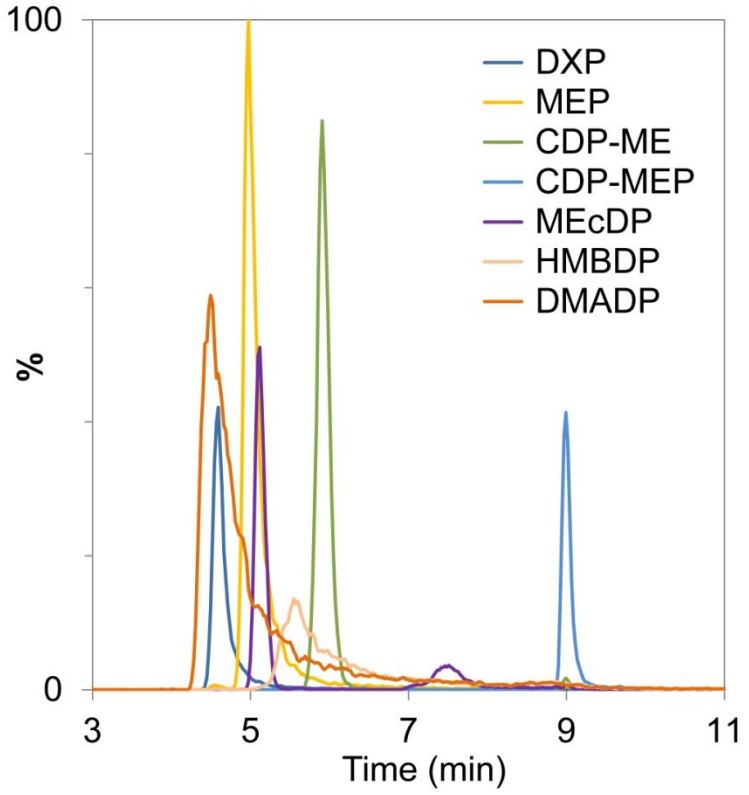

Figure 3.2 Chromatogram of 10 µM standards of MEP pathway metabolites. The standards were separated on a hydrophilic (HILIC) column with a zwitterionic stationary phase. DMADP and IDP could not be differentiated based on fragmentation patterns in this study.

Table 3.2 Retention time and recovery ratios of MEP pathway metabolites in leaf extract. Each number in recovery ratios denotes the mean ± SE (n = 7).

	DXP	MEP	CDP-ME	CDP-MEP	MEcDP	HMBDP	DMADP/IDP
Retention time (min)	4.6	4.9	5.9	9.0	5.1	5.6	4.4
Recovery ratios (%)	67.2 ± 4.0	26.7 ± 1.7	60.7 ± 3.7	3.1 ± 0.4	41.5 ± 4.9	15.5 ± 2.2	18.8 ± 2.5

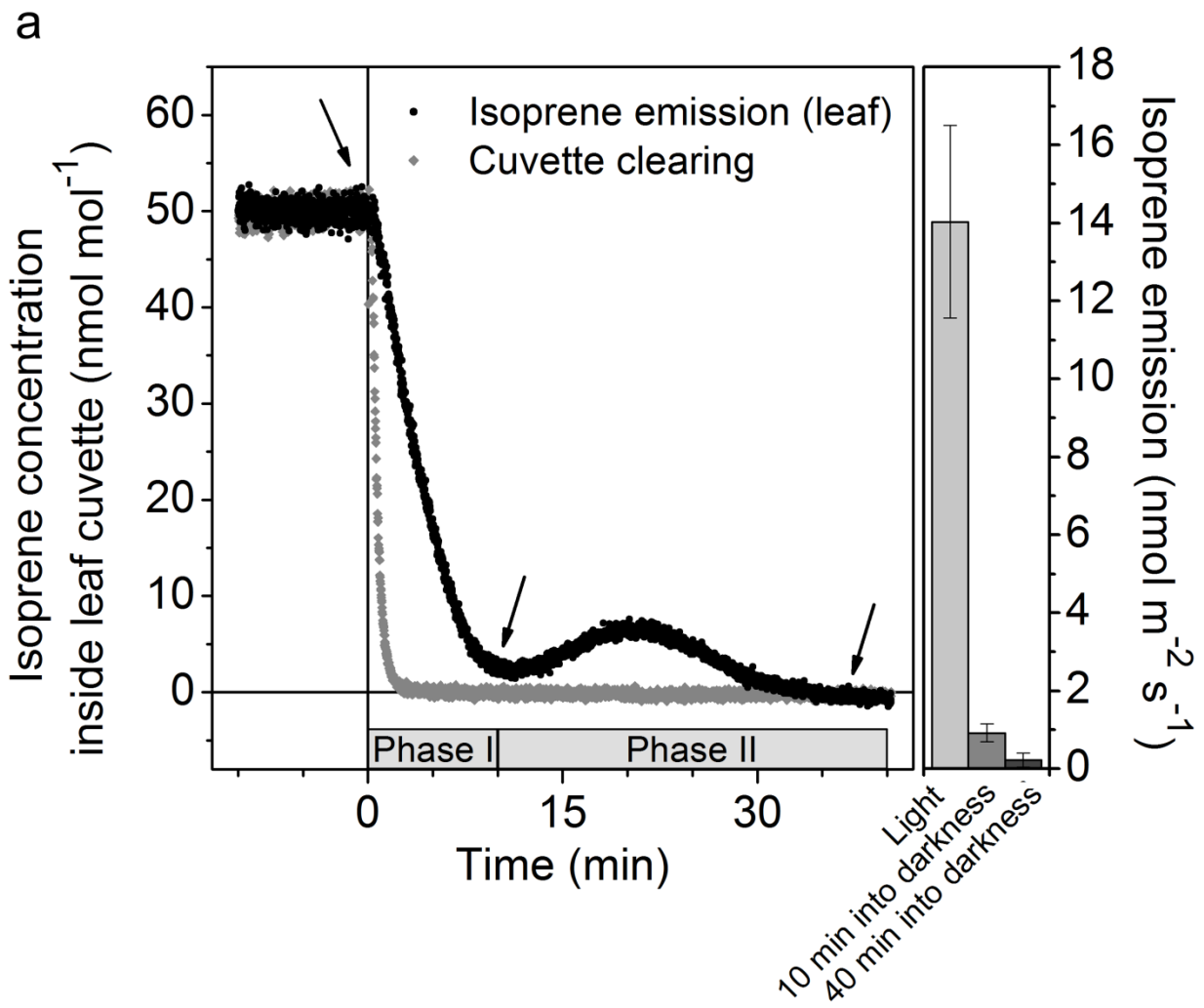

Figure 3.3 MEP pathway metabolites measured during a light-to-dark switch. (a) A typical trace of post-illumination isoprene emission from an aspen leaf under standard conditions. Light was turned off at time 0. Isoprene emission declined rapidly in the first 10 minutes (phase I), and then rose in the dark before dropping off again within 40 minutes ("post-illumination isoprene burst", phase II). Grey-colored data points show clearing of isoprene from the leaf cuvette (a property that depended on flow rate and the gas exchange system itself) used as the reference for integration of post-illumination isoprene emission. The clearing data were generated by first feeding a steady flow of isoprene standard into an empty cuvette, and then immediately withdrawing the isoprene source at the leaf cuvette at time 0. The baseline of the clearing trace was then normalized to isoprene emission from the leaf. Samples were harvested at three time points indicated by the arrows and isoprene emission levels immediately before harvest are shown. (b) Levels of MEP pathway metabolites in leaves harvested at time points shown in (a). LOD = limit of detection. Each column denotes the mean ± SE (n = 3 - 4). The differences in intermediate metabolite levels between the 10 min and 40 min darkness samples were summed and plotted with integrated isoprene emission from phase II in the second panel of (b). CDP-ME contributed a negligible portion (< 0.3%) of the intermediate metabolite pool shown here.

(Figure 3.3 continued)

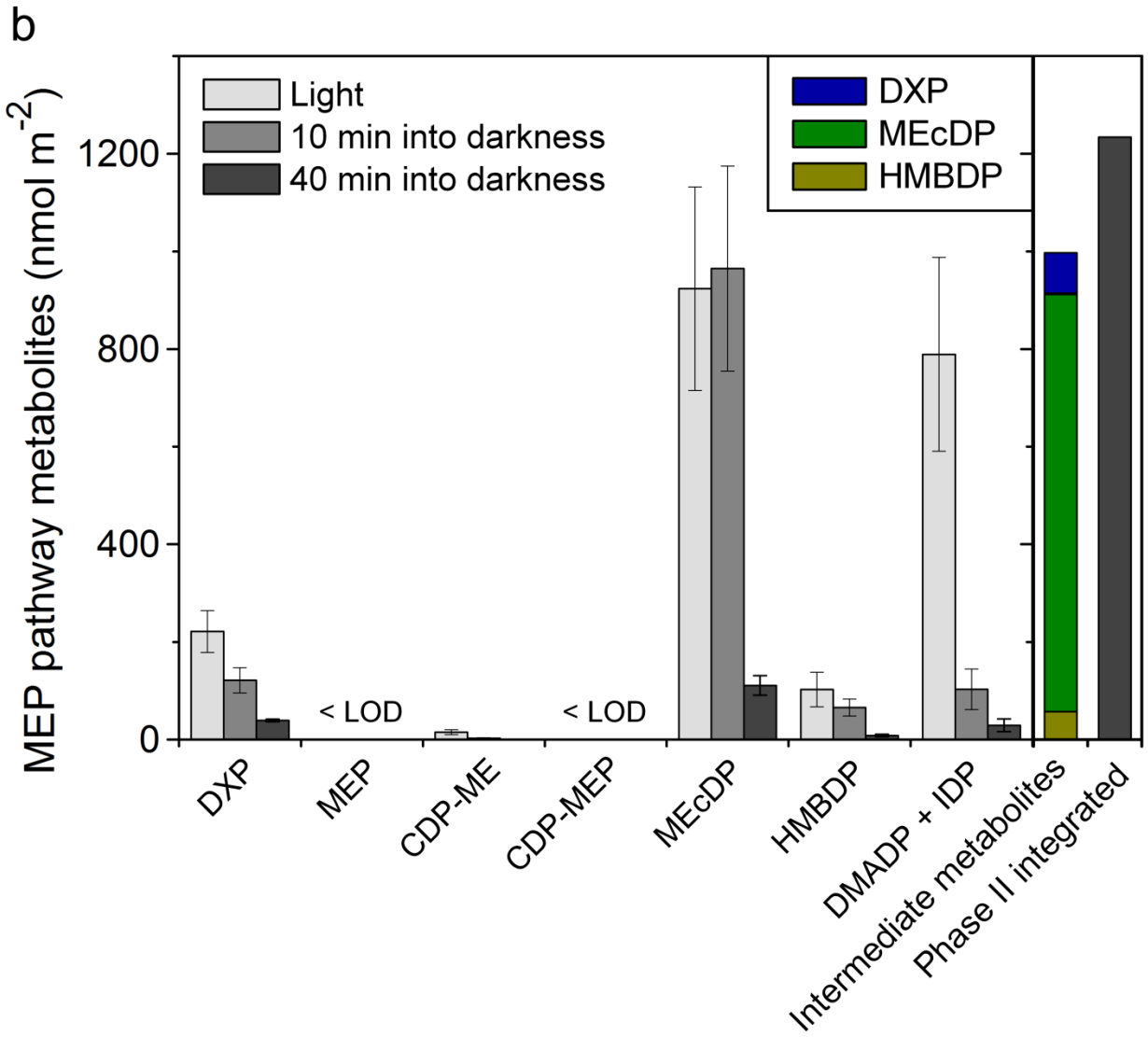

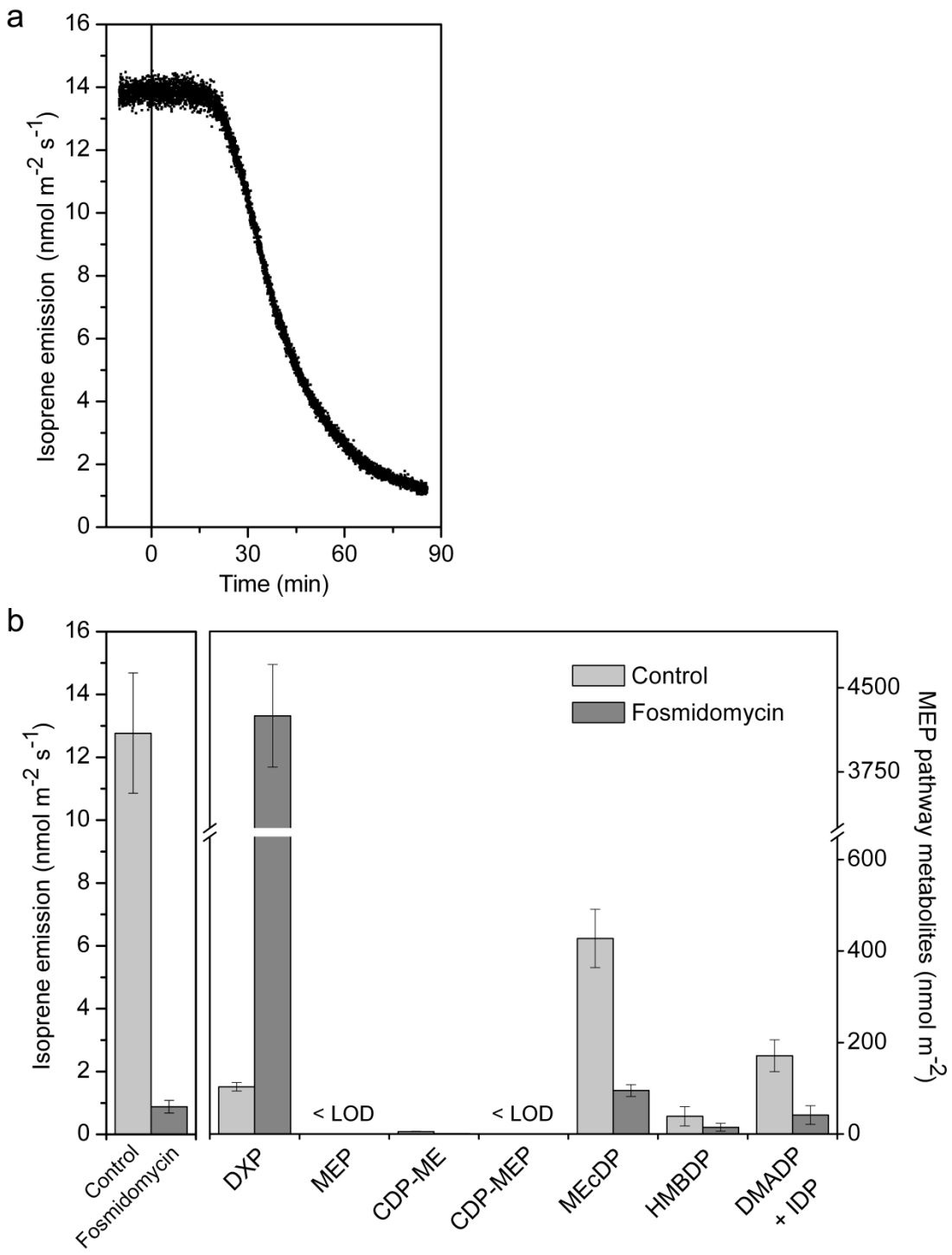

Figure 3.4 Isoprene emission and levels of MEP pathway metabolites in fosmidomycin-fed leaves. (a) Isoprene emission from an aspen leaf fed with 20 μM fosmidomycin for > 80 min. Fosmidomycin feeding was initated at time 0. (b) Levels of isoprene emission and MEP pathway metabolites in fosmidomycin-fed leaves vs. control (detached leaves fed with distilled H_2O). Continuous water column in vascular tissues was maintained by recutting the petiole underwater in both groups. Each column denotes the mean ± SE (n = 3 - 4).

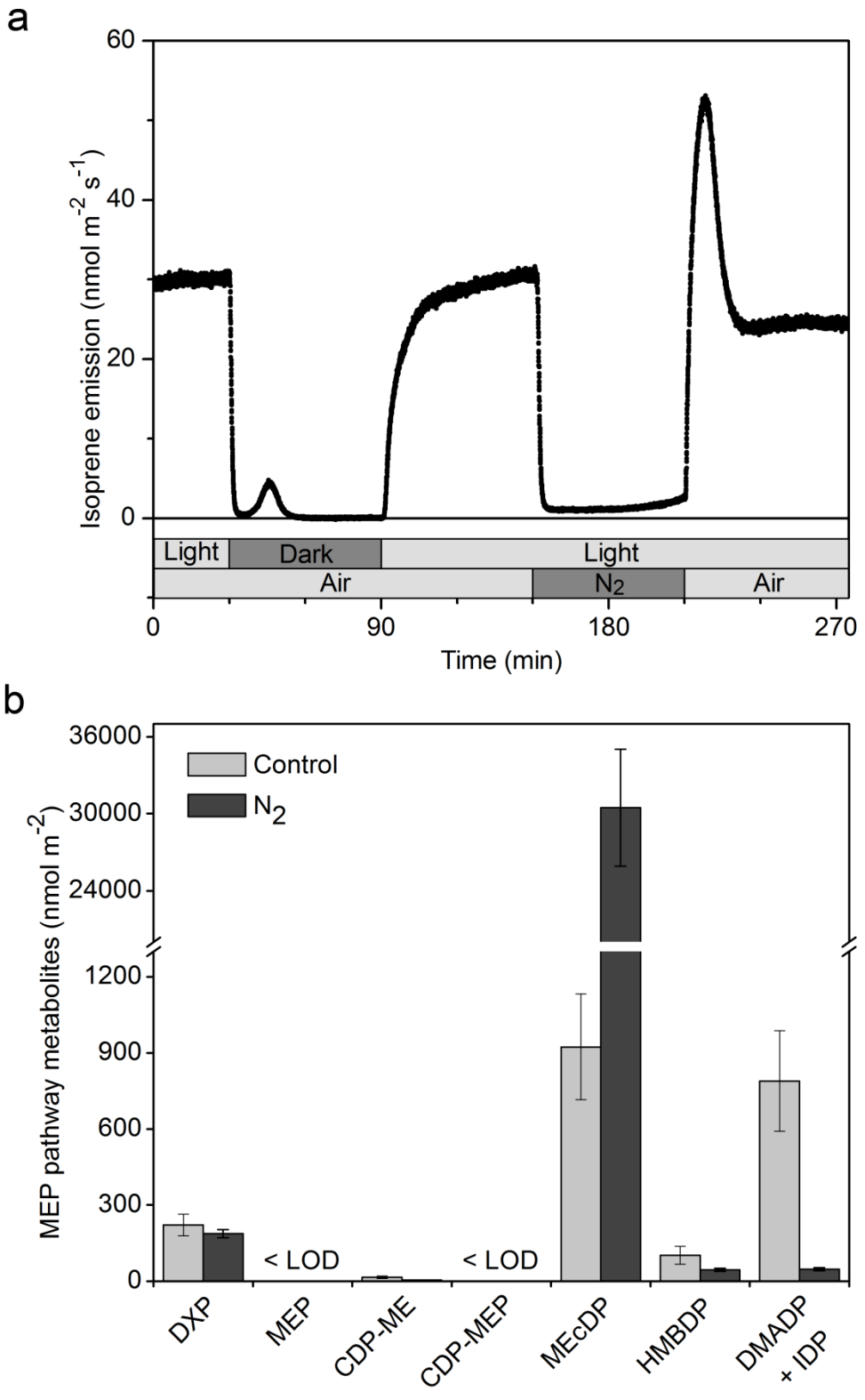

Figuire 3.5 Isoprene emission and levels of MEP pathway metabolites in leaves exposed to pure N_2. (a) Isoprene emission from an aspen leaf in darkness vs. in pure N_2. Light was turned

(Figure 3.5 continued)

off at t = 30 min and turned back on at t = 90 min. CO_2 and O_2 was simultaneously turned off at t = 150 min and turned back on at t = 210 min. Isoprene emission capacity was reduced by ~ 20% after N_2 treatment and did not recover when followed for 2 hours. Similar observations have been repeated three times. (b) Levels of MEP pathway metabolites in leaves acclimated in synthetic air (> 1 hr, control) and acclimated then exposed to N_2 (15 mins). Each column denotes the mean ± SE (n = 3 - 4). Control group used in this experiment was the same control used for light-to-dark transition experiment (Fig. 3.2).

Table 3.3 Compound-dependent parameters used in acquisition of mass spectra of MEP pathway metabolites.

Metabolites (m/z of precursor > product)	Declustering potential (V)	Collision energy (V)
DXP (213 > 97)	-30	-20
MEP (215 > 79)	-30	-25
CDP-ME (520 > 322)	-40	-30
CDP-MEP (600 > 277)	-40	-30
MEcDP (277 > 79)	-20	-35
HMBDP (261 > 79)	-40	-30
DMADP, IDP (245 > 79)	-25	-35

LITERATURE CITED

LITERATURE CITED

Behnke K, Ehlting B, Teuber M, Bauerfeind M, Louis S, Hansch R, Polle A, Bohlmann J, Schnitzler JP (2007) Transgenic, non-isoprene emitting poplars don't like it hot. Plant Journal **51:** 485-499

Chameides WL, Lindsay RW, Richardson J, Kiang CS (1988) The role of biogenic hydrocarbons in urban photochemical smog: Atlanta as a case study. Science **241:** 1473-1475

Charon L, Pale-Grosdemange C, Rohmer M (1999) On the reduction steps in the mevalonate independent 2-C-methyl-D-erythritol 4-phosphate (MEP) pathway for isoprenoid biosynthesis in the bacterium *Zymomonas mobilis*. Tetrahedron Letters **40:** 7231-7234

Guenther A, Karl T, Harley P, Wiedinmyer C, Palmer PI, Geron C (2006) Estimates of global terrestrial isoprene emissions using MEGAN (Model of Emissions of Gases and Aerosols from Nature). Atmospheric Chemistry and Physics Discussions **6:** 107–173

Hecht S, Eisenreich W, Adam P, Amslinger S, Kis K, Bacher A, Arigoni D, Rohdich F (2001) Studies on the nonmevalonate pathway to terpenes: the role of the GcpE (IspG) protein. Proceedings of the National Academy of Sciences of the United States of America **98:** 14837-14842

Kuzuyama T, Takahashi S, Watanabe H, Seto H (1998) Direct formation of 2-C-methyl-D-erythritol 4-phosphate from 1-deoxy-D-xylulose 5-phosphate by 1-deoxy-D-xylulose 5-phosphate reductoisomerase, a new enzyme in the non-mevalonate pathway to isopentenyl diphosphate. Tetrahedron Letters **39:** 4509-4512

Lendzian K, Ziegler H (1970) Über die Regulation der Glucose-6-phosphat-Dehydrogenase in Spinatchloroplasten durch licht. Planta **94:** 27-36

Li Z, Ratliff EA, Sharkey TD (2011) Effect of temperature on post-illumination isoprene emission in oak and poplar. Plant Physiology **155:** 1037-1046

Lois LM, Campos N, Putra SR, Danielsen K, Rohmer M, Boronat A (1998) Cloning and characterization of a gene from *Escherichia coli* encoding a transketolase-like enzyme that catalyzes the synthesis of d-1-deoxyxylulose 5-phosphate, a common precursor for isoprenoid, thiamin, and pyridoxol biosynthesis. Proceedings of the National Academy of Sciences **95:** 2105-2110

Loreto F, Sharkey TD (1990) A gas-exchange study of photosynthesis and isoprene emission in *Quercus rubra* L. Planta **182:** 523-531

Loreto F, Sharkey TD (1993) On the relationship between isoprene emission and photosynthetic metabolites under different environmental conditions. Planta **189:** 420-424

Mandel MA, Feldman KA, Herrera-Estrella L, Rocha-Sosa M, León P (1996) CLA1, a novel gene required for chloroplast development, is highly conserved in evolution. Plant Journal **9:** 649-658

Martin MJ, Stirling CM, Humphries SW, Long SP (2000) A process-based model to predict the effects of climatic change on leaf isoprene emission rates. Ecological Modelling **131:** 161-174

Mongélard G, Seemann M, Boisson A-M, Rohmer M, Bligny R, Rivasseau C (2011) Measurement of carbon flux through the MEP pathway for isoprenoid synthesis by ^{31}P-NMR spectroscopy after specific inhibition of 2-C-methyl-d-erythritol 2,4-cyclodiphosphate reductase. Effect of light and temperature. Plant, Cell and Environment **34:** 1241-1247

Monson RK, Fall R (1989) Isoprene emission from aspen leaves: influence of environment and relation to photosynthesis and photorespiration. Plant Physiology **90:** 267-274

Monson RK, Hills AJ, Zimmerman PR, Fall RR (1991) Studies of the relationship between isoprene emission rate and CO_2 or photon-flux density using a real-time isoprene analyser. Plant, Cell and Environment **14:** 517-523

Niinemets Ü, Tenhunen JD, Harley PC, Steinbrecher R (1999) A model of isoprene emission based on energetic requirements for isoprene synthesis and leaf photosynthetic properties for *Liquidambar* and *Quercus*. Plant, Cell and Environment **22:** 1319-1335

Okada K, Hase T (2005) Cyanobacterial non-mevalonate pathway: (E)-4-hydroxy-3-methylbut-2-enyl diphosphate synthase interacts with ferredoxin in *Thermosynechococcus elongatus* BP-1. Journal of Biological Chemistry **280:** 20672-20679

Phillips MA, León P, Boronat A, Rodríguez-Concepción M (2008) The plastidial MEP pathway: unified nomenclature and resources. Trends in Plant Science **13:** 619-623

Rasulov B, Copolovici L, Laisk A, Niinemets Ü (2009) Postillumination isoprene emission: in vivo measurements of dimethylallyldiphosphate pool size and isoprene synthase kinetics in aspen leaves. Plant Physiology **149:** 1609-1618

Rasulov B, Hüve K, Bichele I, Laisk A, Niinemets Ü (2010) Temperature response of isoprene emission in vivo reflects a combined effect of substrate limitations and isoprene synthase activity: a kinetic analysis. Plant Physiology **154:** 1558-1570

Rasulov B, Hüve K, Laisk A, Niinemets Ü (2011) Induction of a longer term component of isoprene release in darkened aspen leaves: origin and regulation under different environmental conditions. Plant Physiology **156:** 816-831

Rivasseau C, Seemann M, Boisson A-M, Streb P, Gout E, Douce R, Rohmer M, Bligny R (2009) Accumulation of 2-C-methyl-D-erythritol 2,4-cyclodiphosphate in illuminated plant leaves at supraoptimal temperatures reveals a bottleneck of the prokaryotic

methylerythritol 4-phosphate pathway of isoprenoid biosynthesis. Plant, Cell and Environment **32:** 82-92

Rohdich F, Hecht S, Gärtner K, Adam P, Krieger C, Amslinger S, Arigoni D, Bacher A, Eisenreich W (2002) Studies on the nonmevalonate terpene biosynthetic pathway: metabolic role of IspH (LytB) protein. Proceedings of the National Academy of Sciences of the United States of America **99:** 1158-1163

Rosenstiel TN, Fisher AJ, Fall R, Monson RK (2002) Differential accumulation of dimethylallyl diphosphate in leaves and needles of isoprene- and methylbutenol-emitting and nonemitting species. Plant Physiology **129:** 1276-1284

Scheibe R (1987) $NADP^+$ malate dehydrogenase in C3 plants: Regulation and role of a light-activated enzyme. Physiologia Plantarum **71:** 393-400

Seemann M, Bui BTS, Wolff M, Tritsch D, Campos N, Boronat A, Marquet A, Rohmer M (2002) Isoprenoid biosynthesis through the methylerythritol phosphate pathway: the (E)-4-hydroxy-3 methylbut-2-enyl diphosphate synthase (GcpE) is a [4Fe-4S] Protein. Angewandte Chemie International Edition **41:** 4337-4339

Seemann M, Rohmer M (2007) Isoprenoid biosynthesis via the methylerythritol phosphate pathway: GcpE and LytB, two novel iron-sulphur proteins. Comptes Rendus Chimie **10:** 748-755

Seemann M, Tse Sum Bui B, Wolff M, Miginiac-Maslow M, Rohmer M (2006) Isoprenoid biosynthesis in plant chloroplasts via the MEP pathway: direct thylakoid/ferredoxin-dependent photoreduction of GcpE/IspG. FEBS Letters **580:** 1547-1552

Seemann M, Wegner P, Schünemann V, Bui BTS, Wolff M, Marquet A, Trautwein AX, Rohmer M (2005) Isoprenoid biosynthesis in chloroplasts via the methylerythritol phosphate pathway: the (E)-4-hydroxy-3-methylbut-2-enyl diphosphate synthase (GcpE) from *Arabidopsis thaliana* is a [4Fe-4S] protein. Journal of Biological Inorganic Chemistry **10:** 131-137

Sharkey TD, Loreto F, Delwiche CF (1991) The biochemistry of isoprene emission from leaves during photosynthesis. *In* TD Sharkey, EA Holland, HA Mooney, eds, Trace Gas Emissions by Plants. Academic Press, San Diego, pp 153-184

Sharkey TD, Wiberley AE, Donohue AR (2008) Isoprene emission from plants: why and how. Annals of Botany **101:** 5-18

Takahashi S, Kuzuyama T, Watanabe H, Seto H (1998) A 1-deoxy-D-xylulose 5-phosphate reductoisomerase catalyzing the formation of 2-C-methyl-D-erythritol 4-phosphate in an alternative nonmevalonate pathway for terpenoid biosynthesis. Proceedings of the National Academy of Sciences of the United States of America **95:** 9879-9884

Weise SE, Schrader SM, Kleinbeck KR, Sharkey TD (2006) Carbon balance and circadian regulation of hydrolytic and phosphorolytic breakdown of transitory starch. Plant Physiology **141:** 879-886

Wenderoth I, Scheibe R, von Schaewen A (1997) Identification of the cysteine residues involved in redox modification of plant plastidic glucose-6-phosphate dehydrogenase. Journal of Biological Chemistry **272:** 26985-26990

Winter H, Robinson DG, Heldt HW (1994) Subcellular volumes and metabolite concentrations in spinach leaves. Planta **193:** 530-535

Zimmer W, Brüggemann N, Emeis S, Giersch C, Lehning A, Steinbrecher R, Schnitzler JP (2000) Process-based modelling of isoprene emission by oak leaves. Plant, Cell and Environment **23:** 585-595

CHAPTER 4

Conclusions and Future Directions

Part of this chapter was adapted from the following submitted manuscript.
Li Z, Sharkey TD (2012) Biochemical and molecular controls of volatile organic carbon emissions. *In* Biology, controls and models of tree volatile organic compound emissions. Springer, Berlin. http://www.springer.com/series/6644

Introduction

Over the five years of my graduate studies significant progress has been made in the isoprene field towards understanding the factors that govern aspects of regulation of isoprene emission. Two groups of studies, in particular, contributed to our understanding of how isoprene emission respond to environmental variables in the short term: 1) the development of using post-illumination isoprene emission to measure DMADP in vivo under physiological conditions (Rasulov et al., 2009a; Rasulov et al., 2009b; Rasulov et al., 2010; Rasulov et al., 2011); and 2) the discovery that methylerythritol cyclodiphosphate (MEcDP) accumulates to significant levels in leaves (Rivasseau et al., 2009; Mongélard et al., 2011). These studies along with the studies presented in this dissertation show that substrate level is a major determinant of short-term isoprene emission levels, and likely drives the rapid fluctuations in emission levels that are typically observed in nature (Singsaas and Sharkey, 1998; Sharkey et al., 2008). On the other hand, studies that examined MEP pathway enzymes and IspS message levels, protein levels and activities showed that isoprene emission as regulated by seasonal variations (Mayrhofer et al., 2005; Wiberley et al., 2008), circadian rhythm (Loivamäki et al., 2007; Wiberley et al., 2009) and plant development (Wiberley et al., 2005) can be predicted by variations in basal emission rates. An emerging theme, therefore, is that instantaneous responses of isoprene emission are predicted by the enzymes in the Calvin-Benson cycle and the MEP pathway that determine DMADP levels, while the long-term basal emission rates are controlled by IspS, on both transcriptional and translational levels.

Measuring DMADP: strategies and caveats

DMADP measurement is central to answering the question of whether isoprene emission is enzyme- or substrate-regulated. Measuring plastidic DMADP levels has traditionally been a difficult task mainly due to the existence of a variable cytosolic DMADP pool (synthesized through the mevalonic acid pathway). While there is little DMADP exchange between the cytosolic and the plastidic compartments, directly separating the two pools by biochemical methods would still involve complex and time-consuming procedures such as non-aqueous fractionation. The percentage of plastidic DMADP that has been reported varies significantly from 15% - 95% (Table 4.1).

In addition, DMADP isomers such as isopentenyl diphosphate (IDP) exist in chloroplasts. In most cases, it was assumed that IDP constitutes a relatively small portion of the DMADP/IDP pool, as the equilibrium between DMADP and IDP favors DMADP in an approx. 5:1 ratio. Nevertheless, it is not known how closely the in vivo concentrations in plant chloroplasts will resemble equilibrium ratios in vitro. The last step of the MEP pathway (HDR) produces more IDP than DMADP, therefore depending on the relative activities of HDR and isopentenyl diphosphate isomerase (IDI) the actual DMADP and IDP concentrations in the cell under steady state conditions could deviate from the equilibrium ratios determined in vitro. Mass spectrometry (MS) measurement shows a metabolite with the same precursor and product ion m/z as DMADP was present in leaf samples (but not in *E. coli* extracts; Li Z., Weise S.E. and Sharkey T.D., unpublished data), and it is speculated that other DMADP isomers may be present in the cytosolic fraction of cell extracts.

Methods that have been developed to measure DMADP levels are discussed as follows (also summarized in Table 4.1).

1) *Acid hydrolysis (destructive).* This method takes advantage of the fact that DMADP could break down to isoprene non-enzymatically under certain circumstances (usually low pH). A strong acid such as sulfuric acid was often used (Fisher et al., 2001). The breakdown product isoprene can be measured on sensitive detectors such as gas chromatography-flame ionization detectors or chemiluminescent isoprene sensors. To measure the plastidic DMADP pool non-aqueous fractionation of leaf material was typically used. In addition, there were two indirect ways of estimating the plastidic DMADP pool: light-induced DMADP (the difference between total DMADP measured in light and total DMADP measured in dark) and fosmidomycin-induced DMADP inhibition (the difference between total DMADP levels in the presence and absence of fosmidomycin).

Since its introduction, acid hydrolysis has been the mostly widely used method for estimating DMADP levels, for the most part due to a lack of reliable alternatives. One of the advantages of this method was that IDP does not break down to isoprene so DMADP can be separated from IDP. However, there may be other metabolites that convert to isoprene in a similar manner to DMADP. In my opinion, the specificity of this method for DMADP was not satisfactorily demonstrated in Fisher et al. (2001) and has not been addressed in later studies. In the original report, it was shown that DMADP standards and leaf extracts of *P. deltoides* produced a similar methylbutenol (MBO) to isoprene ratio, and the authors concluded that the acid-induced isoprene

emission comes from DMADP exclusively. However, correlation does not imply causality. It is possible that other compounds with similar chemical properties to DMADP also exist in the cell, and they are converted to MBO and isoprene in the same ratio as in DMADP. In fact, we have demonstrated that cytosolic DMADP levels estimated by acid hydrolysis were ~ 10 times higher those measured by LC-MS-MS, while plastidic DMADP levels measured by both methods were approximately the same (Weise S.E., Li Z., Sharkey T.D., in preparation). It is likely that a cytosolic pool of some DMADP analogue is acted upon by acid and converted to isoprene.

2) *Post-illumination isoprene emission (non-destructive).* The method of using post-illumination isoprene emission to measure plastidic DMADP was introduced in 2009 (Rasulov et al., 2009a). The technical details of using post-illumination isoprene emission have been discussed in Chapters 2 and 3. In sum, the integrated isoprene emission in phase I after light was turned off (typically 10 - 15 min) was used to estimate plastidic DMADP. This method is non-destructive and therefore could be repeated on the same leaves under different physiological conditions (provided such conditions are non-stressful and produce a reversible response in plants). This method also provides us with a snapshot of DMADP levels in vivo and allows us to check other destructive methods. DMADP levels measured using the method is often an order of magnitude lower than estimates by acid hydrolysis (Table 4.1).

Nevertheless, the post-illumination isoprene emission method comes with its own limitations. First of all, this method does not differentiate between DMADP and IDP. When light is turned off, plastidic DMADP drops quickly as it converts to isoprene. Assuming IDI is not light- or redox-activated, IDP will isomerize to DMADP and eventually convert to isoprene as well

during phase I of darkness. As discussed at the beginning of this section, while one may assume plastidic IDP is a smaller pool, there is little information on the actual IDP and DMADP concentrations in the cell. Secondly, the effect of darkness during phase I is principally on HDS (step 6 of the MEP pathway, Fig 3.3, Chapter 3), which means some amount of HMBDP will convert to isoprene in phase I. Third, a proportion of MEcDP could convert to downstream metabolites and finally isoprene in phase I. The "leakiness" of HDS inhibition could come from two sources: a slow shutdown of step 6 the moment when light is turned off, or a quick regeneration of electron sources that allow HDS to be jump started in phase I. Since HDS activity directly depends on photosynthetic electron transport, the rate at which HDS is turned off is likely to be very fast. The depletion of reducing equivalents in electron transport is much faster than ATP turnover and likely takes << 50 ms after the light-to-dark switch (Arrivault et al., 2009). Assuming a 30 ms lag time, the amount of MEcDP that is lost to isoprene in phase I could only account for 0.1% of the post-illumination isoprene emission. On the other hand, regeneration of reducing power through other sources may start as soon as darkness is imposed. One way to estimate this proportion of MEcDP is to extrapolate back from the ascending phase of the isoprene emission trace in phase II. MEcDP-converted isoprene due to regeneration of reducing equivalents estimated this way could account for 1 – 10% of phase I post-illumination isoprene emission.

Finally, this method is of limited use at higher temperatures, where phase I and II cannot be separated from each other (Fig. 2.2, Chapter 2). In general, our results in Chapter 3 suggest post-illumination isoprene emission likely overestimates plastidic DMADP levels by 20 – 40%, however the extent of this overestimation is difficult to precisely quantify.

3) *LC-MS (destructive).* The LC-MS method for measuring DMADP was detailed in the materials and methods section of Chapter 3. An important advantage of this method is that due to similar chemical properties of sugar phosphates, a suite of other MEP pathway metabolites can be measured at the same time. It is quite possible that important sugar intermediates in the Calvin-Benson cycle and glycolysis, such as phosphoenolpyruvate, glyceraldehyde 3-phosphate, phosphoglycerates, ribulose 5-phosphate, ribulose 1,5-bisphosphate and 1,3-bisphosphoglycerate can be measured (with a suitable compartment separation procedure) simultaneously with the MEP pathway metabolites. While there has been no precedent published to date where IDP and DMADP in plants can be separated by mass spectrometry without a derivatization procedure first, such separation has been achieved and will be published soon (Rosenstiel, T.N., pers. comm.). In my opinion, tandem mass spectrometry coupled with non-aqueous fractionation is currently the most reliable way of measuring DMADP levels, with only approx. one order of magnitude lower sensitivity in comparison to the acid hydrolysis method, and fewer important assumptions required.

Regulation of isoprene emission: current progress

Response of isoprene emission to temperature

Using post-illumination isoprene emission I was able to measure responses of DMADP levels to temperature. The temperature at which DMADP and other metabolites of the MEP pathway accumulate the most is ~ 35°C (Rasulov et al., 2010; Li et al., 2011; Rasulov et al., 2011). The optimum temperature for IspS on the other hand is ~ 50°C with an activation energy of approximately 40 – 50 kJ mol^{-1} (Monson et al., 1992; Lehning et al., 1999; Rasulov et al., 2010; Li et al., 2011). The combined effect is that observed isoprene emission is greatest at ~ 40°C. It is now generally accepted that response of isoprene emission to temperature is simply due to the thermodynamic properties of the enzymes involved, and the control is shared between the enzyme IspS, and the upstream enzymes (MEP pathway enzymes) that determine DMADP levels. This finding has an important implication for modeling of temperature responses of isoprene emission. Earlier empirical models (e.g. Guenther et al., 1991; Guenther et al., 1993) based on observations rather than theory typically employed an algorithm that made use of the Arrhenius relationship, which describes the kinetic energy of a reaction at any given temperature. It was then suggested later that this formula may have in fact correctly (but inadvertently) represented the biochemical basis of isoprene emission since the temperature dependence of isoprene emission is lent by the strong temperature responses of IspS (Grote et al., 2006; Monson et al., 2012). The co-regulation by multiple enzymes suggested by this study and Rasulov et al. (2010) adds another layer of complexity to constructing the biochemically-correct temperature response model, and additional empirically determined enzyme kinetic parameters and more

tunable coefficients may need to be included, especially if there is a need to include deactivation of isoprene emission at higher temperatures in the current models.

The enzymes in the MEP pathway typically have a temperature optimum that is closer to the ambient temperature (e.g. 37°C for DXR) (Rohdich *et al.*, 2006). The temperature response for IspS is however much stronger; such that, isoprene emission is characterized by a strong temperature response (up to 40 – 45°C), while synthesis of other downstream housekeeping isoprenoids, e.g. carotenoids and quinones, are presumably much less so. It might be interesting to speculate why this has evolved to be the case: isoprene may have a role in protecting plants against moderate heat stress. On a hot summer day, leaf temperature frequently reaches but usually do not go much beyond 40°C (Sharkey et al., 2008).

During a rapid switch from 30°C to 40°C , isoprene emission first increases with an increase in IspS activity and then decreases as DMADP becomes limiting. This observation of the transient response suggests that, at ambient to moderately high temperatures, IspS responds to temperatures faster than upstream enzymes. Once again, this is in line with idea that IspS primarily increase isoprene emission while substrate levels decrease emission levels in response to temperature above 35°C.

Response of isoprene emission to photon flux density

Isoprene emission responds to changes in light levels almost instantaneously. When light is turned off, isoprene emission drops off quickly initially but then rises again forming a transient

burst in the dark. Not all emitting species exhibit the post-illumination burst phenomenon (e.g. kudzu) but most trees (e.g. poplars and oaks) do. In the preceding chapters I provided evidence that the post-illumination isoprene burst comes from intermediate metabolites in the MEP pathway. Profiling of the MEP pathway metabolites during this period shows the intermediate metabolites, primarily MEcDP, stays at approximately the same level during phase I when isoprene emission declined by > 90%, and can account for the post-illumination burst during phase II. The decline of isoprene emission during phase I can be explained by a rapid depletion of reducing power that inhibits HDS (albeit incompletely). The inhibition of HDS is then reversed in the first part of phase II leading to an increase in emission levels. NADPH could be regenerated through the pentose phosphate pathway or plastidic glycolysis; alternatively, the switch of HDS from using ferredoxin to NADPH as a reducing power source may take time. What causes the eventual decline in isoprene emission (later part of phase II) is less clear. NADPH presumably has already been regenerated as seen in the post-illumination isoprene burst, and it is also needed for anabolic cellular processes in the dark. At this time, all of the MEP pathway metabolites dropped to minimal levels (Fig. 3.3, Chapter 3). This suggests steps in the central metabolism upstream of DXS have been turned off, cutting off the carbon supply to the MEP pathway. GAP is likely to be the limiting substrate as GAP levels were quickly reduced upon darkness while levels of 3-PGA, from which pyruvate is made, accumulates in darkness (Sharkey et al., 1986; Loreto and Sharkey, 1993; Arrivault et al., 2009). The darkness-induced reduction in GAP levels likely results from the loss of reducing power to convert 3-PGA to GAP rather than a simple consequence of reduced carbon assimilation, since substantial isoprene emission can be seen under photorespiratory conditions (e.g. 0 ppm CO_2) where the carbon balance is more negative than the carbon balance in darkness. The tight physiological control in

darkness decreased isoprene emission to essentially zero but when light is turned back on emission capacity is fully reversible. This is in sharp contrast to isoprene emission in N_2 (i.e. no O_2 and no CO_2), where the disruption of redox balance is aphysiological; despite a strong inhibition at HDS, a trace amount of isoprene is still emitted in N_2, and isoprene emission capacity is irreversibly damaged after the treatment (Fig. 3.5, Chapter 3).

Therefore, steps in the MEP pathway that require reducing power are likely the points of regulation in response to light. This could explain why the light response of isoprene emission and photosynthesis are similar: both carbon fixation and the MEP pathway require ATP and NADPH. In other words, these two processes depend on the energetic cofactors provided by the light reactions in a similar fashion.

Regulation of the MEP pathway

Rapid regulation of the MEP pathway in plants was first demonstrated by Wolfertz et al. (2003; 2004) and there is now substantial evidence that MEP pathway is feedback regulated (Banerjee A. and Sharkey T.D., unpublished data). DXS, DXR and HDR (the 1^{st}, 2^{nd} and 7^{th} step of the pathway) have also been suggested with regulatory roles in the MEP pathway (reviewed in Sharkey et al., 2008; Wiberley et al., 2009). The discovery that MEcDP accumulates significantly in leaves (Rivasseau et al., 2009) adds a new member to the potential list: HDS. The HDS enzyme catalyzes the penultimate step in the pathway and has two unique properties: 1) it uses an oxygen-sensitive [4Fe-4S] cluster to catalyze the redox reaction; and 2) it can directly utilize illuminated thylakoid membranes as an electron sources, possibly via ferredoxin. The

direct coupling of the activity enzyme to photosynthesis allows this step to be rapidly regulated with energetic cofactors. In addition, the oxygen sensitivity of HDS has been suggested to imply that there may rapid turnover and repair events (Rivasseau et al., 2009; Mongélard et al., 2011), in a similar way to the regulation of photosystem II. The substrate MEcDP possesses a cyclic structure where the extra degree of stability may also aided its accumulation in vivo. The absolute amount of MEcDP I have measured in leaves is similar to DMADP levels. While DMADP level varies quickly with isoprene emission in response to light fluctuations, MEcDP levels are much less responsive and therefore may provide a metabolic buffer to isoprenoid biosynthesis in planta.

Future perspectives

Significant advances are now being made on the front of understanding regulation of isoprene emissions from plants under different physiological conditions. The elucidation of MEP pathway enzymes in the early 2000s, new detection techniques such as proton transfer reaction-time of flight-mass spectrometry (PTR-TOF-MS) developed for isoprene measurements and the advent of the omics era all contribute to the increasing repertoire of knowledge about the regulation of isoprene emission from plants. In particular, the potential for using the MEP pathway in bacteria as chemical factories for producing commercially profitable compounds, as well as targeting the bacterial MEP pathway in drug development, has sparked tremendous interest that funded studies to elucidate the control mechanisms of the MEP pathway. However, caution should be taken as we extrapolate existing knowledge about the MEP pathway in microorganisms to understand isoprene emission in plants, as the two systems may not be entirely identical. A

notable example, as mentioned previously, is the 6th step of the pathway. The plant HDS enzyme accepts electrons directly from photosynthesis and may be an important regulatory step in nature. The bacterial homolog IspG, on the other hand, uses NADPH as the source of reducing power. The MEP pathway metabolic profile extracted from *E. coli* also appears to be distinct from that of plant extract (Weise, S.E., Li, Z., Sharkey, T.D., unpublished data). Nevertheless, significant additional progress in understanding molecular and biochemical control of isoprene emission from trees is likely in the near future. A low-hanging fruit, as it seems now, is to employ current techniques to elucidate the biochemical mechanisms underlying CO_2 responses of isoprene emission. In addition, metabolic flux analysis of the MEP pathway will go a long way towards understanding how each individual enzyme controls the synthesis of DMADP.

Table 4.1 Measurements of leaf DMADP levels published to date.

Reference	DMADP (μmol m^{-2})		Plastidic fraction	Method of detection	Method used to separate plastidic and cytosolic fractions
	Chloroplast	Cytosol			
Rosenstiel et al., 2002	10	4.0	68%	Acid Hydrolysis	Non-aqueous fractionation
Wolfertz et al., 2003	5 - 80	-	-	Acid Hydrolysis	Non-aqueous fractionation
Loreto et al., 2004	~ 28		36%	Acid Hydrolysis	^{13}C pulse-chase
Behnke et al., 2007	~ 1		-	Acid Hydrolysis	-
Rasulov et al., 2009a	1.3	9.0	15%	Acid Hydrolysis	Measurements in light vs. in dark (6 min), and in the presence vs. absence of fosmidomycin
Li and Sharkey, 2012 (in press)	0.80	0.013	95%	LC-MS-MS	Measurements in light vs. in dark (40 min)
Weise, Corrion, Li and Sharkey, unpublished data	~ 2	~ 2	50%	Acid Hydrolysis	Measurements in light vs. in dark (40 min)

LITERATURE CITED

LITERATURE CITED

Arrivault S, Guenther M, Ivakov A, Feil R, Vosloh D, Van Dongen JT, Sulpice R, Stitt M (2009) Use of reverse-phase liquid chromatography, linked to tandem mass spectrometry, to profile the Calvin cycle and other metabolic intermediates in *Arabidopsis* rosettes at different carbon dioxide concentrations. The Plant Journal **59:** 826-839

Behnke K, Ehlting B, Teuber M, Bauerfeind M, Louis S, Hansch R, Polle A, Bohlmann J, Schnitzler JP (2007) Transgenic, non-isoprene emitting poplars don't like it hot. Plant Journal **51:** 485-499

Fisher AJ, Rosenstiel TN, Shirk MC, Fall R (2001) Nonradioactive assay for cellular dimethylallyl diphosphate. Analytical Biochemistry **292:** 272-279

Grote R, Mayrhofer S, Fischbach RJ, Steinbrecher R, Staudt M, Schnitzler JP (2006) Process-based modelling of isoprenoid emissions from evergreen leaves of Quercus ilex (L.). Atmospheric Environment **40:** S152-S165

Guenther AB, Monson RK, Fall R (1991) Isoprene and monoterpene emission rate variability: Observations with Eucalyptus and emission rate algorithm development. Journal of Geophysical Research **96:** 10,799-710,808

Guenther AB, Zimmerman PR, Harley PC (1993) Isoprene and monoterpene emission rate variability: Model evaluations and sensitivity analysis. Journal of Geophysical Research **98:** 12,609-612,617

Lehning A, Zimmer I, Steinbrecher R, Bruggemann N, Schnitzler JP (1999) Isoprene synthase activity and its relation to isoprene emission in *Quercus robur* L. leaves. Plant, Cell and Environment **22:** 495-504

Li Z, Ratliff EA, Sharkey TD (2011) Effect of temperature on post-illumination isoprene emission in oak and poplar. Plant Physiology **155:** 1037-1046

Loivamäki M, Louis S, Cinege G, Zimmer I, Fischbach RJ, Schnitzler J-P (2007) Circadian rhythms of isoprene biosynthesis in grey poplar leaves. Plant Physiology **143:** 540-551

Loreto F, Pinelli P, Brancaleoni E, Ciccioli P (2004) ^{13}C labelling reveals chloroplastic and extra-chloroplastic pools of dimethylallyl piroposphate and their contribution to isoprene formation. Plant Physiology **135:** 1903-1907

Loreto F, Sharkey TD (1993) On the relationship between isoprene emission and photosynthetic metabolites under different environmental conditions. Planta **189:** 420-424

Mayrhofer S, Teuber M, Zimmer I, Louis S, Fischbach RJ, Schnitzler JP (2005) Diurnal and seasonal variation of isoprene biosynthesis-related genes in grey poplar leaves. Plant Physiology **139:** 474-484

Mongélard G, Seemann M, Boisson A-M, Rohmer M, Bligny R, Rivasseau C (2011) Measurement of carbon flux through the MEP pathway for isoprenoid synthesis by ^{31}P-NMR spectroscopy after specific inhibition of 2-C-methyl-d-erythritol 2,4-cyclodiphosphate reductase. Effect of light and temperature. Plant, Cell and Environment **34:** 1241-1247

Monson RK, Grote R, Niinemets Ü, Schnitzler J-P (2012) Modeling the isoprene emission rate from leaves. New Phytologist **195:** 541-559

Monson RK, Jaeger CH, Adams WW, Driggers EM, Silver GM, Fall R (1992) Relationships among isoprene emission rate, photosynthesis, and isoprene synthase activity as influenced by temperature. Plant Physiology **98:** 1175-1180

Rasulov B, Copolovici L, Laisk A, Niinemets Ü (2009a) Postillumination isoprene emission: in vivo measurements of dimethylallyldiphosphate pool size and isoprene synthase kinetics in aspen leaves. Plant Physiology **149:** 1609-1618

Rasulov B, Hüve K, Bichele I, Laisk A, Niinemets Ü (2010) Temperature response of isoprene emission in vivo reflects a combined effect of substrate limitations and isoprene synthase activity: a kinetic analysis. Plant Physiology **154:** 1558-1570

Rasulov B, Hüve K, Laisk A, Niinemets Ü (2011) Induction of a longer term component of isoprene release in darkened aspen leaves: origin and regulation under different environmental conditions. Plant Physiology **156:** 816-831

Rasulov B, Hüve K, Valbe M, Laisk A, Niinemets Ü (2009b) Evidence that light, carbon dioxide, and oxygen dependencies of leaf isoprene emission are driven by energy status in hybrid aspen. Plant Physiology **151:** 448-460

Rivasseau C, Seemann M, Boisson A-M, Streb P, Gout E, Douce R, Rohmer M, Bligny R (2009) Accumulation of 2-C-methyl-D-erythritol 2,4-cyclodiphosphate in illuminated plant leaves at supraoptimal temperatures reveals a bottleneck of the prokaryotic methylerythritol 4-phosphate pathway of isoprenoid biosynthesis. Plant, Cell and Environment **32:** 82-92

Rohdich F, Lauw S, Kaiser J, Feicht R, Köhler P, Bacher A, Eisenreich W (2006) Isoprenoid biosynthesis in plants – 2C-methyl-d-erythritol-4-phosphate synthase (IspC protein) of *Arabidopsis thaliana*. FEBS Journal **273:** 4446-4458

Rosenstiel TN, Fisher AJ, Fall R, Monson RK (2002) Differential accumulation of dimethylallyl diphosphate in leaves and needles of isoprene- and methylbutenol-emitting and nonemitting species. Plant Physiology **129:** 1276-1284

Sharkey TD, Seemann JR, Pearcy RW (1986) Contribution of metabolites of photosynthesis to postillumination CO_2 assimilation in response to lightflecks. Plant Physiology **82:** 1063-1068

Sharkey TD, Wiberley AE, Donohue AR (2008) Isoprene emission from plants: why and how. Annals of Botany **101:** 5-18

Singsaas EL, Sharkey TD (1998) The regulation of isoprene emission responses to rapid leaf temperature fluctuations. Plant, Cell and Environment **21:** 1181-1188

Wiberley AE, Donohue AR, Meier ME, Westphal MM, Sharkey TD (2008) Regulation of isoprene emission in *Populus trichocarpa* leaves subjected to changing growth temperature. Plant Cell and Environment **31:** 258-267

Wiberley AE, Donohue AR, Westphal MM, Sharkey TD (2009) Regulation of isoprene emission from poplar leaves throughout a day. Plant Cell and Environment **32:** 939-947

Wiberley AE, Linskey AR, Falbel TG, Sharkey TD (2005) Development of the capacity for isoprene emission in kudzu. Plant Cell and Environment **28:** 898-905

Wolfertz M, Sharkey TD, Boland W, Kuhnemann F (2004) Rapid regulation of the methylerythritol 4-phosphate pathway during isoprene synthesis. Plant Physiology **135:** 1939-1945

Wolfertz M, Sharkey TD, Boland W, Kuhnemann F, Yeh S, Weise SE (2003) Biochemical regulation of isoprene emission. Plant, Cell and Environment **26:** 1357-1364

APPENDIX 1

Additional Studies: Characterization of Photosynthesis in *Arabidopsis* ER-to-Chloroplast Lipid Trafficking Mutants

---

Research described in this chapter was a collaborative work with Jinpeng Gao and Christoph Benning originally published in Photosynthesis Research.
Li Z, Gao J, Benning C, Sharkey TD (2012) Characterization of photosynthesis in *Arabidopsis* ER-to-plastid lipid trafficking mutants. Photosynthesis Research **112:** 49-61

Abstract

Vascular plants use two pathways to synthesize galactolipids, the predominant lipid species in chloroplasts – a prokaryotic pathway that resides entirely in the chloroplast, and a eukaryotic pathway that involves assembly in the endoplasmic reticulum. Mutants deficient in the endoplasmic reticulum pathway, *trigalactosyldiacylglycerol* (*tgd1-1 and tgd2-1*) mutants, had been previously identified with reduced contents of monogalactosyldiacylglycerol and digalactosyldiacylglycerol, and altered lipid molecular species composition. Here we report that the altered lipid composition affected photosynthesis in lipid trafficking mutants. It was found that proton motive force as measured by electrochromic shift was reduced by ~ 40% in both *tgd* mutants. This effect was accompanied by an increase in thylakoid conductance attributable to ATPase activity and so the rate of ATP synthesis was nearly unchanged. Thylakoid conductance to ions also increased in *tgd* mutants. However, gross carbon assimilation in *tgd* mutants as measured by gas exchange was only marginally affected. Rubisco activity, electron transport rate, and photosystem I and II oxidation status were not altered. Despite the large change in proton motive force, responses to heat and high light stress were similar between *tgd* mutants and the wild type.

Introduction

Chloroplasts of vascular plants have an unusual membrane lipid composition different from membrane lipids in animals and other plant tissues (Dörmann and Benning, 2002). While phospholipids dominate animal cell membranes, galactolipids such as monogalactosyldiacylglycerol (MGDG) and digalactosyldiacylglycerol (DGDG), and sulfolipids are the primary constituents of plastid membranes in plants (Toni, 1997; Joyard et al., 1998). The chloroplast membranes (including the plastid envelope membranes and the thylakoids) play important roles, not only in the regulation of metabolite transport into and out of the chloroplast, but also in light-dependent photosynthetic electron transport. Membrane lipids such as MGDG and DGDG have also been shown to be an integral part of photosystem I (PSI), photosystem II (PSII), light harvesting complexes and cytochrome b_6/f complexes (Jordan et al., 2001; Stroebel et al., 2003; Liu et al., 2004; Loll et al., 2005; Mizusawa and Wada, 2011). Therefore, studies of synthesis, trafficking and function of galactolipids have been of great interests to plant biologists.

In many plants, including *Arabidopsis thaliana*, galactolipids are produced by galactosylation of diacylglycerols from two separate pathways (Roughan and Slack, 1982; Frentzen, 1986). Diacylglycerol precursors can be either synthesized entirely in plastids or assembled in the endoplasmic reticulum (ER) from plastid-derived fatty acids. Lipids derived from these two different pathways can be differentiated by the fatty acid compositions: lipids derived from the plastid pathway have a 16-carbon chain at the *sn-2* position while the lipids derived from the ER pathway contain an 18-carbon chain at this position. The ER pathway requires lipid transport between the ER and plastid. Mutants lacking putative transporters in this pathway have been

identified using a forward genetics approach. These mutants were named *tgd* mutants since they contained trigalactosyldiacylglycerols (TGDG) and other oligogalactolipids produced from a galactolipid:galactolipid galactosyltransferase (GGGT) that was activated when ER-plastid interaction was disrupted (Xu et al., 2003; Moellering et al., 2010). Four *tgd* loci had been identified, three of which encode components of an ATP-binding cassette transporter in the inner envelope membrane and a fourth protein associated with ER and chloroplast outer envelope membrane (Benning, 2009; Wang et al., 2012).

The lipid profile of *tgd1-1* revealed an overall reduced level of MGDG and DGDG, increased levels of phosphotidylcholine (PC), phosphotidic acid (PA) and triacylglycerol (TAG), as well as an increased percentage of 16-carbon fatty acid at the *sn-2* position (indicative of plastid pathway dominance) (Xu et al., 2003; Xu et al., 2005). The *tgd2-1* mutant displayed a similar lipid phenotype and the TGD2 protein was shown to be part of a super complex larger than 500 kDa that specifically binds PA (Awai et al., 2006; Lu and Benning, 2009; Roston et al., 2011). It has been postulated that TGD1, 2 and 3 constitute different domains of a transporter complex involved in ER-to-plastid lipid trafficking (Lu et al., 2007; Benning, 2009).

Many parts of the photosynthetic machinery are housed on thylakoid membranes and an alteration in plastidic lipid composition may affect photosynthesis. For instance, *mgd1-1* mutants where MGDG levels were reduced by 42% showed reduced capacity for non-photochemical quenching (Aronsson et al., 2008). In addition, thylakoid membrane energization as measured by electrochromic shift (ECS) was lower in *mgd1-1* mutant, and the xanthophyll cycle was partially impaired (Aronsson et al., 2008). In the DGDG-deficient *dgd* mutants, PSII levels were reduced

which affected overall thylakoid organization and thermostability (Härtel et al., 1997; Hölzl et al., 2009; Krumova et al., 2010). The original purpose of this work was to understand the underlying mechanism of thylakoid membrane structures under stressed conditions so that the function of isoprene on protecting membrane integrity can be better assessed. While isoprene fumigation did not affect the *tgd* mutants differently from the wild-type plants (data not shown), we observed a noticeable difference in photosynthetic parameters between the *tgd* mutants and the wild-types. A custom-built spectrophotometer (NoFOSpec, Sacksteder et al., 2001) was used in this study to measure the proton motive force (*pmf*) as well as thylakoid conductance derived from ECS kinetics. The proton flux derived from ECS kinetics results mostly from chloroplast ATPase activity and can be related to electron transport rate (Sacksteder and Kramer, 2000; Cruz et al., 2001; Avenson et al., 2005; Baker et al., 2007). The conductance of the thylakoid membranes to ions (Mg^{2+} and Cl^{-}) were derived from the inverse phase of ECS decay (Cruz et al., 2001; Takizawa et al., 2007). In addition, parameters of the two photosystems and carbon assimilation were also measured.

Here we report an increased thylakoid membrane conductance to protons and ions for the *tgd* mutants, while the extent of *pmf* was reduced compared with wild-type plants. However, carbon assimilation, linear electron transport rate, PSI oxidation status and PSII quantum efficiency remained largely the same. The effect of changes in lipid composition on photosynthesis in the *tgd* mutants is discussed.

Results

Growth and lipid phenotypes of tgd mutants

As a prerequisite to completely cover the optical path of NoFOSpec (diameter = 1.6 cm) and to obtain the optimum gas exchange data, Arabidopsis plants were grown under short photoperiod (8 hr) to obtain large leaves. All lines grew slower under these conditions than under longer daylength but at approximately the same developmental progression (Fig. A1.1a). At the seedling stage, both *tgd1-1* and *tgd2-1* mutants frequently had two different-sized cotyledons, with the larger cotyledon sometimes bilobed in shape (Fig. A1.1b). The smaller "cotyledon" possesses true leaf-like characteristics such as trichomes. Three cotyledons were occasionally observed (Fig. A1.1b). This is in contrast with wild-type plants where two identical-sized, trichome-less cotyledons were always observed. Most adult leaves were fully developed at eight weeks after germination and floral stems developed approximately 10 weeks after germination. While both *tgd* mutants had small and curly leaves under 14 hr photoperiod (not shown), under 8 hr photoperiod the sizes of leaves on these mutants were comparable to those of wild-type leaves. Both *tgd* mutants had a slightly smaller rosette size than wild type, and leaves of both *tgd* mutants appeared paler (Fig. A1.1a). Both *tgd* mutants showed a reduction in chlorophyll levels, while carotenoid levels did not change significantly ($p < 0.05$), in comparison to wild-type plants (Fig. A1.1c).

TGDG was present in leaves of both *tgd* mutants and absent from wild-type plants as confirmed by thin layer chromatography. Analysis of lipid profiles showed that levels of MGDG and

DGDG both decreased in *tgd* mutants, accompanied with an increase in PE and PC (Fig. A1.2a). A breakdown of molecular species in each lipid categories revealed that the 18:3 fatty acids decreased in all lipid categories in *tgd* mutants, reflecting a shift from eukaryotic to prokaryotic species at the *sn-2* position (Fig. A1.2b). 16:0 fatty acids were increased in DGDG but this may have taken place at the *sn-1* position (Fig. A1.2b).

Dark interval relaxation kinetics of tgd mutants

The size of proton motive force (*pmf*) as measured by total electrochromic shift (Δ_{ECS}) was reduced by approximately 40% in the *tgd* mutants (Fig. A1.3a, c, $p < 0.001$, one-way ANOVA). Conductance of thylakoid membranes to protons significantly increased in *tgd* mutants, as shown by a decrease in the time constants of ECS dissipation (τ_{ECS}, Fig. A1.3a, c, $p = 0.001$, ANOVA on ranks). Conductance of thylakoid membrane to counter-ion flows (primarily Mg^{2+} influx and Cl^- efflux) (Cruz et al., 2001) also significantly increased in *tgd* mutants as shown by a decrease in time constants of the inverse phases of ECS decay (τ_{ion}, Fig. A1.3b, c, $p < 0.001$, one-way ANOVA). Since ATP synthase activity in the thylakoid is primarily responsible for the observed proton conductance (Baker et al., 2007), we also measured the amount of ATPase protein in the chloroplast. ATPase protein levels in the *tgd* mutants were similar to the levels in the wild type (Fig. A1.4).

Since it was shown that the proton motive force as measured by Δ_{ECS} also decreased under moderate heat stress (Zhang et al., 2009; Zhang and Sharkey, 2009), we investigated whether the effect of the *tgd* mutations on *pmf* was independent of the effect of heat stress on *pmf*. A 30-min

heat treatment that held leaf temperature at 40°C decreased *pmf* in both wild type and *tgd* mutants by approximately 20% at the end of the heat treatment (Fig. A1.5). In *tgd* mutants, *pmf* initially dropped by ~35% within the first minute of heat stress and gradually recovered to ~80% of pre-stress levels. In all three lines, *pmf* recovered to ~90% of pre-stress levels after the heat stress. τ_{ECS} decreased instantaneously upon heat treatment, and increased instantaneously upon returning to normal temperature (25°C), by approximately the same percentage in all lines (Fig. A1.5).

Carbon assimilation and electron transport in tgd mutants

Photosynthesis as measured by carbon assimilation was slightly reduced in both *tgd* mutants by 10-15% when compared with wild type, under all light intensities (Fig. A1.6). To better understand different processes limiting photosynthesis of *tgd* mutants, we determined CO_2 response curves of assimilation in each line (Fig. A1.7a). No apparent triose phosphate utilization limitation was present in either wild-type or *tgd* mutants, as assimilation was seen to continue to increase with $[CO_2]$ up to a $C_i > 160$ Pa (the point with the highest $[CO_2]$ in the graph). Most data points were sufficiently explained as assimilation-limited by RuBP regeneration. Maximum carboxylation rate of Rubisco (V_{cmax}) and electron transport rate (J) as derived from CO_2 response curves of assimilation (according to methods described in Sharkey et al., 2007) were both unaffected in *tgd* mutants (Fig. A1.7b). Photosystem I (P700) oxidation status was similar in both wild-type and mutant plants (Fig. A1.7b). Rubisco levels on a leaf area basis were similar between the *tgd* mutants and the wild-types, while levels of light harvesting complexes and cytochrome b_6/f complexes were somewhat lower in the mutants (Fig. A1.4d, 4e).

To investigate whether photoprotection was affected in *tgd* mutants, we measured PSII parameters by chlorophyll *a* fluorescence before, during and after a 1-hr 3000 μmol m^{-2} s^{-1} high light stress (Fig. A1.8). Under low light conditions (170 μmol m^{-2} s^{-1}), both F_v'/F_m' and ΦPSII were similar between *tgd* mutants and wild type, indicating that electron transport rate through PSII were similar. F_v'/F_m' dropped sharply upon high light treatment, and then gradually declined; while ΦPSII dropped to essentially zero. Both parameters gradually recovered to ~50% of pre-stress level during the 1-hr recovery phase. Responses to this high light treatment were similar in all three lines.

Discussion

Both *tgd1-1* and *tgd2-1* mutants have significantly reduced *pmf*, along with increased thylakoid conductance to protons and ions (Fig. A1.3), while electron transport, assimilation rate and photoprotection were all largely unaffected (Fig. A1.6, A1.7, A1.8). The size of *pmf* is important thermodynamically as it must be ≥ the ΔG of ATP formation. On the other hand, the ATP synthase is an enzyme whose rate can be described in terms of K_m and V_{max}. As we show in the following paragraph, despite the changes in *pmf*, the rate of ATP synthesis is approximately the same in *tgd* mutants as in wild type indicating a compensatory change to balance the reduced *pmf*.

In this study *pmf* was measured as the extent of electrochromic shift (ECS). Specifically, the electrochromic shift at 517 nm (ΔA_{517}) measures energization of the thylakoid membranes as changes in carotenoid absorbance (Witt, 1979). Carotenoid levels were similar between *tgd* mutants and wild type (Fig. A1.1c), therefore, the difference in Δ_{ECS} (i.e. ΔA_{517}) here reflects a difference in steady-state *pmf*. Assuming proton flux across thylakoid membrane follows the Ohm's law model as developed by Cruz et al. (2001),

$$(1) \quad \nu_{H^+} = \frac{\Delta_{ECS}}{R} = g_{H^+} \cdot \Delta_{ECS}$$

where ν_H^+ is the initial rate of proton flow during the dark interval which infinitely approaches the steady-state proton flux in light, Δ_{ECS} is the extent of ECS, R is the thylakoid membrane resistance to protons (mathematically equivalent to the time constant of ECS decay, τ_{ECS}), and g_H^+ is the thylakoid conductance to protons (inverse of resistance). The conductance is an intrinsic property of the thylakoid membrane and independent of the ECS amplitude. Δ_{ECS} in the two *tgd* mutants decreased by ~42% on average, but this is compensated by a ~34% decrease in τ_{ECS}.

$$(2) \quad \nu_{H^+, tgd} = \frac{\Delta_{ECS, tgd}}{\tau_{ECS, tgd}} = \frac{0.58 \cdot \Delta_{ECS, WT}}{0.66 \cdot \tau_{ECS, WT}} = 0.88 \cdot \nu_{H^+, WT}$$

The net effect is proton flux in *tgd* mutants decreased by only 12% compared with wild-type plants. This is also evident from the individual ECS traces of *tgd* mutants and wild types (Fig. A1.3a), that despite the differences in ECS amplitudes and time constants, the two traces had a similar initial slope. The predicted rate of ATP synthesis would therefore be similar. This is consistent with the electron transport rates determined from chlorophyll fluorescence and carbon

fixation (Fig. A1.7b, 8) and may explain why assimilation rates were only marginally affected in the *tgd* mutants (Fig. A1.6).

The major lipid phenotypes in *tgd1-1* and *tgd2-1* mutants were a simultaneous reduction in MGDG and DGDG levels while PC levels were increased (Fig. A1.2, Xu et al., 2003; Xu et al., 2005; Awai et al., 2006). A small amount of TGDG was also produced. It has been reported that in the MGDG-deficient mutant *mgd1-1*, Δ_{ECS} (*pmf*) was significantly affected at light conditions >200 μmol m^{-2} s^{-1} and non-photochemical quenching was affected (Aronsson et al., 2008). The contents of major protein complexes on thylakoid membranes, however, were unaffected in the *mgd1-1* mutant. In addition, chloroplasts in the *mgd1-1* mutant were found to be smaller in size and contained fewer thylakoid membranes (Jarvis et al., 2000). In the *dgd1* mutant with a DGDG content ~10% of wild type, thylakoid stacking structure was disrupted and PSII to PSI ratio was altered, although photosynthesis as measured by oxygen evolution was not affected (Dörmann et al., 1995; Härtel et al., 1997; Härtel et al., 1998; Hölzl et al., 2009). *dgd1* mutants possessed more reduced PSI and were less likely to undergo state transitions indicating PSI-acceptor side limitations (Ivanov et al., 2006). Thylakoid conductance as measured by half-time of single turnover flash ECS decay (= $\tau_{ECS} \cdot \ln 2$ in dark-adapted leaves) was increased in *dgd1* mutants at 35°C but unaffected at room temperature (Krumova et al., 2010). The changes in thylakoid membrane energization in *tgd* mutants we observed here further underscores the important roles of lipid content in membranes.

Lipid compositions of the thylakoid membrane have a role in determining membrane architecture. MGDG has a "conical" shape and spontaneously adopts the hexagonal-II (H_{II}) phase in aqueous

mixtures (a non-bilayer-forming lipid), while DGDG is more cylindrical and classified as a bilayer-forming lipid (Sen et al., 1981). It was hence argued that the ratio of MGDG:DGDG must be tightly regulated (Dörmann and Benning, 2002). The *tgd* mutants presents an interesting case in which levels of both MGDG and DGDG were reduced, yet the MGDG:DGDG ratio remains approximately the same as wild type (Fig. A1.2). In addition, since the ER pathway of lipid synthesis was blocked in *tgd* mutants, the level of 18:3 fatty acids decreased in all lipid types resulting in an overall increase in lipid saturation level (Fig. A1.2). In our opinion, it is thus unlikely that thylakoid membranes in *tgd* mutants have been disrupted to the extent that H_{II} structures formed and protons leaked through membranes bypassing the ATPases. This is supported by the observation that linear electron transport rates derived from PSII fluorescence (generation of proton gradient), ECS decay (relaxation of proton gradient, ATP generation) and carbon fixation (ATP usage) were all similar between *tgd* mutants and wild type.

Given that the amount of ATP synthase was unchanged (Fig. A1.4), it is likely that ATPase activity was affected by the altered lipid composition causing the observed ECS phenotype. Lipids are an integral part in crystal structures of most large protein complexes on the thylakoid, but the structure of thylakoid ATP synthase remains to be determined (Mizusawa and Wada, 2011). While the mechanism remains unknown, it has been shown that chloroplast ATPase activity in vitro is lipid-dependent; in fact, MGDG is the only chloroplast lipid that activates ATP hydrolysis on its own, and fatty acids with higher degrees of saturation inhibit the activation (Gounaris and Barber, 1983; Pick et al., 1984; Pick et al., 1987). Suppression of ATP synthase using antisense lines and translation initiation mutants was recently shown to strongly reduce electron transport and assimilation rate, by causing an increased steady-state *pmf* (Rott et al.,

2011; Yamori et al., 2011). Interestingly, conductance of thylakoid membranes to ions also increased in *tgd* mutants by >50% in this study (Fig. A1.2b, c). This may indicate that ion channels were also affected by the altered lipid composition, in a similar way to the ATPases.

The presence of TGDG is unlikely to cause a significant change in membrane architecture, due to its small amount in the membranes (Fig. A1.2). TGDG in *tgd* mutants is likely to be formed from DGDG by the processive galactolipidtransferase activity of GGGT (van Besouw and Wintermans, 1978; Dorne et al., 1982; Cline and Keegstra, 1983; Kelly et al., 2003; Moellering et al., 2010). GGGT confers freezing tolerance to plants and is activated under osmotic stress conditions when membrane structures are affected (Moellering et al., 2010). Heat stress has been shown to cause chloroplast swelling (Zhang et al., 2011), and *pmf* and thylakoid conductance are affected by heat stress in a similar way to those in *tgd* mutants (Zhang et al., 2009; Zhang and Sharkey, 2009). However, it appears that the effects on ECS parameters caused by heat stress and *tgd* mutation are independent (Fig. A1.5).

tgd1-1 and *tgd2-1* mutants grown under our conditions (100 μmol m^{-2} s^{-1}, 8 hr photoperiod) showed a reduction in both chlorophyll *a* and chlorophyll *b* levels, as has been reported before (Fig. A1.1c, Awai et al., 2006), and a small reduction in levels of light harvesting complexes and Cyt b_6/f complexes. The reduced expression of Cyt b_6/f complexes in *tgd* mutants may be because less protein were needed to maintain the same electron transport rate, as Cyt b_6/f specific activity may be increased due to reduced *pmf*. Both *tgd* mutants also displayed a previously unreported abnormal cotyledon phenotype (Fig. A1.1b), revealing possible roles for lipids in early plant development. Disruption of lipid transport into chloroplast may interfere

with embryonic development mediated by abscisic acid signaling, as shown by studies with leaf cotyledon (*lec*) mutants (Meinke et al., 1994). Overall, photosynthetic and growth phenotypes of *tgd1-1* and *tgd2-1* are nearly identical. These observations are consistent with the idea that TGD1 and TGD2 are in the same complex responsible for lipid transport in the ER pathway (Benning, 2009).

It is surprising that despite the vast changes in lipid composition, *pmf* and possible disruptions in early development, the *tgd* mutants display only a very marginally affected photosynthetic rate as well as growth phenotype. The loss in *pmf* is compensated by a higher activity (higher conductance) of the ATP synthase. This increased conductance was not caused by an increased amount of ATP synthase proteins but could have been caused by post-translational modification (or lack thereof) of the ATP synthase or by changes in the concentrations of ATP, ADP, or inorganic phosphate. Either one of these mechanisms can explain how *pmf* can be substantially lower in the *tgd* mutants with nearly the same rate of ATP synthesis. The lower *pmf* is likely associated with a higher luminal pH and so it is also surprising that thermo- and photoprotection mechanisms are not compromised in *tgd* mutants. This study along with others (Zhang et al., 2009; Zhang and Sharkey, 2009; Zhang et al., 2011) underscores the important roles of thylakoid membrane structures in maintaining the proton motive force where isoprene emission in plants has been shown to exert a protective role (Velikova et al., 2011).

Materials and Methods

Growth Conditions

Arabidopsis mutants and wild-type plants were germinated on soil (Baccto planting mix; Michigan Peat Co., Houston, TX, USA) in plastic containers with tapered ends ("Cone-tainers", Steuwe and Sons, Tangent, OR, USA), after a 2-day vernalization period at 4°C. The plants were grown in a growth chamber set to 100 μmol m^{-2} s^{-1} PPFD at leaf level, 8 hr photoperiod, and 20°C/18°C day/night temperatures. Plants were watered every four days with half-strength Hoagland solution. Under these growth conditions, all lines reached flowering stage at approximately 10 weeks after germination. Fully-expanded, attached rosette leaves at eight weeks after germination were used for all experiments.

Pigment measurements

Leaf pigment levels were extracted in 96% ethanol and measured spectrophotometrically on a Uvikon 930 spectrophotometer (Kontron Instruments, Germany) according to procedures in Zhang and Sharkey (2009). Chlorophyll *a*, chlorophyll *b* and carotenoid levels were calculated from leaf absorbance at 470, 649 and 665 nm using the following equations (Wellburn and Lichtenthaler, 1984):

Chlorophyll *a* (mg/l) = 13.95 A_{665} – 6.88 A_{649};

Chlorophyll *b* (mg/l) = 24:96 A_{649} – 7.32 A_{665};

Carotenoid (mg/l) = (1,000 A_{470} – 2.05 Chl *a* – 114.8 Chl *b*) / 245

The following molecular weights were used to convert units of pigments to μmol m^{-2} (Lichtenthaler, 1987): chlorophyll *a*, 893.5 g mol^{-1}, chlorophyll *b*, 907.5 g mol^{-1} and carotenoids, 550 g mol^{-1}.

Protein measurements

Leaf punches of 1 cm^2 were quickly frozen in liquid nitrogen and immediately ground in a standard SDS-PAGE loading buffer. Chloroplast ATPases were quantified by western blot using antibodies against CF_1-γ (AtpC) subunit of ATP synthase (AntiProt, Martinsried, Germany). Levels of Rubisco, light harvesting complexes and cytochrome b_6/f complexes were quantified using antibodies against RbcL, Lhcb1 and Cyt b_6 (Agrisera, Vännäs, Sweden), respectively. Since most of the photosynthesis measurements were made on a leaf area basis, protein levels were also normalized to leaf areas rather than chlorophyll levels. Although chlorophyll levels were different between the mutants and the wild type (Fig. A1.1c), total proteins per leaf area were approximately the same (Fig. A1.4b). Intensities of the bands on the membrane were quantified using the ImageJ software (http://rsbweb.nih.gov/ij/).

Lipid profiling

Lipids were extracted from liquid nitrogen-frozen leaf punches according to procedures in Dörmann et al. (1995). Fatty acid methyl esters were prepared and analyzed by gas-liquid chromatography as described by Rossak et al. (1995) and Wang and Benning (2011).

Spectrophotometry and gas exchange

Electrochromic shift (ECS) and P700 measurements were made on a custom-built non-focusing optics flash spectrophotometer/fluorometer (NoFOSpec, Sacksteder et al., 2001; Kanazawa and Kramer, 2002) with modifications with parts of a LI-6400 (LI-COR Biosciences, Lincoln, NE, USA, Zhang et al., 2009). The ECS is a light-induced absorbance change that results from effects of *pmf* on carotenoids embedded in thylakoid membranes (Sewe and Reich, 1977; Witt, 1979). This light-induced absorbance change peaks at 517 nm (ΔA_{517}). The NoFOSpec measures kinetics of ΔA_{520} changes during a rapid light-to-dark transition (dark-interval relaxation kinetics, or DIRK) with a temporal resolution on a sub-millisecond scale. The light source is a light-emitting diode attached to a compound parabolic concentrator to concentrate and homogeneously diffuse the red actinic light (spectrum peak at 635 nm). The compound parabolic concentrator was attached to a beam splitter that split part of the light to a "reference" detector against which the "measurement" channel was standardized. On the measurement channel, a LI-6400 leaf chamber where the leaf was clamped in was installed before the detector to simultaneously allow light to pass and provide constant gas flow to the leaf. Light that passed through leaf was then measured with the measurement channel detector.

During a DIRK measurement, light was turned off for either 500 ms (rapid ECS decay, measures Δ_{ECS} and τ_{ECS}) or 30 s (slow ECS decay, measures τ_{ion}) during steady illumination under actinic light. In the 30 s DIRK measurements, absorbances at three wavelengths [505 nm (A_{505}), 520 nm (A_{520}) and 535 nm (A_{535})] were measured so that confounding effects from zeaxanthin accumulation and energy-dependent quenching (Q_E) on the longer time scale (Noctor et al., 1993) can be separated by multi-wavelength deconvolution. The procedures using a 10 min light interval relaxation kinetic measurement in Zhang et al. (2009) was followed to determine the deconvolution formula. The deconvolution formula determined was:

$$\Delta_{ECS} = 1.775 \cdot A_{520} - 0.807 \cdot A_{505} - 0.949 \cdot A_{535}$$

This formula is slightly different from the deconvolution formula used in Zhang et al. (2009) which may be due to the fact that a different species (Arabidopsis, vs. tobacco) was used here.

P700 measurements were carried out on NoFOSpec and as described by Klughammer and Schreiber (1994) and Siebke et al. (1997). $P700^+$ oxidation level was measured as absorbances at 810 nm (A_{810}) minus absorbance at 905 nm (A_{905}) to factor out contributions from other absorbing species (such as plastocyanin and ferredoxin) to A_{810}. Full oxidation under actinic light (A_{sat}) was achieved by giving a 300 ms far red pulse in actinic light followed by a 200 ms saturating light pulse. $P700^+$ oxidation ratio was calculated as $(A_{sat} - A_{actinic}) / (A_{sat} - A_{dark})$.

When the NoFOSpec was used, gas exchange data such as carbon assimilation and stomatal conductance was monitored with LI-6400 in real time to ensure that leaf was operating under physiological conditions. The LI-6400 fluorescence chamber had a small gas exchange area of 2 cm^2 that allowed Arabidopsis leaves grown under abovementioned conditions to cover the entire light path and be large enough to provide reliable gas exchange data with good signal-to-noise ratio. Leaf temperature control was provided by LI-6400. In experiments with heat treatments (40°C), however, we have found that Peltier heat exchange provided by LI-6400 did not raise the temperature fast enough and could not hold leaf temperature above 38°C at a room temperature of 25°C. In this case, a custom-built nickel-plated copper chamber was used instead. A small water chamber (separate from the gas chamber) was built into this leaf chamber behind an optical glass that allows light to pass. The adaxial side of the leaf was then attached to the optical glass by applying a very thin layer of vacuum grease to the glass. This setup did not affect gas exchange nor optical measurements while allowing for rapid heat transfer between the leaf sample and water (Zhang and Sharkey, 2009). The water chamber was connected to a six-way valve that allowed rapid switching between two water baths preset at 25°C (normal temperature) and 40°C (high temperature). With this setup, we were able to raise leaf temperature from 25°C to 40°C within 15 seconds. The copper leaf chamber was connected on-line with a LI-6400 for monitoring of gas exchange parameters.

Measurement of carbon assimilation rates under different light conditions (light response curve) were made on LI-6400 alone (with a regular leaf chamber, chamber area = 6 cm^2). Although an Arabidopsis leaf could not cover the entire chamber, the LI-6400 regular leaf chamber measured a larger area than the fluorescence chamber and thus gave a better signal-to-noise ratio. Leaf area

was estimated by tracing out the profile of measured leaf area on paper and weighing the cutout against a piece of paper of a standard area.

Chlorophyll *a* fluorescence measurements were made on the FAST-Est gas exchange system provided by Tartu University (Laisk et al., 2002), as previously described (Zhang and Sharkey, 2009). This system provided the high light needed (3000 μmol m^{-2} s^{-1} PPFD) for the light stress experiment. Gas exchange parameters were also monitored.

In all experiments with gas exchange and optical measurements, leaves were fed with an artificial air mixture consisting of 20% O_2, 80% N_2 and 400 ppm CO_2. Leaf temperatures were held at 25°C and light used to illuminate leaves was set to 500 μmol m^{-2} s^{-1} PPFD, unless otherwise noted. Leaves were acclimatized at 25°C and under 500 μmol m^{-2} s^{-1} PPFD for at least 45 min before the start of each experiment, except in the light stress experiment where 170 μmol m^{-2} s^{-1} PPFD was used.

Data Analysis

Different limits on CO_2 assimilation were fitted using the utility developed by Sharkey et al. (2007) according to the model developed by Farquhar et al. (1980). No obvious triose phosphate utilization limit was observed at high CO_2 concentrations. Mesophyll conductance was allowed to vary when solving for best fit of the model.

Comparisons between groups were made using one-way ANOVA and *t* tests ($P < 0.05$) in SigmaPlot (Systat software, Chicago, IL, USA). Where normality tests failed, Kruskal-Wallis ANOVA on ranks were performed instead of one-way ANOVA.

Acknowledgement

This project was a collaborative work with Jinpeng Gao and Christoph Benning. The chlorophyll and carotenoid levels (Fig. A1.1e), lipid profiles (Fig. A1.2) and AtpC levels (Fig. A1.4a, b) were measured by Jinpeng in Christoph Benning's lab. I also thank Drs. Ru Zhang and David Kramer for their helpful advices on using the NoFOSpec and Dr. Sean E. Weise for his technical assistance with LI-6400. This project was funded by National Science Foundation Grants IOS-0950574 to T.D.S. and MCB-0741395 to C.B.

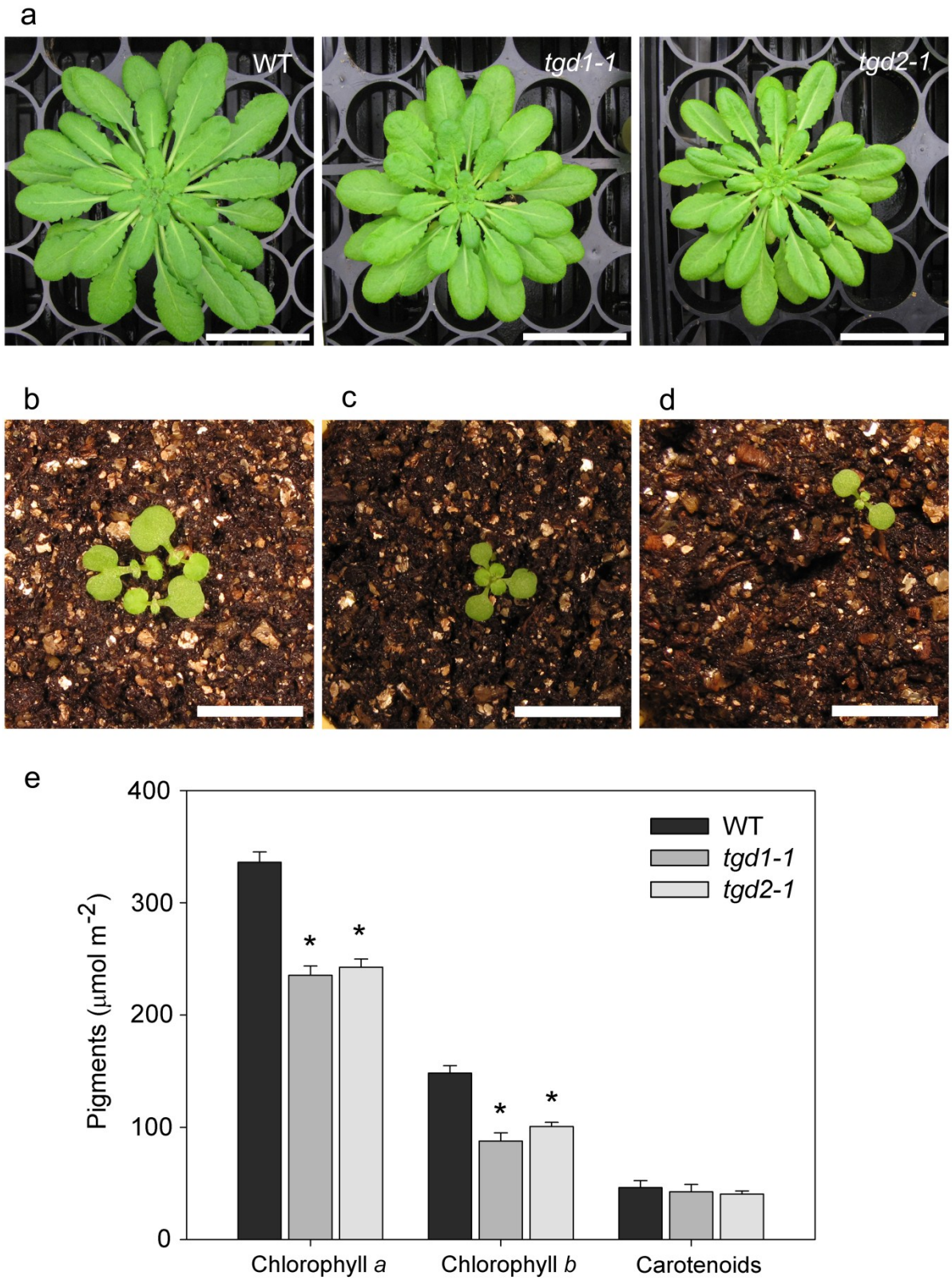

Figure A1.1 Phenotypes and pigment levels of *tgd* mutants. (a) phenotypes of *tgd1-1* and *tgd2-1* mutants vs. wild type (WT) 8 weeks after germination when grown under 8 hr

(Figure A1.1 continued)

photoperiod. Bar = 5 cm. (b, c) cotyledons of *tgd1-1* mutants 8 days after germination. Bar = 1 cm. Cotyledons of *tgd2-1* mutants appear similar to *tgd1-1* mutants. (d) cotyledons of wild-type plants 8 days after germination. Bar = 1 cm. (e) pigment levels in *tgd* mutants vs. wild-types. Each bar denotes the mean ± standard error (n = 4-5). Asteroids indicate significant difference from wild type (one-way ANOVA, $P < 0.001$).

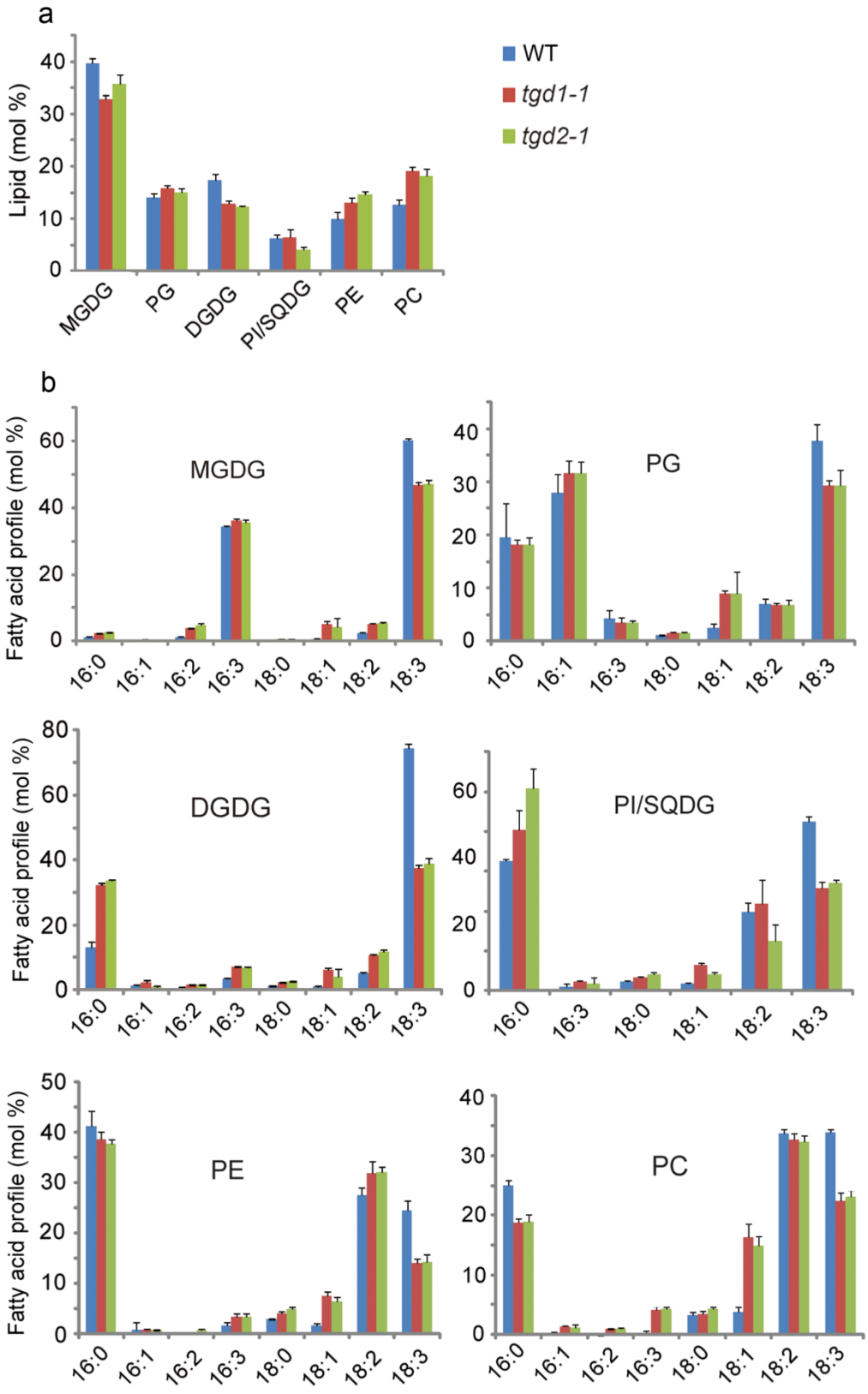

Figure A1.2 Lipid profile of chloroplasts of *tgd* mutants. (a) lipid profile of chloroplasts of

(Figure A1.2 continued)

tgd mutants and wild-type plants. MGDG = monogalactosyldiacylglycerol, PG = phosphotidylglycerol, DGDG = digalactosyldiacylglycerol, PI = phosphotidylinositol, SQDG = sulfoquinovosyldiacylglycerol, PE = phosphotidylethanolamine, PC = phosphotidylcholine. (b) fatty acid profile for each type of lipid. Each bar denotes the mean ± standard error (n = 3).

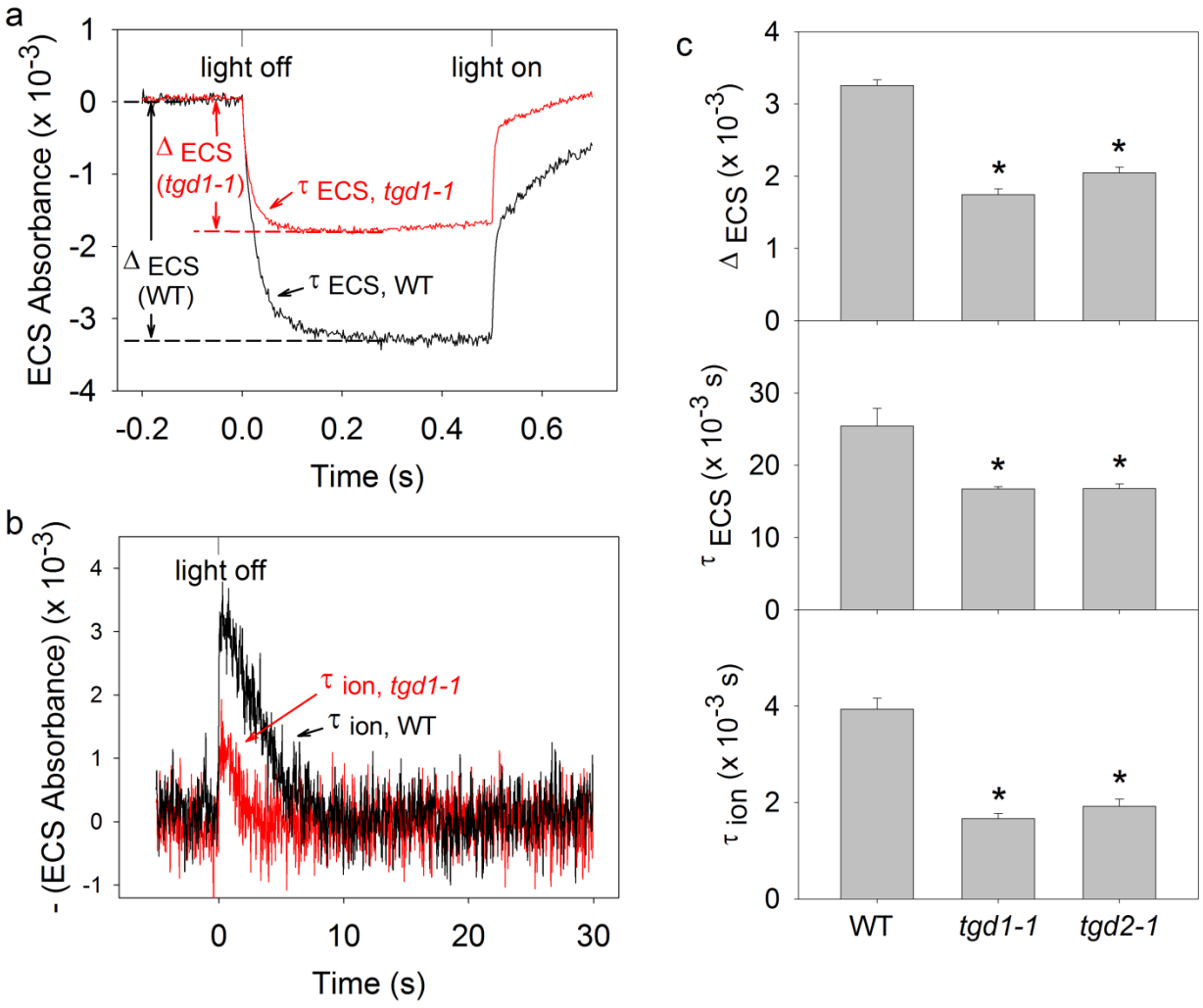

Figure A1.3 Dark interval relaxation kinetics (DIRK) of ECS in *tgd* mutants vs. wild type. Black lines represent data from wild-type Col-2 and red lines represent data from a *tgd* mutant (in this case, a *tgd1-1* mutant). Light was turned off at time 0. (a) representative traces of 500ms DIRK in wild type and *tgd1-1* mutant. Δ_{ECS} = amplitude of the ECS. τ_{ECS} = exponential time constant of the rapid phase (within 100 ms) of ECS decay. τ_{ECS} measures the conductance of thylakoid membranes to protons. (b) representative traces of 30s DIRK in wild type and *tgd1-1* mutant. Both traces had been smoothed with 10-point adjacent averaging for better visualization. τ_{ion} = exponential time constant of the slow and inverse phase (0.2 – 30s) of ECS decay. τ_{ion} measures the conductance of thylakoid membrane to counterions (primarily Mg^{2+} and Cl^-, Cruz et al., 2001). DIRK traces in *tgd2-1* mutants were similar to those in *tgd1-1* mutants. (c) Δ_{ECS}, τ_{ECS} and τ_{ion} were significantly reduced in *tgd* mutants. Each bar denotes the mean ± standard error (n = 6-8). Asteroids indicate significant difference from wild type (one-way ANOVA and ANOVA on ranks, $P < 0.001$).

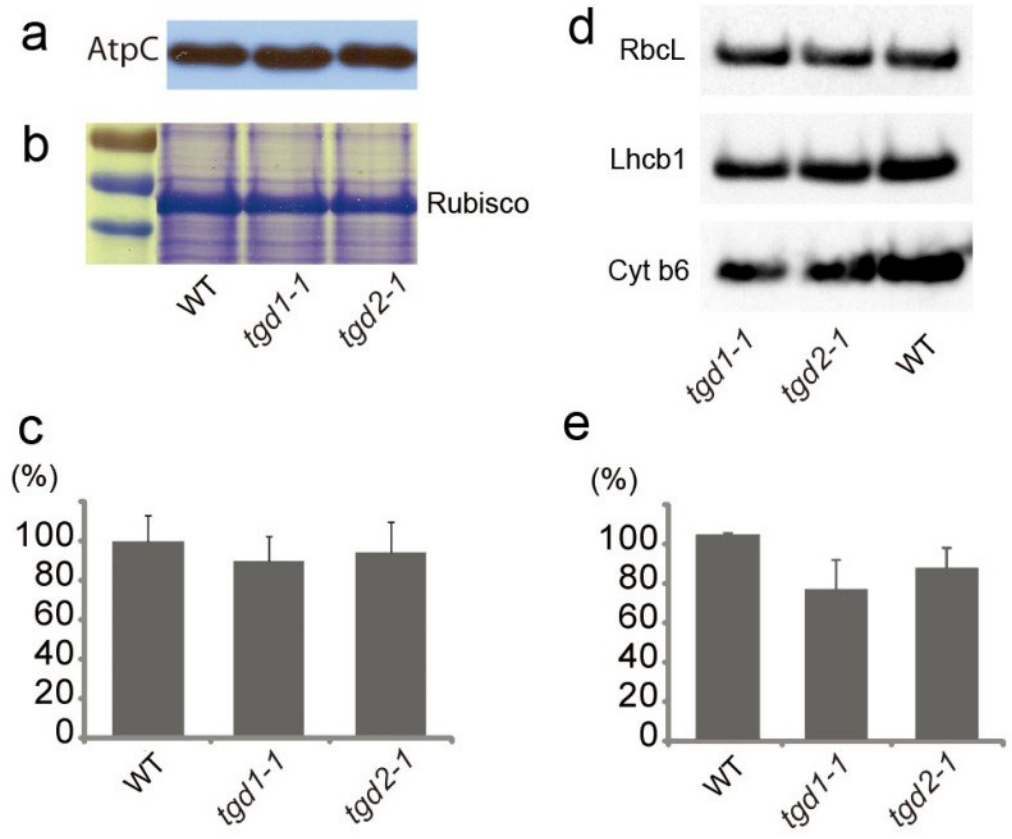

Figure A1.4 Levels of photosynthesis-related proteins in *tgd* mutants vs. wild type. (a) AtpC levels measured by western blot. (b) total proteins extracted (loading control) as stained by Coomassie blue. (c) band intensities in A as quantified by ImageJ. (d) Levels of RbcL, Lhcb1 and Cyt b6 measured by western blot. (e) band intensities of Cyt *b6* as quantified by ImageJ. In figures (c) and (e) band intensities of all three lines were normalized to the intensity of wild type band. Each bar denotes the mean ± standard error (n = 3).

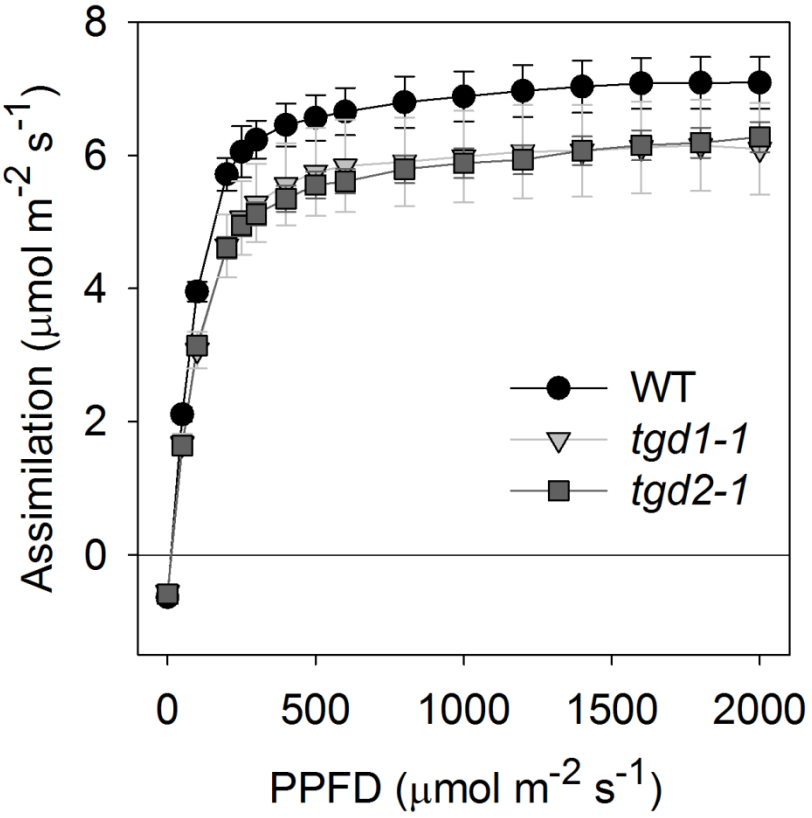

Figure A1.5 Light response curve of carbon assimilation in *tgd* mutants. PPFD = photosynthetic photon flux density. Each point denotes the mean ± standard error (n = 4-5).

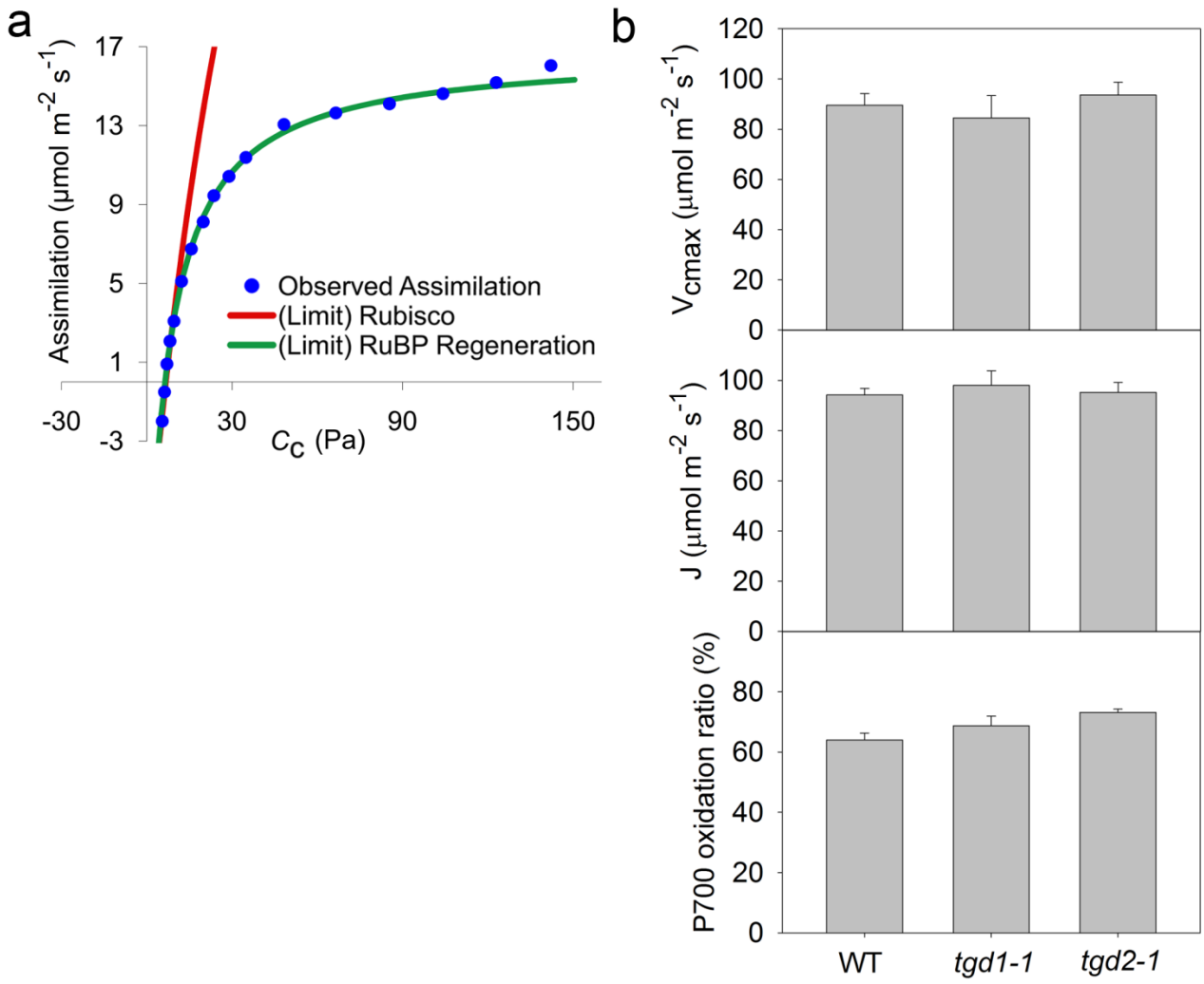

Figure A1.6 Different processes limiting assimilation under different CO_2 concentrations were determined according to Sharkey et al., 2007. (a) an example A-C_c (Assimilation – CO_2 concentration at site of carboxylation) curve of a wild-type arabidopsis plant. (b) Maximum carboxylation rate of RuBisCO (V_{cmax}), linear electron transport rate (J) and P700 oxidation ratio of *tgd* mutants vs. wild-types. Each point denotes the mean ± standard error (n = 4-5). V_{cmax} and J were derived from the A-C_c curves. P700 oxidation ratio was determined separately on NoFOSpec as $[(A_{810} - A_{905})_{sat + fr} - (A_{810} - A_{905})_{actinic}] / [(A_{810} - A_{905})_{sat + fr} - (A_{810} - A_{905})_{dark}]$.

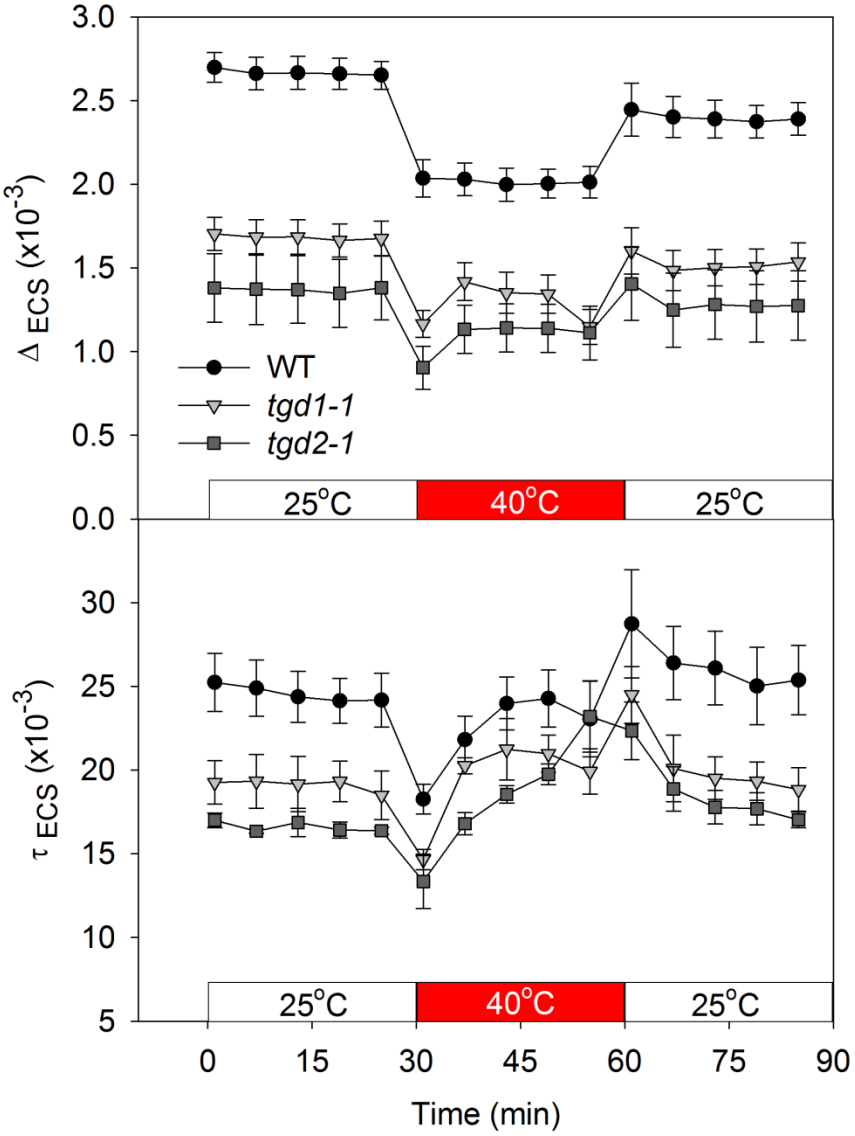

Figure A1.7 Effect of heat stress on *tgd* mutants. Each plant was acclimatized for at least 40 minutes before start of the experiment. ECS parameters of a 500ms DIRK was measured every 6 minutes as leaf temperature was held at 25°C for 30 min, raised and held at 40°C for 30 min, and then dropped to 25°C and held for another 30 min. Δ_{ECS} (*pmf*) of both wild-type and *tgd* mutants decreased during the heat treatment. τ_{ECS} (g_H^+)in all lines decreased immediately at the beginning of the heat treatment and soon recovered. τ_{ECS} also increased instantaneously as leaf temperature returned to 25°C and then gradually recovered to pre-stress levels.

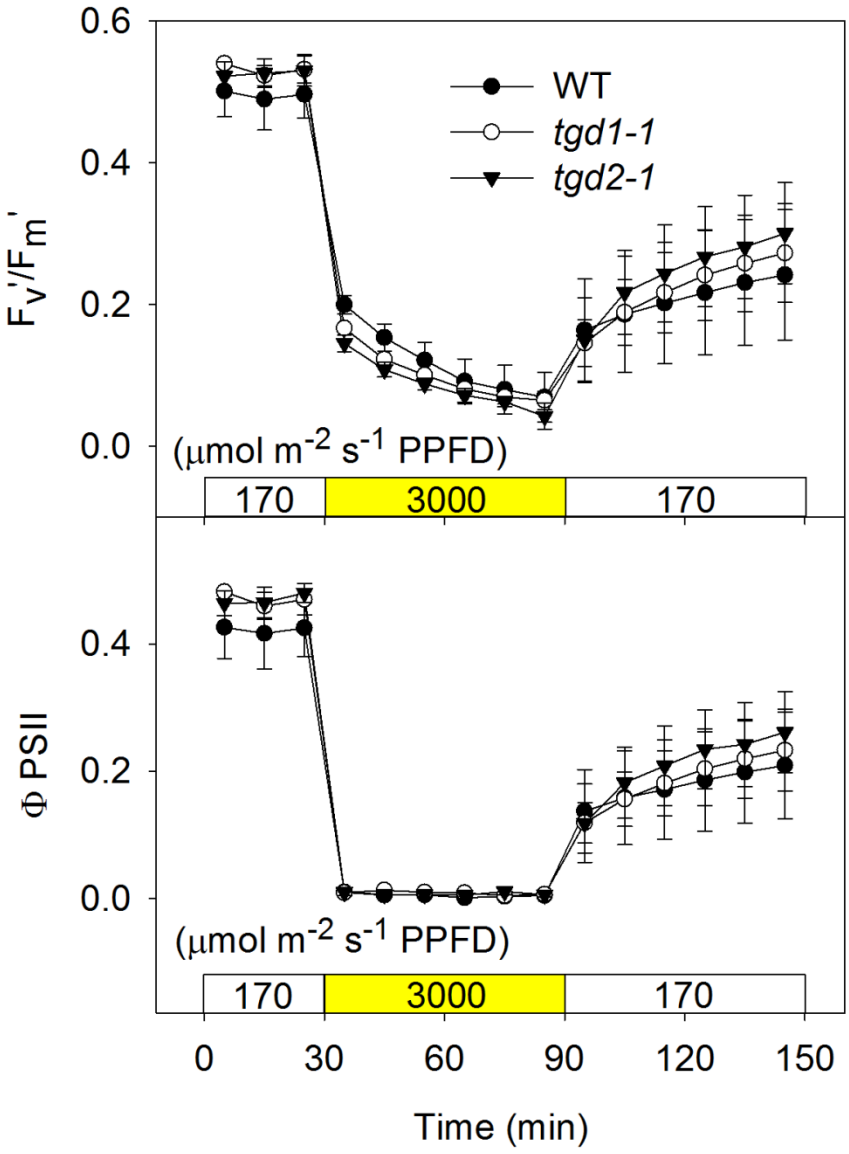

Figure A1.8 PSII fluorescence in *tgd* mutants and wild type during high light stress. PSII maximum efficiency (F_v'/F_m') and PSII operating efficiency (ΦPSII) were measured as leaves were held under 170 μmol m^{-2} s^{-1} PPFD for 30 min, placed under 3000 μmol m^{-2} s^{-1} PPFD for 60 min and returned to 170 μmol m^{-2} s^{-1} PPFD and monitored for another 60 min. Both PSII parameters were indifferent between the mutant and wild type at the beginning of experiment, during and after the high light treatment.

LITERATURE CITED

LITERATURE CITED

Aronsson H, Schöttler MA, Kelly AA, Sundqvist C, Dörmann P, Karim S, Jarvis P (2008) Monogalactosyldiacylglycerol deficiency in arabidopsis affects pigment composition in the prolamellar body and impairs thylakoid membrane energization and photoprotection in leaves. Plant Physiology **148:** 580-592

Avenson TJ, Cruz JA, Kanazawa A, Kramer DM (2005) Regulating the proton budget of higher plant photosynthesis. Proceedings of the National Academy of Sciences **102:** 9709-9713

Awai K, Xu C, Tamot B, Benning C (2006) A phosphatidic acid-binding protein of the chloroplast inner envelope membrane involved in lipid trafficking. Proceedings of the National Academy of Sciences **103:** 10817

Baker NR, Harbinson J, Kramer DM (2007) Determining the limitations and regulation of photosynthetic energy transduction in leaves. Plant, Cell and Environment **30:** 1107-1125

Benning C (2009) Mechanisms of lipid transport involved in organelle biogenesis in plant cells. Annual Review of Cell and Developmental Biology **25:** 71-91

Cline K, Keegstra K (1983) Galactosyltransferases involved in galactolipid biosynthesis are located in the outer membrane of pea chloroplast envelopes. Plant Physiology **71:** 366-372

Cruz JA, Sacksteder CA, Kanazawa A, Kramer DM (2001) Contribution of electric field ($\Delta\psi$) to steady-state transthylakoid proton motive force (*pmf*) in vitro and in vivo. Control of *pmf* parsing into $\Delta\psi$ and ΔpH by ionic strength. Biochemistry **40:** 1226-1237

Dörmann P, Benning C (2002) Galactolipids rule in seed plants. Trends in Plant Science **7:** 112-118

Dörmann P, Hoffmann-Benning S, Balbo I, Benning C (1995) Isolation and characterization of an Arabidopsis mutant deficient in the thylakoid lipid digalactosyl diacylglycerol. The Plant Cell **7:** 1801-1810

Dorne AJ, Block MA, Joyard J, Douce R (1982) The galactolipid: galactolipid galactosyltransferase is located on the outer surface of the outer membrane of the chloroplast envelope. FEBS Letters **145:** 30-34

Frentzen M (1986) Biosynthesis and desaturation of the different diacylglycerol moieties in higher plants. Journal of Plant Physiology **124:** 193-209

Gounaris K, Barber J (1983) Monogalactosyldiacylglycerol: The most abundant polar lipid in nature. Trends in Biochemical Sciences **8:** 378-381

Härtel H, Lokstein H, Dörmann P, Grimm B, Benning C (1997) Changes in the composition of the photosynthetic apparatus in the galactolipid-deficient *dgd1* mutant of *Arabidopsis thaliana*. Plant Physiology **115:** 1175-1184

Härtel H, Lokstein H, Dörmann P, Trethewey RN, Benning C (1998) Photosynthetic light utilization and xanthophyll cycle activity in the galactolipid deficient *dgd1* mutant of *Arabidopsis thaliana*. Plant Physiology and Biochemistry **36:** 407-417

Hölzl G, Witt S, Gaude N, Melzer M, Schöttler MA, Dörmann P (2009) The role of diglycosyl lipids in photosynthesis and membrane lipid homeostasis in arabidopsis. Plant Physiology **150:** 1147-1159

Ivanov AG, Hendrickson L, Krol M, Selstam E, Oquist G, Hurry V, Huner N (2006) Digalactosyl-diacylglycerol deficiency impairs the capacity for photosynthetic intersystem electron transport and state transitions in Arabidopsis thaliana due to photosystem I acceptor-side limitations. Plant and Cell Physiology **47:** 1146

Jarvis P, Dörmann P, Peto CA, Lutes J, Benning C, Chory J (2000) Galactolipid deficiency and abnormal chloroplast development in the *Arabidopsis MGD synthase 1* mutant. Proceedings of the National Academy of Sciences of the United States of America **97:** 8175-8179

Jordan P, Fromme P, Witt HT, Klukas O, Saenger W, Krausz N (2001) Three-dimensional structure of cyanobacterial photosystem I at 2.5 Å resolution. Nature **411:** 909-917

Joyard J, Teyssier E, Miège C, Berny-Seigneurin D, Maréchal E, Block MA, Dorne A-J, Rolland N, Ajlani G, Douce R (1998) The Biochemical Machinery of Plastid Envelope Membranes. Plant Physiology **118:** 715-723

Kelly AA, Froehlich JE, Dörmann P (2003) Disruption of the two digalactosyldiacylglycerol synthase genes *DGD1* and *DGD2* in Arabidopsis reveals the existence of an additional enzyme of galactolipid synthesis. The Plant Cell **15:** 2694-2706

Krumova S, Laptenok S, Kovács L, Tóth T, van Hoek A, Garab G, van Amerongen H (2010) Digalactosyl-diacylglycerol-deficiency lowers the thermal stability of thylakoid membranes. Photosynthesis Research **105:** 229-242

Liu Z, Yan H, Wang K, Kuang T, Zhang J, Gui L, An X, Chang W (2004) Crystal structure of spinach major light-harvesting complex at 2.72[thinsp]A resolution. Nature **428:** 287-292

Loll B, Kern J, Saenger W, Zouni A, Biesiadka J (2005) Towards complete cofactor arrangement in the 3.0Å resolution structure of photosystem II. Nature **438:** 1040-1044

Lu B, Benning C (2009) A 25-amino acid sequence of the *Arabidopsis* TGD2 protein is sufficient for specific binding of phosphatidic acid. Journal of Biological Chemistry **284:** 17420-17427

Lu B, Xu C, Awai K, Jones AD, Benning C (2007) A small ATPase protein of *Arabidopsis*, TGD3, involved in chloroplast lipid import. Journal of Biological Chemistry **282:** 35945-35953

Meinke DW, Franzmann LH, Nickle TC, Yeung EC (1994) *Leafy Cotyledon* Mutants of Arabidopsis. The Plant Cell **6:** 1049-1064

Mizusawa N, Wada H (2011) The role of lipids in photosystem II. Biochimica et Biophysica Acta (BBA) - Bioenergetics **DOI:** 10.1016/j.bbabio.2011.1004.1008

Moellering ER, Muthan B, Benning C (2010) Freezing tolerance in plants requires lipid remodeling at the outer chloroplast membrane. Science **330:** 226-228

Pick U, Gounaris K, Admon A, Barber J (1984) Activation of the CF_0-CF_1, ATP synthase from spinach chloroplasts by chloroplast lipids. Biochimica et Biophysica Acta, Bioenergetics **765:** 12-20

Pick U, Weiss M, Gounaris K, Barber J (1987) The role of different thylakoid glycolipids in the function of reconstituted chloroplast ATP synthase. Biochimica et Biophysica Acta, Bioenergetics **891:** 28-39

Roston R, Gao J, Xu C, Benning C (2011) Arabidopsis chloroplast lipid transport protein TGD2 disrupts membranes and is part of a large complex. Plant Journal **DOI:** 10.1111/j.1365-1313X.2011.04536.x

Rott M, Martins NF, Thiele W, Lein W, Bock R, Kramer DM, Schottler MA (2011) ATP synthase repression in tobacco restricts photosynthetic electron transport, CO_2 assimilation, and plant growth by overacidification of the thylakoid lumen. Plant Cell **23:** 304-321

Roughan PG, Slack CR (1982) Cellular organization of glycerolipid metabolism. Annual Review of Plant Physiology **33:** 97-132

Sacksteder CA, Jacoby ME, Kramer DM (2001) A portable, non-focusing optics spectrophotometer (NoFOSpec) for measurements of steady-state absorbance changes in intact plants. Photosynthesis Research **70:** 231-240

Sacksteder CA, Kramer DM (2000) Dark-interval relaxation kinetics (DIRK) of absorbance changes as a quantitative probe of steady-state electron transfer. Photosynthesis Research **66:** 145-158

Sen A, Williams WP, Quinn PJ (1981) The structure and thermotropic properties of pure 1,2-diacylgalactosylglycerols in aqueous systems. Biochimica et Biophysica Acta, Lipids and Lipid Metabolism **663:** 380-389

Sharkey TD, Bernacchi CJ, Farquhar GD, Singsaas EL (2007) Fitting photosynthetic carbon dioxide response curves for C_3 leaves. Plant, Cell and Environment **30:** 1035-1040

Stroebel D, Choquet Y, Popot J-L, Picot D (2003) An atypical haem in the cytochrome b6f complex. Nature **426:** 413-418

Takizawa K, Cruz JA, Kanazawa A, Kramer DM (2007) The thylakoid proton motive force *in vivo*. Quantitative, non-invasive probes, energetics, and regulatory consequences of light-induced *pmf*. Biochimica et Biophysica Acta, Bioenergetics **1767:** 1233-1244

Toni S (1997) Galactolipid biosynthesis genes and endosymbiosis. Trends in Plant Science **2:** 161-162

van Besouw A, Wintermans JFGM (1978) Galactolipid formation in chloroplast envelopes: I. Evidence for two mechanisms in galactosylation. Biochimica et Biophysica Acta, Lipids and Lipid Metabolism **529:** 44-53

Velikova V, Várkonyi Z, Szabó M, Maslenkova L, Nogues I, Kovács L, Peeva V, Busheva M, Garab G, Sharkey TD, Loreto F (2011) Increased thermostability of thylakoid membranes in isoprene-emitting leaves probed with three biophysical techniques. Plant Physiology **157:** 905-916

Wang Z, Xu C, Benning C (2012) TGD4 involved in endoplasmic reticulum-to-chloroplast lipid trafficking is a phosphatidic acid binding protein. The Plant Journal **DOI:** 10.1111/j.1365-1313X.2012.04900.x

Witt HT (1979) Energy conversion in the functional membrane of photosynthesis. Analysis by light pulse and electric pulse methods. The central role of the electric field. Biochimica et Biophysica Acta **505:** 355

Xu C, Fan J, Froehlich JE, Awai K, Benning C (2005) Mutation of the TGD1 chloroplast envelope protein affects phosphatidate metabolism in Arabidopsis. The Plant Cell **17:** 3094

Xu C, Fan J, Riekhof W, Froehlich JE, Benning C (2003) A permease-like protein involved in ER to thylakoid lipid transfer in Arabidopsis. EMBO Journal **22:** 2370-2379

Yamori W, Takahashi S, Makino A, Price GD, Badger MR, von Caemmerer S (2011) The roles of ATP synthase and the cytochrome b_6/f complexes in limiting chloroplast electron transport and determining photosynthetic capacity. Plant Physiology **155:** 956-962

Zhang R, Cruz JA, Kramer DM, Magallanes-Lundback ME, Dellapenna D, Sharkey TD (2009) Moderate heat stress reduces the pH component of the transthylakoid proton motive force in light-adapted, intact tobacco leaves. Plant, Cell and Environment **32:** 1538-1547

Zhang R, Sharkey TD (2009) Photosynthetic electron transport and proton flux under moderate heat stress. Photosynthesis Research **100:** 29-43

Zhang R, Wise RR, Struck KR, Sharkey TD (2011) Moderate heat stress of *Arabidopsis thaliana* leaves causes chloroplast swelling and plastoglobule formation. Photosynthesis Research **105:** 123-134

APPENDIX 2

Additional Studies: Effect of drought stress on biogenic volatile organic carbon (BVOC) emissions from *Populus* sp.

Research described in this chapter was a collaborative work with Werner Jud, Elisa Vanzo, and Jörg-Peter Schnitzler (Munich Helmholtz Center)

Introduction

I travelled to Munich, Germany in November 2011 to participate in the MOMEVIP campaign (Molecular and Metabolic Bases of Volatile Isoprenoid-induced Resistance to Stresses). The goal of the project that I participated in was to assess the effects of drought stress on BVOC emissions emitting species (e.g. poplar) and to better understand the molecular mechanism by which BVOC may confer resistance to abiotic stresses. Transgenic poplar species with isoprene emission knocked down by RNA interference (RNAi) was employed to study the interaction between BVOC emissions and drought stress.

Materials and methods

Growth conditions and experimental design

Four lines of poplar species were used in this study: 1) wild type (WT); 2) wild type transformed with a GUS reporter gene (GUS); 3) and 4), RNAi lines against poplar IspS (RA1, RA2). The transgenic lines have been previously generated in the Schnitzler lab (Behnke et al., 2010; Behnke et al., 2011).

Poplar trees were grown in gas-tight growth chambers where incoming gas compositions were tightly controlled. Whole-chamber gas exchange parameters were measured and recorded. The

light sources of the growth chambers used gradual light-up and dim-down at dawn and dusk. Four treatments were used: 1) control treatment at 380 ppm CO_2 (current ambient CO_2 concentrations); 2) three rapid drought episodes at 380 ppm CO_2, plants were re-watered after each drought episode; 3) a mild drought stress that last for an extended period of time, at 380 ppm CO_2; and 4) control treatment at 500 ppm CO_2 (projected future CO_2 levels). A blocked random design was used for both the treatments as well as selecting individual plants for further analysis. Leaves conditions were first assessed using non-destructive methods such as gas exchange experiments, and then harvested and further processed by other groups specializing in genomic, transcriptomic, metabolic, lipidomic measurements, molecular biology, root biology and ecophysiology.

Gas exchange and BVOC measurement

My role in this project was to set up gas exchange systems and carry out photosynthetic measurement in collaboration with biophysicists that specialize in BVOC measurements. Leaves were clamped in an open-path gas exchange system (GFS-3000, Walz, Effeltrich, Germany) online with a custom-built proton-transfer-reaction-time-of-flight-mass-spectrometer (PTR-TOF-MS) where plant volatile emissions were monitored. Gas exchange measurements were carried out at growth CO_2 concentrations (i.e. 380 ppm CO_2 for treatments 1, 2 and 3 and 500 ppm CO_2 for treatment 4). A flow rate of 800 μmol s^{-1} was used. For each measurement, the leaf was acclimated at photosynthetic photon flux density of 1000 μmol m^{-2} s^{-1} and 30°C leaf temperature for 30 – 40 min (unless otherwise noted), and then measured for 10 min in light followed by 20 min in dark. Assimilation and transpiration measurements were averaged over

the light period and dark respiration measurements were averaged over the first 10 min of the dark period.

All BVOC measurements were normalized to a standard mix of VOCs at the beginning of every measurement day. Background data was recorded for 10 min after the dark period for each measurement and subtracted from observed values during post-analysis. Raw BVOC data were stored in .hdf5 format. Plastidic dimethylallyl diphosphate levels were measured using post-illumination isoprene emission according to Rasulov et al. (2009). Clearing of the chamber and tubings was determined to be less than five seconds and therefore neglected from integration calculations. System clearing measurements were repeated three times at each CO_2 concentrations. Isoprene synthase constants were estimated by dividing steady-state isoprene emission levels in light by DMADP levels.

Results and discussions

Photosynthesis in plants under drought stress

The transformed lines (GUS, RA1 and RA2) displayed reduced assimilation and transpiration compared with the wild-type lines (Fig. A2.9a, b). This data suggests the transformation events may have confounding effects on the physiological state of the plants. In all four lines, both types of drought stresses significantly decreased carbon assimilation and transpiration, while dark

respiration was not affected (Fig. A2.9a, b, c). The extended drought stress affected photosynthesis more than short, acute drought stresses. Unexpectedly, assimilation measured in high CO_2 was lower than assimilation measured in low CO_2 levels; this is likely because measurements were made at CO_2 concentrations of growth conditions, and basal assimilation rates were probably lower in plants that had time to adapt to a high CO_2 environment. Higher water use efficiencies (A/E) were observed during drought stresses (Fig. A2.9d). The decrease in transpiration was more significant than the decrease in assimilation at higher CO_2 concentrations thus water use efficiency was also enhanced. The drop in transpiration under stressed conditions was caused by a decrease in stomatal conductance (Fig. A2.9e, f).

BVOC emissions from plants under drought stress

Isoprene emission under steady state conditions was effectively suppressed in RNAi lines (Fig. A2.10a). While isoprene emission was only marginally affected in the GUS lines, IspS activity was significantly affected by the transformation event and was ~10 fold lower than in the wild-type (Fig. A2.10b, c). The lower IspS activity in GUS lines was confirmed by measuring the rate of isoprene decline in light-to-dark transition (data not shown). Interestingly, plastidic DMADP was higher in the GUS lines so that isoprene emission was much less affected. Under drought stress, DMADP levels in both WT and GUS lines were significantly reduced; however this was accompanied by an increase in IspS activity, such that, isoprene emission was at approximately the same level as in non-stressed conditions. These observations suggest isoprene emission is tightly regulated in emitting species. Drought stresses significantly affect carbon assimilation, and this could reduce the carbon supply in the MEP pathway causing a drop in DMADP levels. It

appears that the loss of substrate is compensated by an up-regulation of enzyme levels (IspS) so that approximately the same level of isoprene emission is maintained. This further suggests that isoprene emission likely has an adaptive function in plants, and there is an "incentive" for plants to keep emitting isoprene under different conditions.

A rapid light-to-dark switch causes a burst of various VOCs, such as acetaldehyde and green leaf volatiles (GLVs); and the integrated emission of these VOCs were measured here (Fig. A2.10d, f). Emissions of these VOCs did not correlate with isoprene emission, as the VOC bursts were also observed in IspS-RNAi lines, approximately to the same amplitude as the wild-type and GUS

lines. Drought stress effectively abolished the post-illumination bursts of acetaldehyde and green leaf volatile, as well as the light-independent methanol emission (Fig. A2.10d, e, f).. This was also seen for the other VOCs (GLV83, GLV143, pentenal fragments) measured (data not shown). These observations contradict findings of Brilli et al. (2011), where a weak correlation between isoprene emission and the acetaldehyde burst was observed ($R^2 = 0.55$). The release of acetaldehyde and GLVs has not been well characterized. It has been suggested that the post-illumination acetaldehyde may represent a pyruvate overflow mechanism, where excess pyruvate upon switching to darkness are rapidly converted to acetaldehyde by pyruvate decarboxylase (Karl et al., 2002). The use of enzyme inhibitors to artificially enhance cellular pyruvate levels, however, did not support this hypothesis (Graus et al., 2004). Regardless of its origin, the acetaldehyde and GLV bursts were significantly reduced in drought stress. This suggest release of VOCs such as acetaldehyde is a consequence of cellular processes and is not an adaptive

response (at least to abiotic stresses), in stark contrast to isoprene emission which likely possess an important physiological function in stress response in plants.

Acknowledgements

Assistance from Werner Jud, Christoph Hasler, Elisa Vanzo, Federico Brilli, Zhen Bi and Katja Behnke is gratefully acknowledged. Data collection on PTR-TOF-MS is mostly carried out by Werner, who also wrote the program for data storage as well as pre-post-processing. I also thank Jörg-Peter Schnitzler for his thought-provoking discussions and guidance throughout the project.

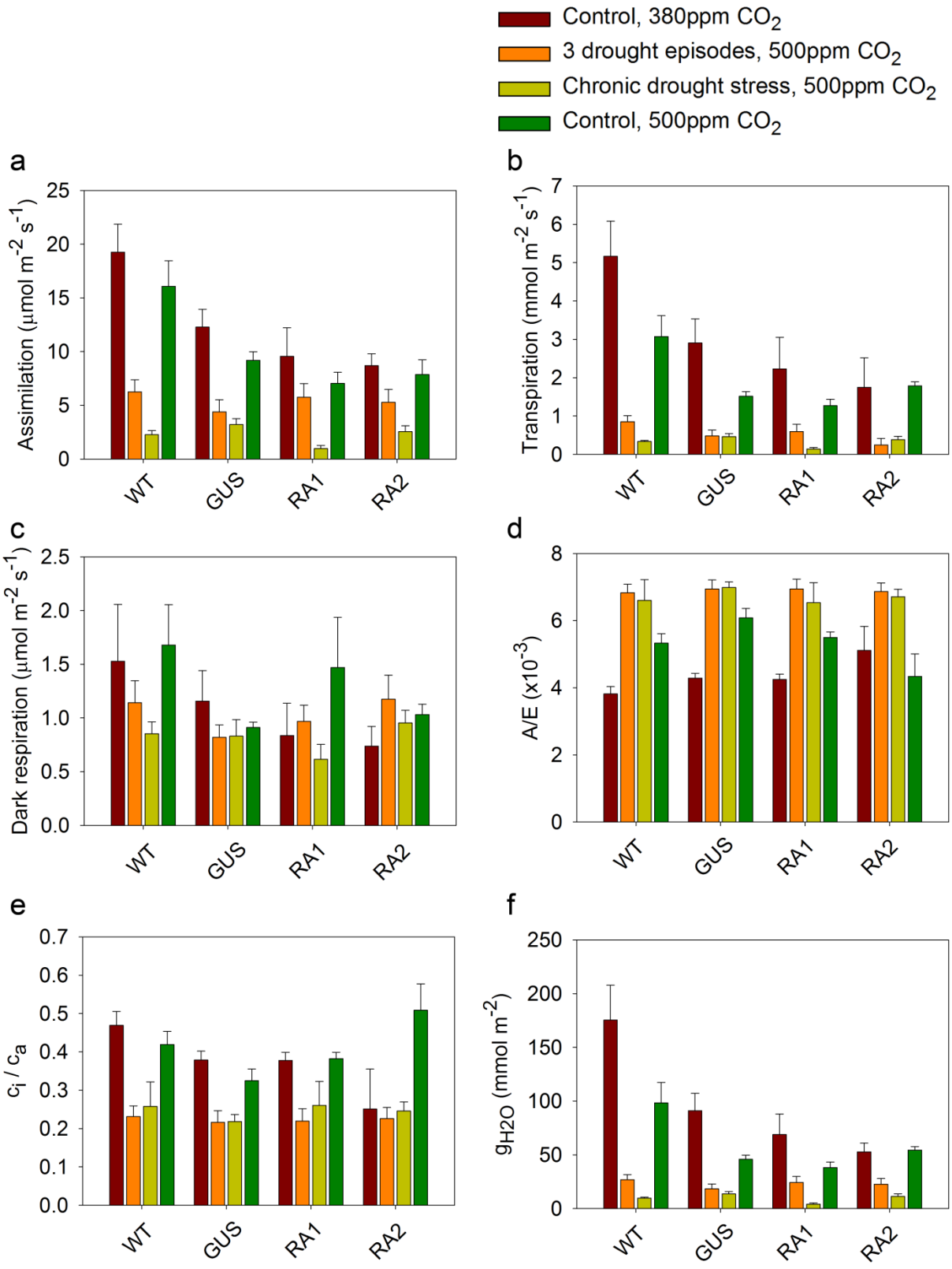

Figure A2.1 Photosynthetic parameters of drought-stressed poplar leaves vs. control leaves as measured during the MOMEVIP campaign, 2011 – 2012. RA1 and RA2, RNAi

(Figure A2.1 continued)

lines against poplar IspS. GUS, control line transformed with a GUS reporter gene. Carbon assimilation **(a)**, transpiration **(b)**, dark respiration **(c)**, A/E **(d)**, c_i/c_a **(e)** and g_{H2O} **(f)** were measured on a GFS-3000 (Walz) in line with PTR-TOF-MS. Each column denotes the mean ± standard error (n = 4).

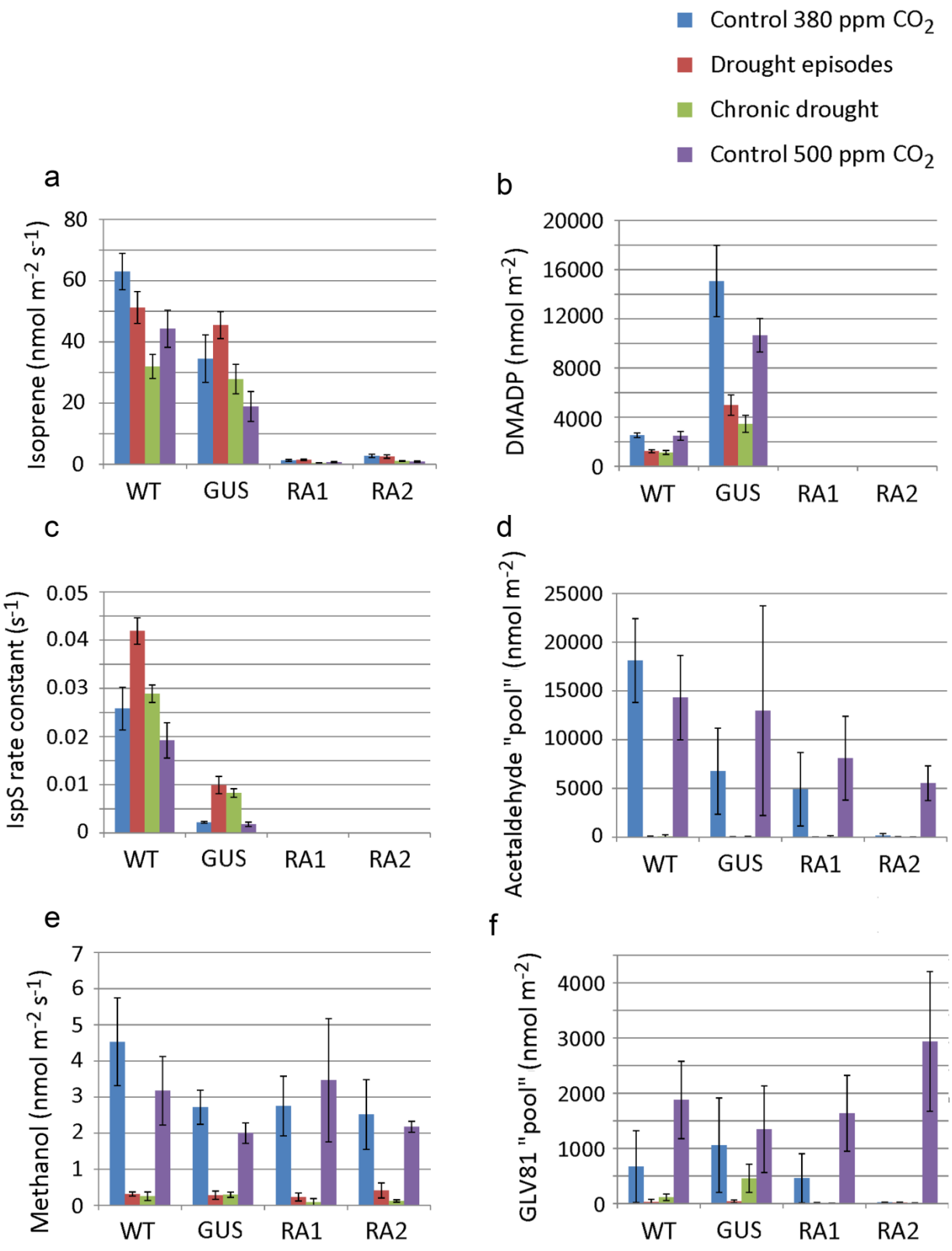

Figure A2.2 VOC emissions from four lines of poplar leaves under drought stress. Mass-to-charge ratios (m/z) of VOCs measured here were: isoprene, 69.07; acetaldehyde, 45.05;

(Figure A2.2 continued)

methanol, 33.03; green leaf volatile, 81.07. Other VOCs measured but not included in this figure were: acrolein, m/z = 57.03; methyl vinyl ketone, m/z = 71.04; pentenal fragments, m/z = 71.09; green leaf volatiles, m/z = 83.09 and 143.11; α-pinene, m/z = 137.13. Each column denotes the mean ± standard error (n = 4). **a** Isoprene emission from leaves under steady-state light conditions. **b** Plastidic DMADP levels as calculated from post-illumination isoprene emission. Trace amount of isoprene emission from RA1 and RA2 lines were not light dependent and thus DMADP levels cannot be determined. **c** IspS rate constant estimated from isoprene emission and DMADP values. **d** Integrated light-to-dark-transition-induced acetaldehyde burst. **e** Light-independent steady-state methanol emission. **f** Integrated light-to-dark-transition-induced green leaf volatile (m/z = 81.07) burst.

LITERATURE CITED

LITERATURE CITED

Behnke K, Grote R, Brüggemann N, Zimmer I, Zhou G, Elobeid M, Janz D, Polle A, Schnitzler J-P (2011) Isoprene emission-free poplars – a chance to reduce the impact from poplar plantations on the atmosphere. New Phytologist **194:** 70-82

Behnke K, Kaiser A, Zimmer I, Bruggemann N, Janz D, Polle A, Hampp R, Hansch R, Popko J, Schmitt-Kopplin P, Ehlting B, Rennenberg H, Barta C, Loreto F, Schnitzler JP (2010) RNAi-mediated suppression of isoprene emission in poplar transiently impacts phenolic metabolism under high temperature and high light intensities: a transcriptomic and metabolomic analysis. Plant Molecular Biology **74:** 61-75

Brilli F, Ruuskanen TM, Schnitzhofer R, Muller M, Breitenlechner M, Bittner V, Wohlfahrt G, Loreto F, Hansel A (2011) Detection of plant volatiles after leaf wounding and darkening by proton transfer reaction "time-of-flight" mass spectrometry (PTR-TOF). PLoS ONE **6:** 12

Graus M, Schnitzler JP, Hansel A, Cojocariu C, Rennenberg H, Wisthaler A, Kreuzwieser J (2004) Transient release of oxygenated volatile organic compounds during light-dark transitions in grey poplar leaves. Plant Physiology **135:** 1967-1975

Karl T, Curtis AJ, Rosenstiel TN, Monson RK, Fall R (2002) Transient releases of acetaldehyde from tree leaves - products of a pyruvate overflow mechanism? Plant Cell and Environment **25:** 1121-1131

Rasulov B, Copolovici L, Laisk A, Niinemets Ü (2009) Postillumination isoprene emission: in vivo measurements of dimethylallyldiphosphate pool size and isoprene synthase kinetics in aspen leaves. Plant Physiology **149:** 1609-1618